Constructing “chaotic coordinates” for non-integrable dynamical systems

S. R. Hudson, Princeton Plasma Physics Laboratory

Abstract

Action-angle coordinates can be constructed for so-called integrable Hamiltonian dynamical systems, for which there exists a foliation of phase space by surfaces that are invariant under the dynamical flow.

Perturbations generally destroy integrability.

However, we know that periodic orbits will survive, as will cantori, as will the “KAM” surfaces that have sufficiently irrational frequency, depending on the perturbation. There will also be irregular “chaotic” trajectories.

By “fitting” the coordinates to the invariant structures that are robust to perturbation, action-angle coordinates may be generalized to non-integrable dynamical systems. These coordinates “capture” the invariant dynamics and neatly partition the chaotic regions. These so-called chaotic coordinates are based on a construction of almost-invariant surfaces known as ghost surfaces. The theoretical definition and numerical construction of ghost surfaces and chaotic coordinates will be described and illustrated.

Ghost Surfaces: theoretical definition

Classical Mechanics 101:

The action integral is a functional of a curve in phase space.

1. The <u>action</u>, S, is the line integral along an arbitrary "trial" curve $\{\mathcal{C} : q \equiv q(t)\}$, of the Lagrangian,

$$\mathcal{L} \equiv \underbrace{T(\dot{q}, q)}_{\text{kinetic}} - \underbrace{U(q,t)}_{\text{potential}}, \quad S \equiv \int_{\mathcal{C}} \mathcal{L}(q, \dot{q}, t) dt$$

2. For magnetic fields, $\mathbf{B}$, the action is the line integral, of the vector potential, $\mathbf{B} = \nabla \times \mathbf{A}$,

$$S \equiv \oint_{\mathcal{C}} \mathbf{A} \cdot d\mathbf{l}, \text{ along } \{\mathcal{C} : \theta \equiv \theta(\zeta), \rho \equiv \rho(\theta)\}. \qquad \oint \mathbf{A} \cdot d\mathbf{l} = \int \mathbf{B} \cdot d\mathbf{s} = \text{flux}$$

3. Physical trajectories (magnetic fieldlines) extremize the action:

$$\delta S = \int_{\mathcal{C}} d\zeta \left(\delta\theta \frac{\partial S}{\partial \theta} + \delta\rho \frac{\partial S}{\partial \rho} \right), \text{ where } \boxed{\frac{\partial S}{\partial \theta} \equiv \sqrt{g} B^{\rho} - \dot{\rho}\sqrt{g} B^{\zeta}} \text{ and } \boxed{\frac{\partial S}{\partial \rho} \equiv \dot{\theta}\sqrt{g} B^{\zeta} - \sqrt{g} B^{\theta}}.$$

extremal curves satisfy $\dot{\rho} = B^{\rho}/B^{\zeta}$, and $\dot{\theta} = B^{\theta}/B^{\zeta}$.

4. Action-extremizing periodic curves may be minimizing or minimax.

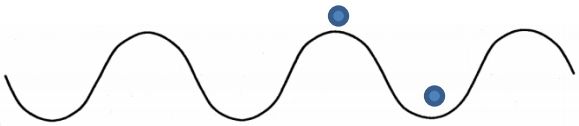

5. [Ghost surfaces are defined by an action-gradient flow between the minimax and minimizing periodic orbit.]

1954 : Kolmogorov, Dokl. Akad. Nauk SSSR 98, 469 ,1954

1963 : Arnold, Russ. Math. Surveys 18, 9,1963

1962 : Moser, Nachr. Akad. Wiss. Goett. II, Math.-Phys. Kl. 1, 1,1962

1. A dynamical system is integrable if there exists action-angle (ψ, θ) s.t. $H = H_0(\psi)$.
2. Arbitrary perturbation $H = H_0(\psi) + \sum_{m,n} H_{m,n}(\psi) \exp[i(m\theta - n\zeta)]$, where $\zeta \equiv t$ is "time".
3. Generating function to new action-action coordinates, $(\bar{\psi}, \bar{\theta})$, is

$$S(\bar{\psi}, \bar{\theta}) = \bar{\psi} \cdot \bar{\theta} + i \sum \frac{H_{m,n}}{(m\,\dot{\theta} - n)} \exp[i(m\theta - n\zeta)]. \tag{1}$$

   i. small denominators: rationals are dense; $\exists (m, n)$ s.t. $m\,\dot{\theta} - n$ is arbitrarily small.

4. KAM: adjust ψ, iteratively, to ensure that $\iota \equiv \dot{\theta}$ is sufficiently irrational,

Diophantine condition $\boxed{\left| \iota - \frac{n}{m} \right| > \frac{r}{m^k}}$, for all n & m, where $r \geq 0$ and $k > 1$.

5. If ι is sufficiently irrational then for sufficiently small $H_{m,n}(\psi)$, Eqn(1) converges.
   i. action-angle coordinates can be constructed locally if $\iota \equiv \dot{\theta}$ is irrational.

"one of the most important concepts is labelling orbits by their frequency" [J. D. Meiss, Reviews of Modern Physics, 64(3):795 (1992)]

The structure of phase space is related to the structure of rationals and irrationals.

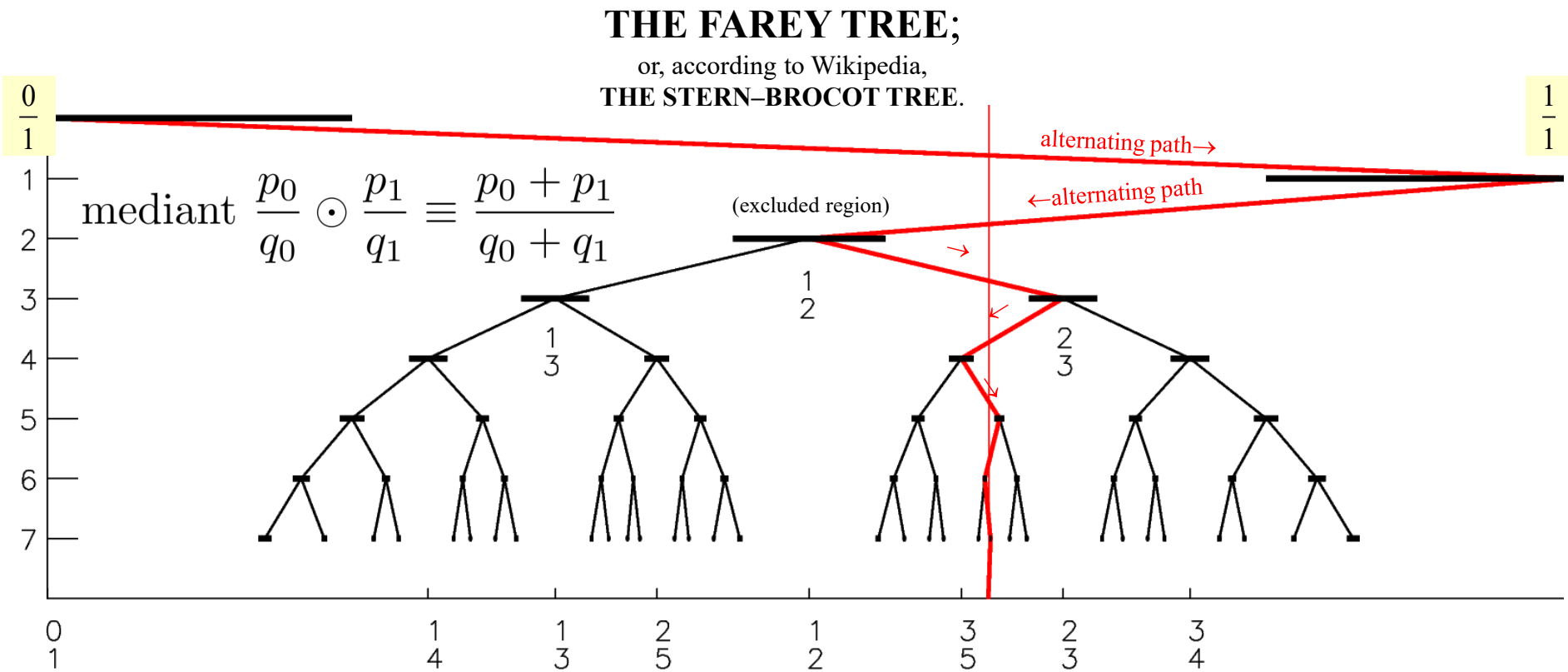

1. Islands, and chaos, emerge at every rational.

2. Noble irrationals $\equiv$ limit of ultimately alternating paths $\equiv$ limit of Fibonacci ratios

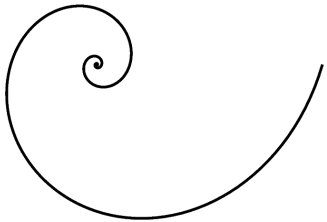

Irrational KAM surfaces break into cantori when perturbation exceeds critical value.
Both KAM surfaces and cantori restrict transport.

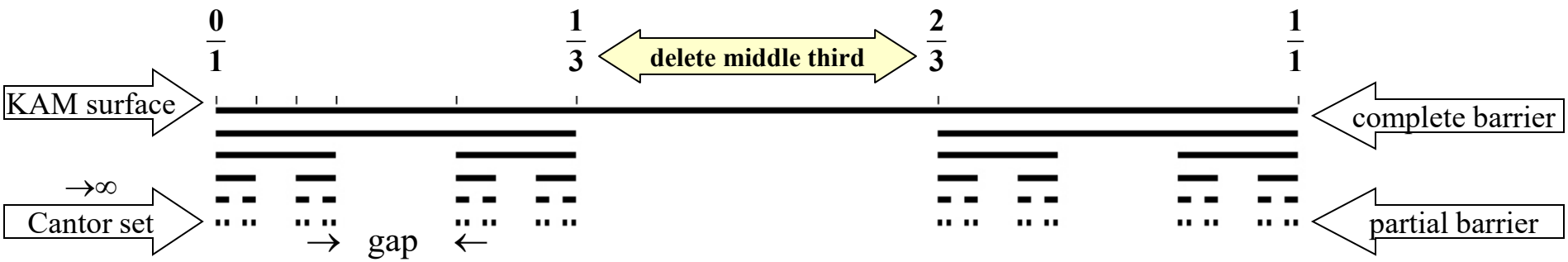

→ KAM surfaces are closed, toroidal surfaces that **stop** radial field line transport

→ Cantori have "gaps" that fieldlines can pass through; however, **cantori can severely restrict** radial transport

→ Example: all flux surfaces destroyed by chaos, but even after **100 000 transits** around torus the fieldlines **don't get past cantori !**

→ Regions of chaotic fields can provide some confinement because of the cantori partial barriers.

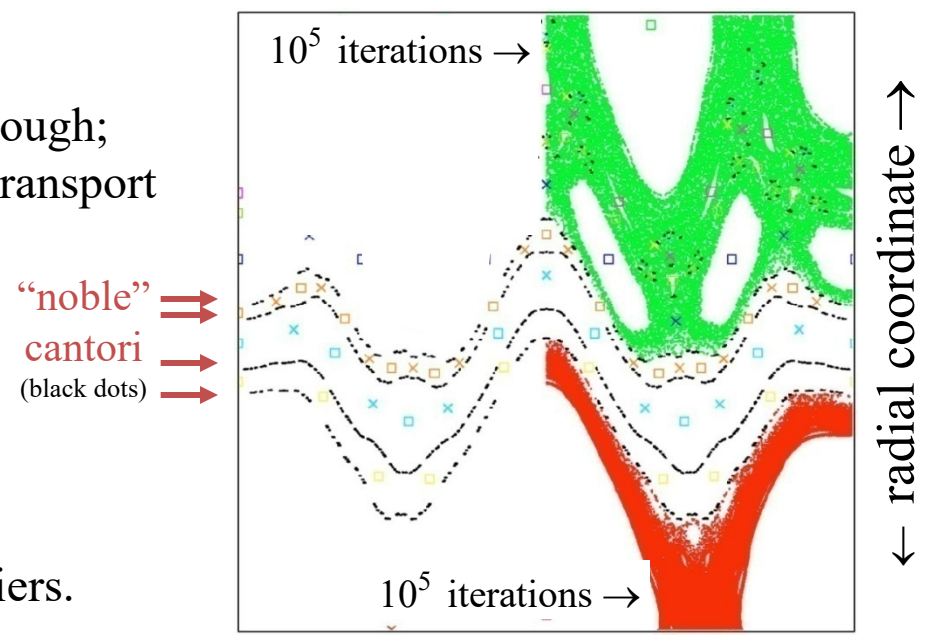

Simple physical picture of cantori

[Percival, 1979]

1. Consider masses, m, linked by springs in a periodic potential.
2. For $m = 0$, potential is irrelevant: minimum energy state has masses equally spaced.

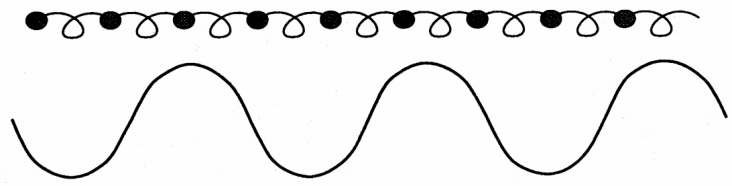

3. For large m, springs are irrelevant: all the masses lie at the potential minimum, and there are "gaps".

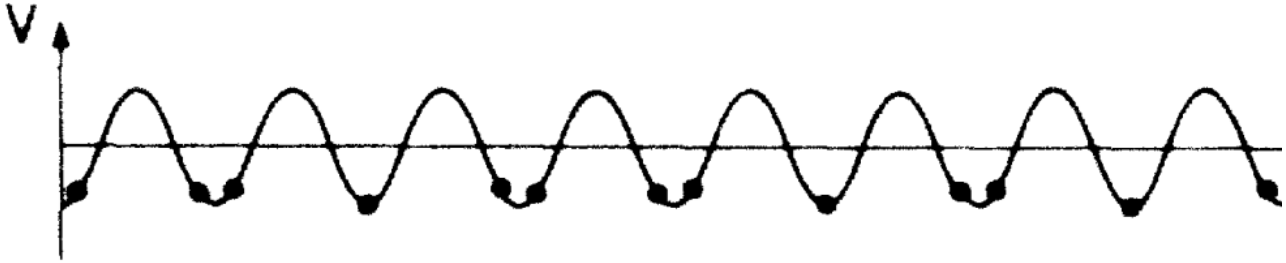

[Schellnhuber, Urbschat & Block, Physical Review A, 33(4):2856 (1986)]

The construction of extremizing curves of the action generalized extremizing surfaces of the quadratic-flux

1. $\delta S = \int_{\mathcal{C}} d\zeta \left(\delta\theta \frac{\partial S}{\partial \theta} + \delta\rho \frac{\partial S}{\partial \rho} \right)$, where $\boxed{\frac{\partial S}{\partial \theta} \equiv \sqrt{g} B^{\rho} - \dot{\rho}\sqrt{g} B^{\zeta}}$ and $\boxed{\frac{\partial S}{\partial \rho} \equiv \dot{\theta}\sqrt{g} B^{\zeta} - \sqrt{g} B^{\theta}}$.

2. Extremal curves satisfy $\frac{\partial S}{\partial \theta} = 0$, i.e. $\dot{\rho} = B^{\rho}/B^{\zeta}$, and $\frac{\partial S}{\partial \rho} = 0$, i.e. $\dot{\theta} = B^{\theta}/B^{\zeta}$.

3. Introduce toroidal surface, $\rho \equiv P(\theta, \zeta)$, and *family* of angle curves, $\theta_{\alpha}(\zeta) \equiv \alpha + p\,\zeta/q + \tilde{\theta}(\zeta)$, where α is a fieldline label; p and q are integers that determine periodicity; and $\tilde{\theta}(0) = \tilde{\theta}(2\pi q) = 0$.

4. On *each* curve, $\rho_{\alpha}(\zeta) = P(\theta_{\alpha}(\zeta), \zeta)$ and $\theta_{\alpha}(\zeta)$, can <u>enforce</u> $\frac{\partial S}{\partial \rho} = 0$; generally $\nu \equiv \frac{\partial S}{\partial \theta} \neq 0$.

5. The *pseudo* surface dynamics is defined by $\dot{\theta} \equiv B^{\theta}/B^{\zeta}$ and $\dot{\rho} \equiv \partial_{\theta} P\, \dot{\theta} + \partial_{\zeta} P$.

6. Corresponding *pseudo* field $\mathbf{B}_{\nu} \equiv \dot{\rho}\, B^{\zeta}\, \mathbf{e}_{\rho} + \dot{\theta}\, B^{\zeta}\, \mathbf{e}_{\theta} + B^{\zeta} \mathbf{e}_{\zeta}$; simplifies to $\mathbf{B}_{\nu} = \mathbf{B} - \frac{\nu}{\sqrt{g}}\, \mathbf{e}_{\rho}$.

7. Introduce the <u>**quadratic-flux functional**</u>: $\boxed{\varphi_2 \equiv \frac{1}{2} \iint d\theta d\zeta \left(\frac{\partial S}{\partial \theta} \right)^2}$

8. Allowing for δP, the first variation is $\delta\varphi_2 = \iint d\theta d\zeta\, \delta P\, \sqrt{g}\, \underbrace{\left(B^{\theta} \partial_{\theta} + B^{\zeta} \partial_{\zeta} \right) \nu}_{\text{Euler-Lagrange for QFMs}}$.

At each poloidal angle, compute radial "error" field that must be subtracted from **B** to create a periodic curve, and so create a rational, pseudo flux surface.

0. Usually, there are only the "stable" periodic fieldline and the unstable periodic fieldline,

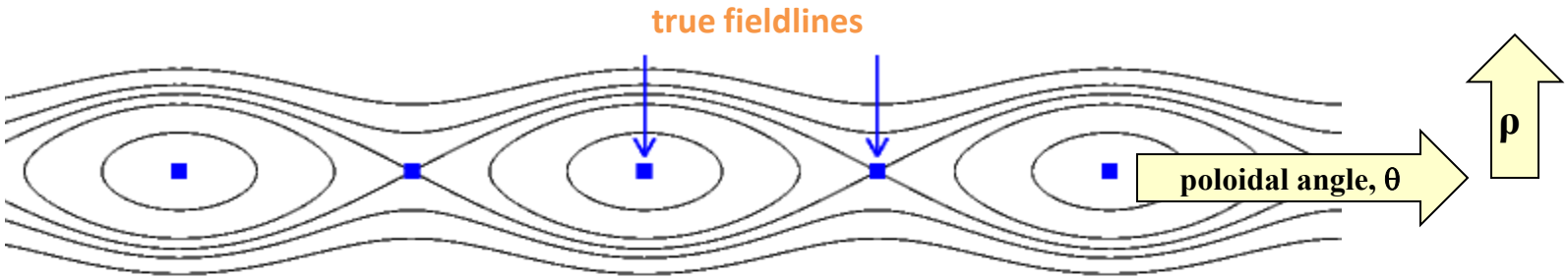

1. At every $\theta = \alpha$, determine $\nu(\alpha)$ via numerical search so that $\mathbf{B} - \nu\, \mathbf{e}_\rho/\sqrt{g}$ yields a periodic integral curve; where α is a fieldline label.

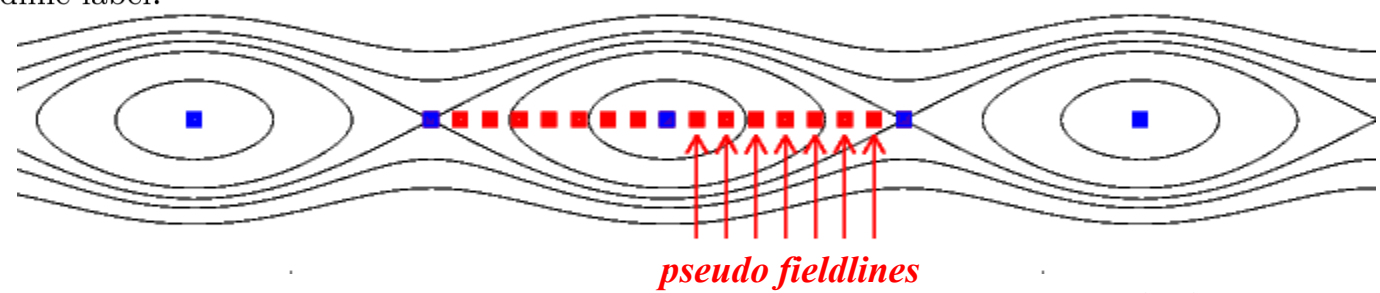

2. At the true periodic fieldlines, the required additional radial field is zero: i.e. $\nu(\alpha_0) = 0$ and $\nu(\alpha_X) = 0$.

3. Typically, $\nu(\alpha) \approx \sin(q\alpha)$.

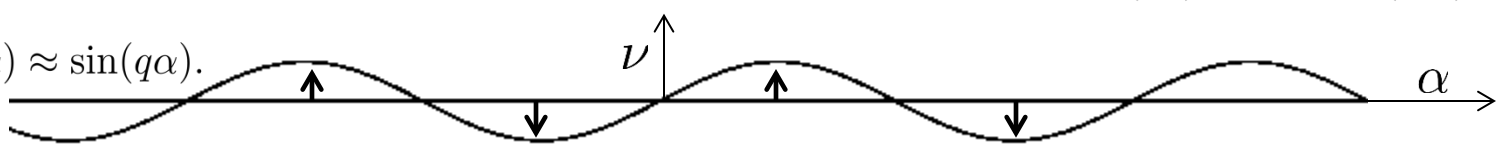

4. The pseudo fieldlines "capture" the true fieldlines; QFM surfaces pass through the islands.

Ghost surfaces, another class of almost-invariant surface, are defined by an action-gradient flow between the action minimax and minimizing fieldline.

1. Action, $S[\mathcal{C}] \equiv \int_{\mathcal{C}} \mathbf{A} \cdot d\mathbf{l}$, and action gradient, $\dfrac{\partial S}{\partial \theta} \equiv \sqrt{g} B^{\rho} - \dot{\rho} B^{\zeta}$.

2. Enforce $\dfrac{\partial S}{\partial \rho} \equiv \dot{\theta} B^{\zeta} - \sqrt{g} B^{\theta} = 0$, i.e. invert $\dot{\theta} \equiv B^{\theta}/B^{\zeta}$ to obtain $\rho = \rho(\dot{\theta}, \theta, \zeta)$; so that trial curve is completely described by $\theta(\zeta)$, and the action reduces from $S \equiv S[\rho(\zeta), \theta(\zeta)]$ to $S \equiv S[\theta(\zeta)]$

3. Define action-gradient flow: $\boxed{\dfrac{\partial \theta(\zeta;\tau)}{\partial \tau} \equiv -\dfrac{\partial S[\theta]}{\partial \theta}}$, where τ is an arbitrary integration parameter.

4. Ghost-surfaces are constructed as follows:

   i. Begin at action-minimax ("O", "not-always-stable") periodic fieldline, which is a saddle;
   ii. initialize integration in decreasing direction (given by negative eigenvalue/vector of Hessian);
   iii. the entire curve "flows" down the action gradient, $\partial_{\tau}\theta = -\partial_{\theta} S$;
   iv. action is decreasing, $\partial_{\tau} S < 0$;
   v. finish at action-minimizing ("X", unstable) periodic fieldline.
   vi. ghost surface described by $\mathbf{x}(\zeta, \tau)$, where τ is a fieldline label.

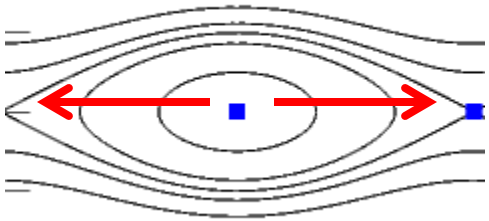

Ghost surfaces are (almost) indistinguishable from QFM surfaces

can redefine poloidal angle to unify ghost surfaces with QFMs.

1. Ghost-surfaces are defined by an (action gradient) flow.
2. QFM surfaces are defined by minimizing $\int (\text{action gradient})^2 d\mathbf{s}$.
3. Not obvious if the different definitions give the same surfaces.
4. For model chaotic field:
   (a) ghosts = thin solid lines;
   (b) QFMs = thick dashed lines;
   (c) agreement is excellent;
   (d) difference $= \mathcal{O}(\epsilon^2)$, where ϵ is perturbation.
5. Can redefine θ to obtain unified theory of ghosts & QFMs; straight *pseudo* fieldline angle.

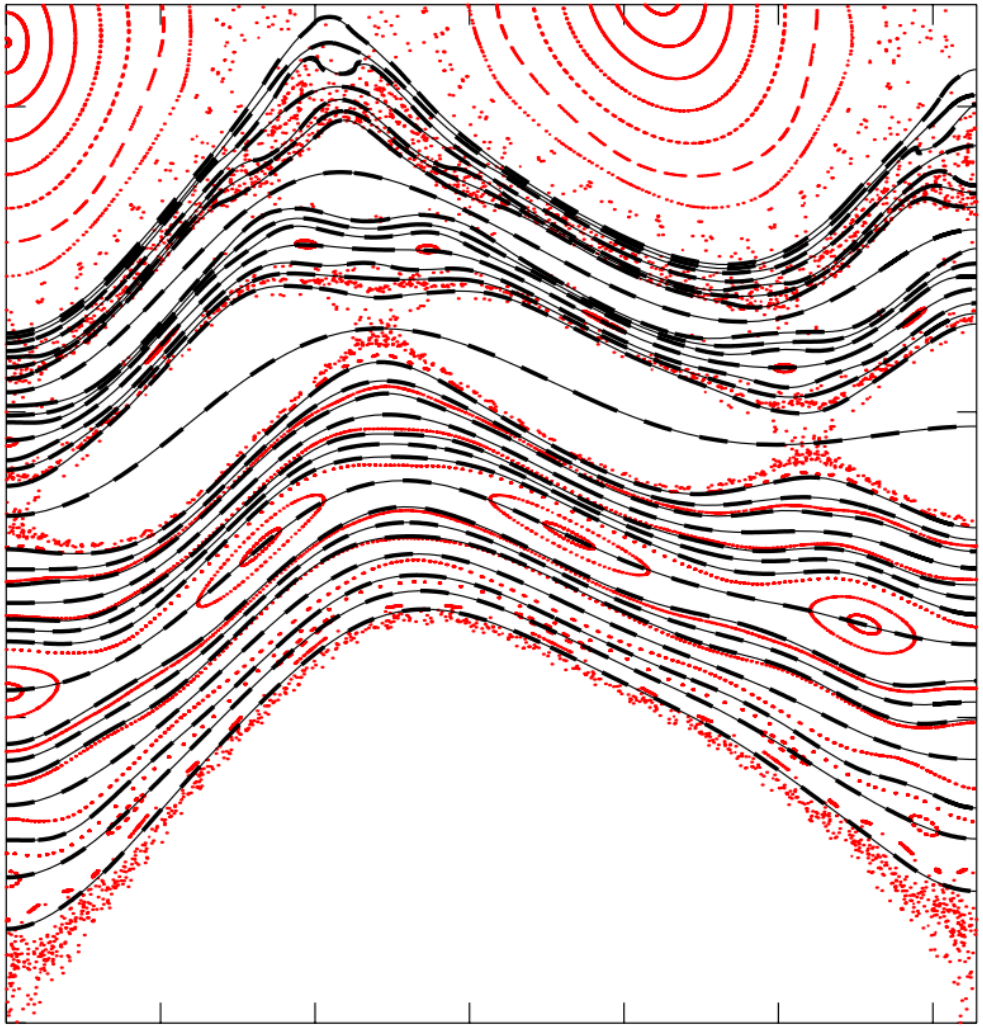

Chaotic Coordinates: intuitive description

Simplied Diagram showing the invariant structures: integrable

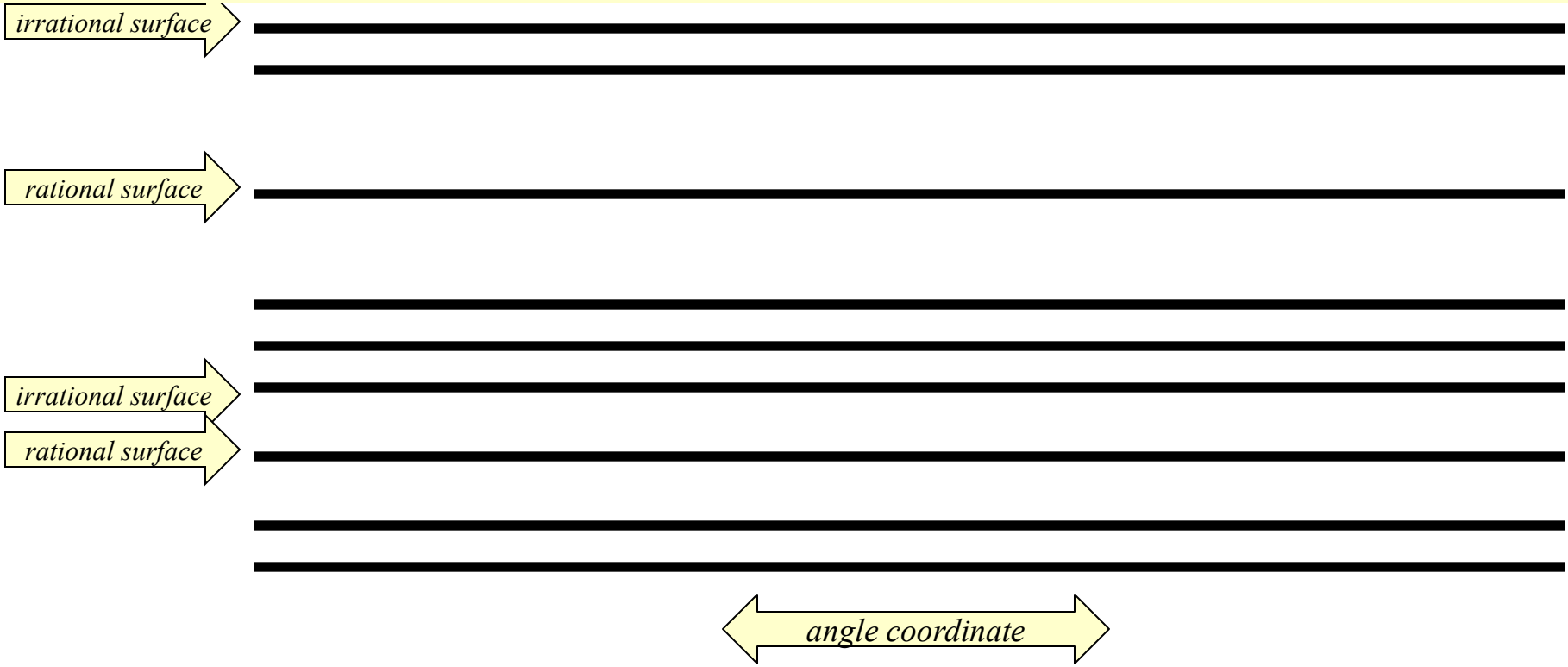

Action-angle coordinates can be constructed for "integrable" fields

1. the "action" coordinate coincides with the invariant surfaces
2. dynamics then appears simple

Simplied Diagram showing the invariant structures: perturbed

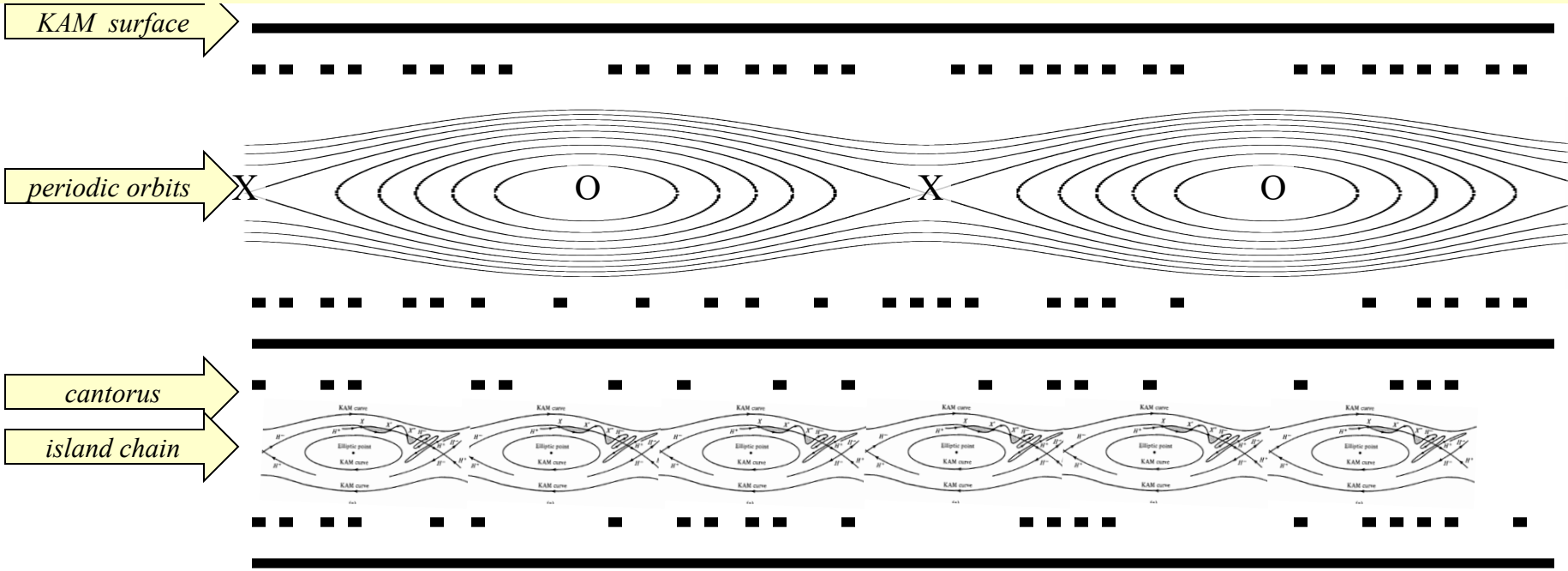

After perturbation:

the <u>rational</u> surfaces break into islands, “stable” and “unstable” periodic orbits survive,

some <u>irrational</u> surfaces break into cantori,

some <u>irrational</u> surfaces survive (KAM surfaces), break into cantori as perturbation increases,

$\rightarrow$ action-angle coordinates can no longer be constructed globally

Simplied Diagram showing the invariant structures: perturbed

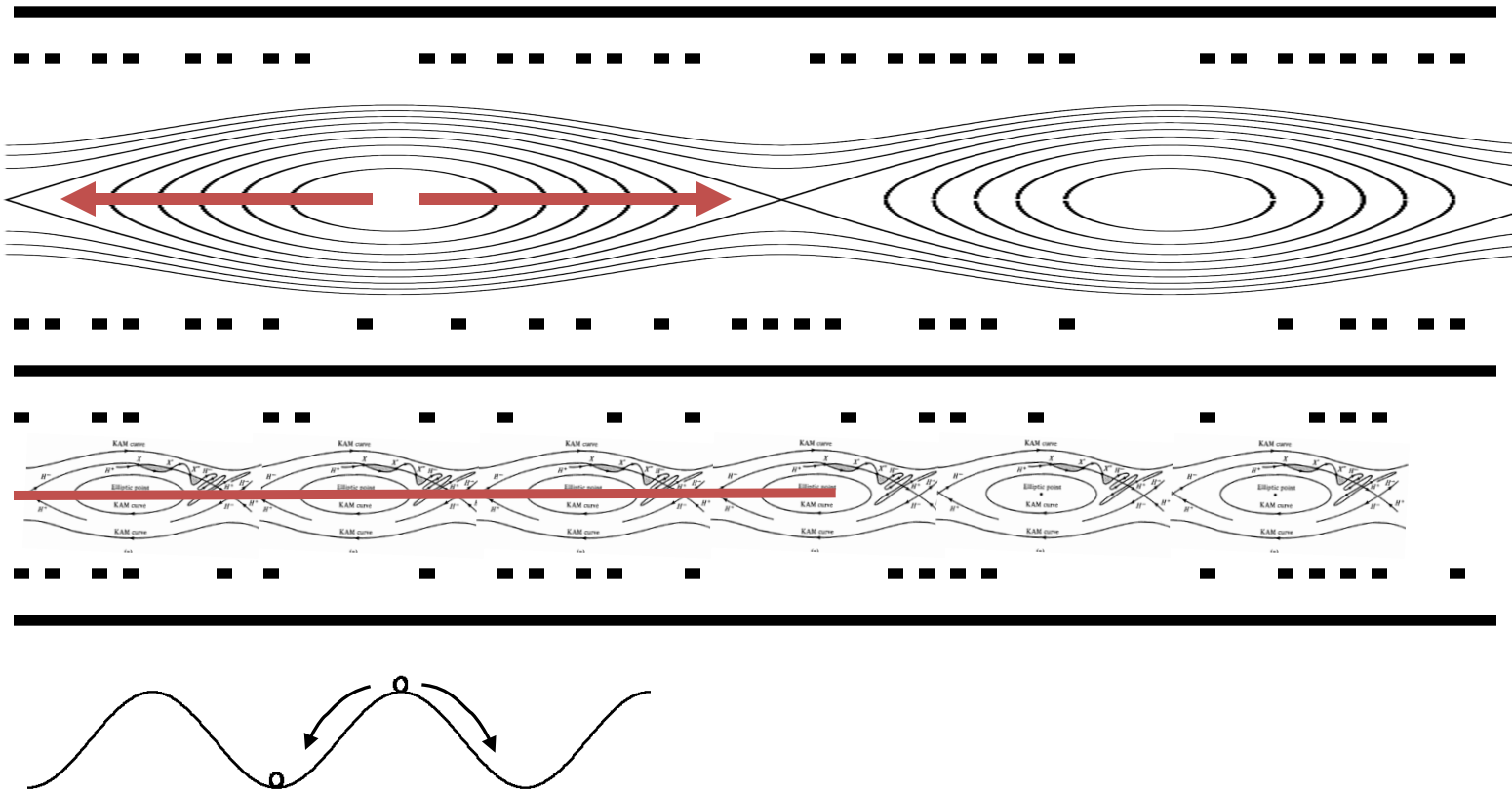

Simplied Diagram showing the invariant structures: perturbed, but with coordinates adapted to invariant sets

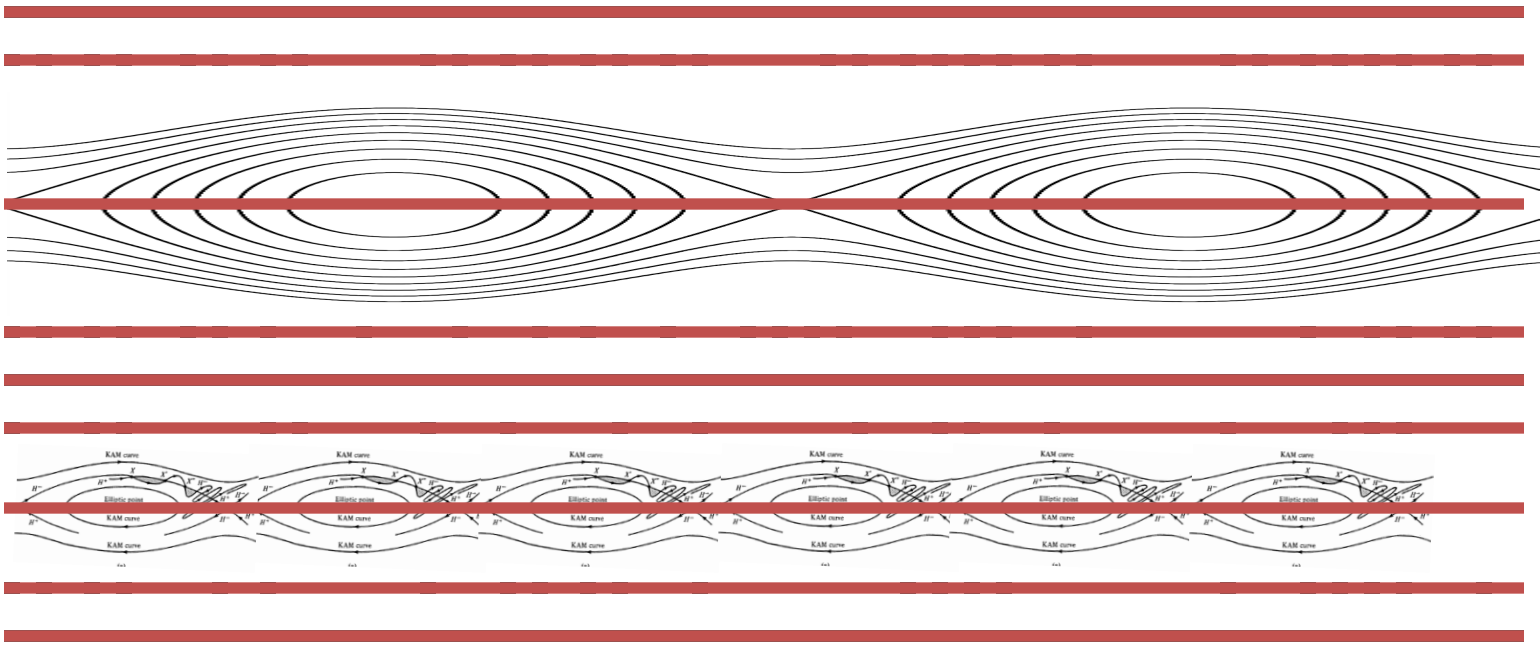

“Chaotic-coordinates” coincide with the invariant sets

1. coordinate surfaces are adapted to fractal hierarchy of remaining invariant sets
2. ghost surfaces ≡ quadratic-flux minimizing surfaces are “almost-invariant”
3. dynamics appears “almost-simple”

Simplied Diagram showing the invariant structures: example

Poincaré plot of chaotic field
(in **action-angle** coordinates of **unperturbed** field)

Poincaré plot of chaotic field
in chaotic coordinates

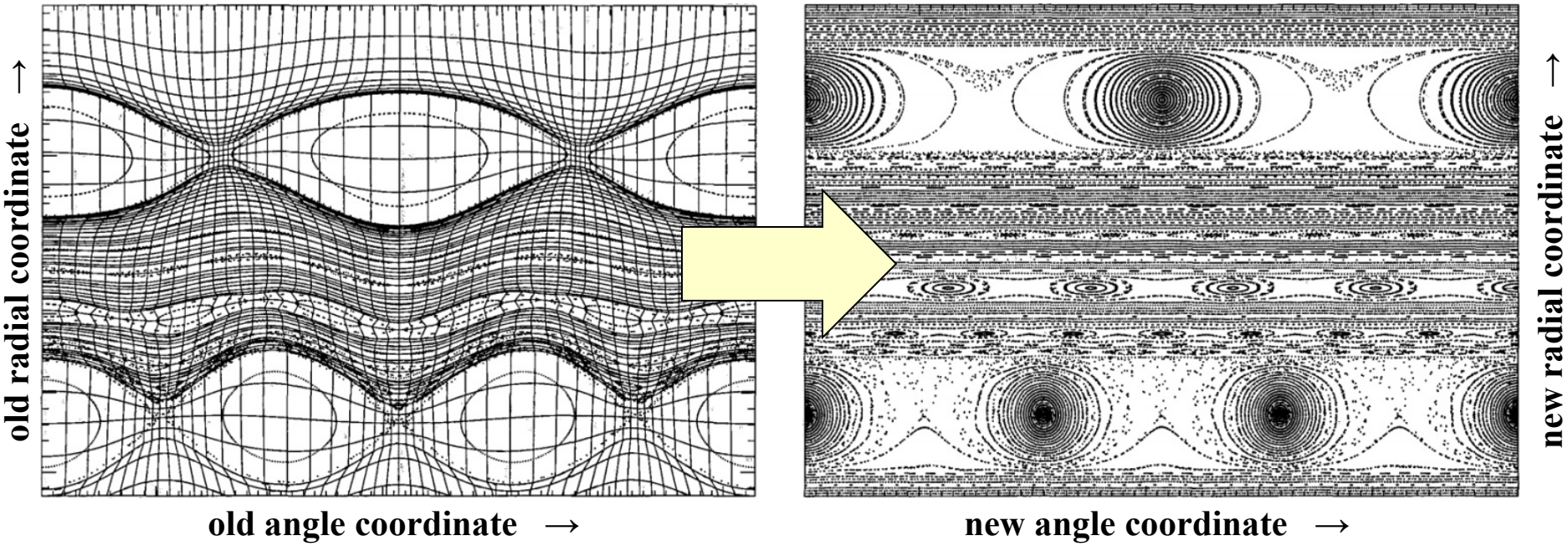

phase-space is partitioned into (1) regular "irrational" regions
and (2) irregular "rational" regions

Chaotic Coordinates: construction for stellarator fields

Large Helical Device (LHD) is a stellarator in Japan

1. The magnetic field consistent with an MHD equilibrium,
   $\nabla p \approx \mathbf{j} \times \mathbf{B}, \qquad \mathbf{j} \equiv \nabla \times \mathbf{B}$
   is provided by the HINT-2 code.

2. The field near the edge is chaotic.

3. A selection of ghost surfaces is constructed,
   $p/q = 10/23, 10/22, 10/21, \ldots$ near the axis,
   $p/q = 10/9, 10/8, 10/7, 10/6$ near the edge.
   (shown in lower half of figure)

4. These ghost surfaces, and a suitable interpolation provide a new coordinate system.

5. The following slides shall concentrate on edge region.

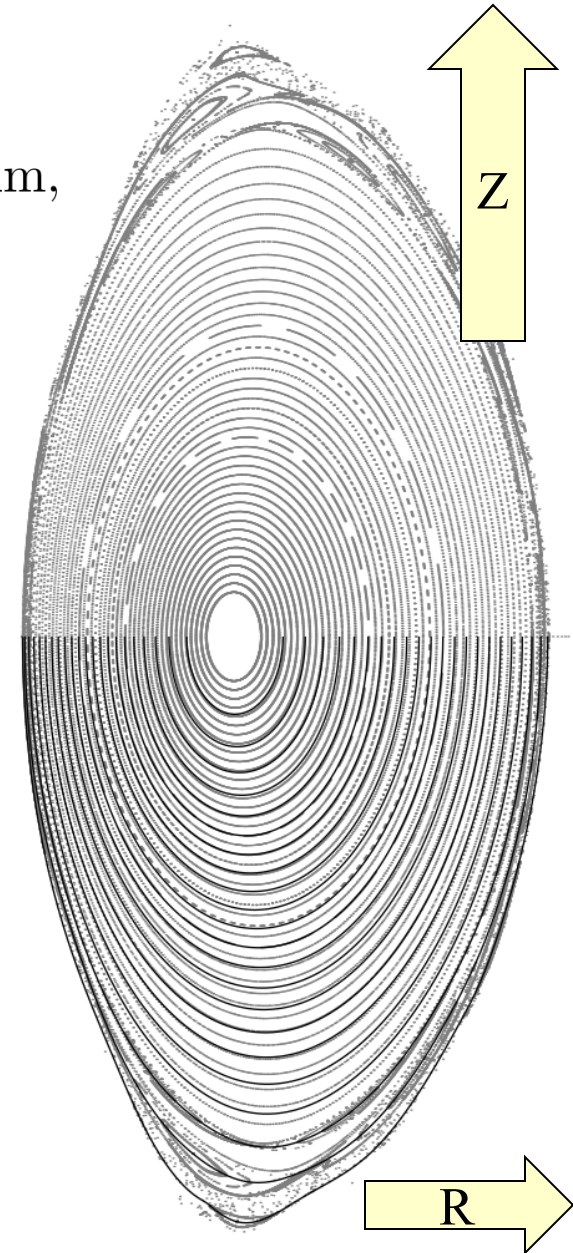

The corresponding islands lie on a coordinate surface

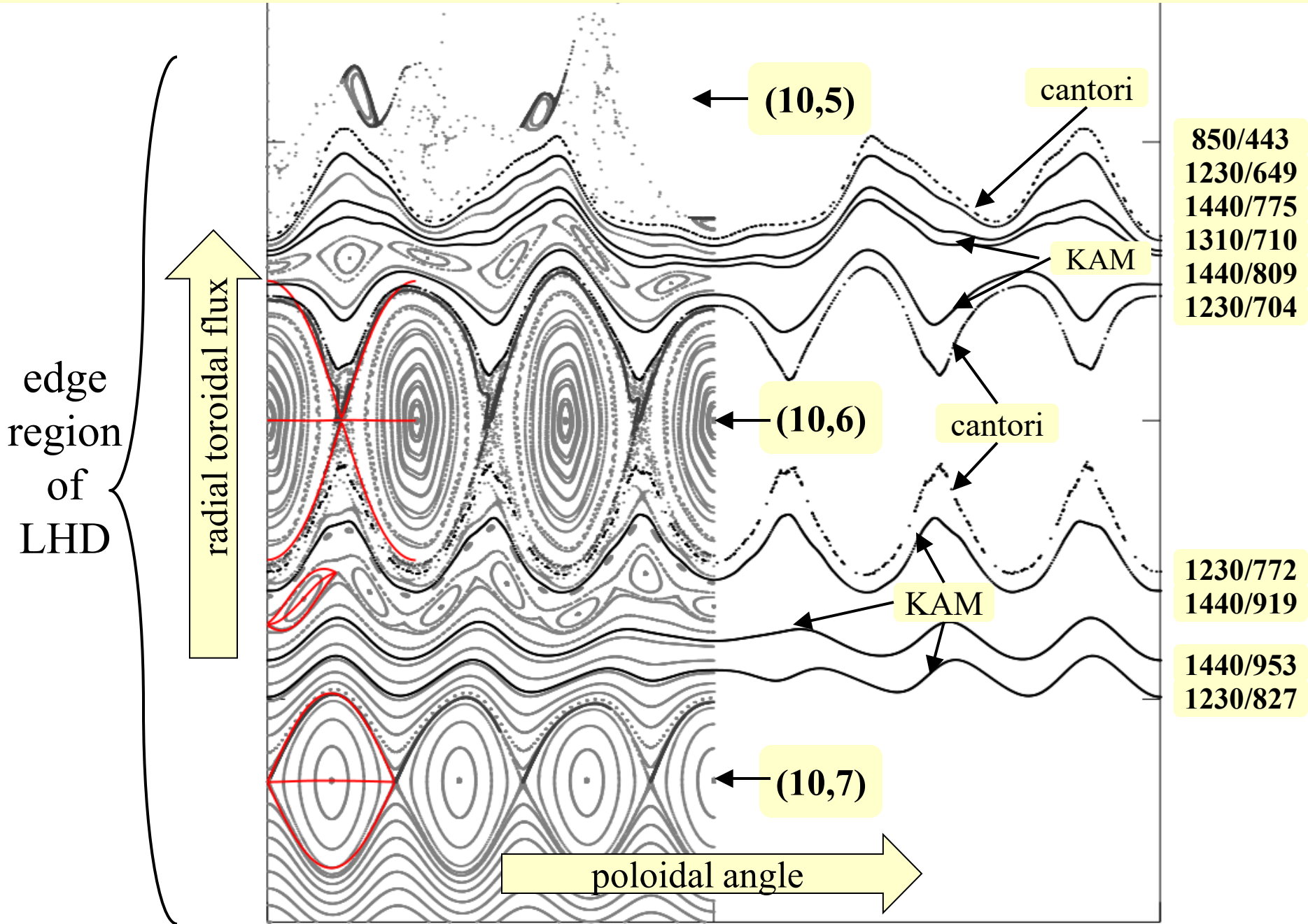

The Flux Farey tree shows the flux across the rational surfaces, the importance of the hierarchy of partial barriers can be quantified

1. $\oint_{\partial\mathcal{V}} \mathbf{B}\cdot d\mathbf{S} = \int_{\mathcal{V}} \nabla\cdot\mathbf{B}\, dv = 0$; the total flux across any closed surface is zero.

2. Consider any "ribbon" surface with boundary coinciding with X and O fieldlines; define "upward" flux
$$\Psi_{p/q} \equiv \oint_{\mathcal{S}} \mathbf{B}\cdot d\mathbf{S} = \int_O \mathbf{A}\cdot d\mathbf{l} - \int_X \mathbf{A}\cdot d\mathbf{l}.$$

3. Surfaces with small flux are "partial" barriers.

4. If $\Phi_{p/q}$ is suff. small, collisional transport can dominate.

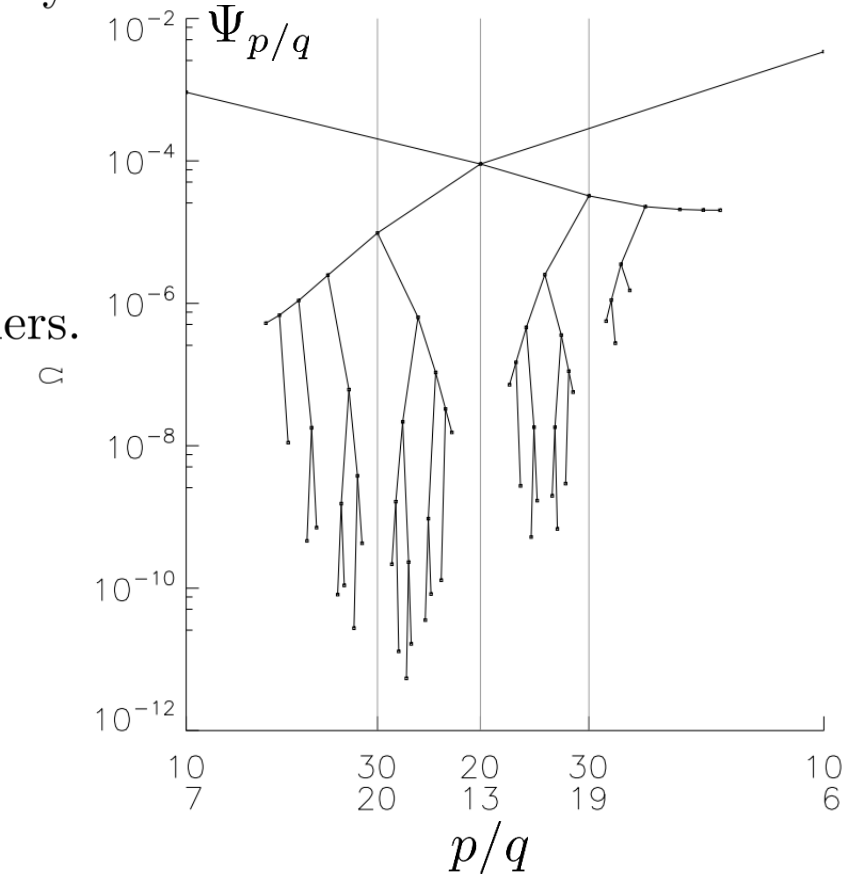

Now, construct more ghost surfaces (resolve the fractal structure iteratively)

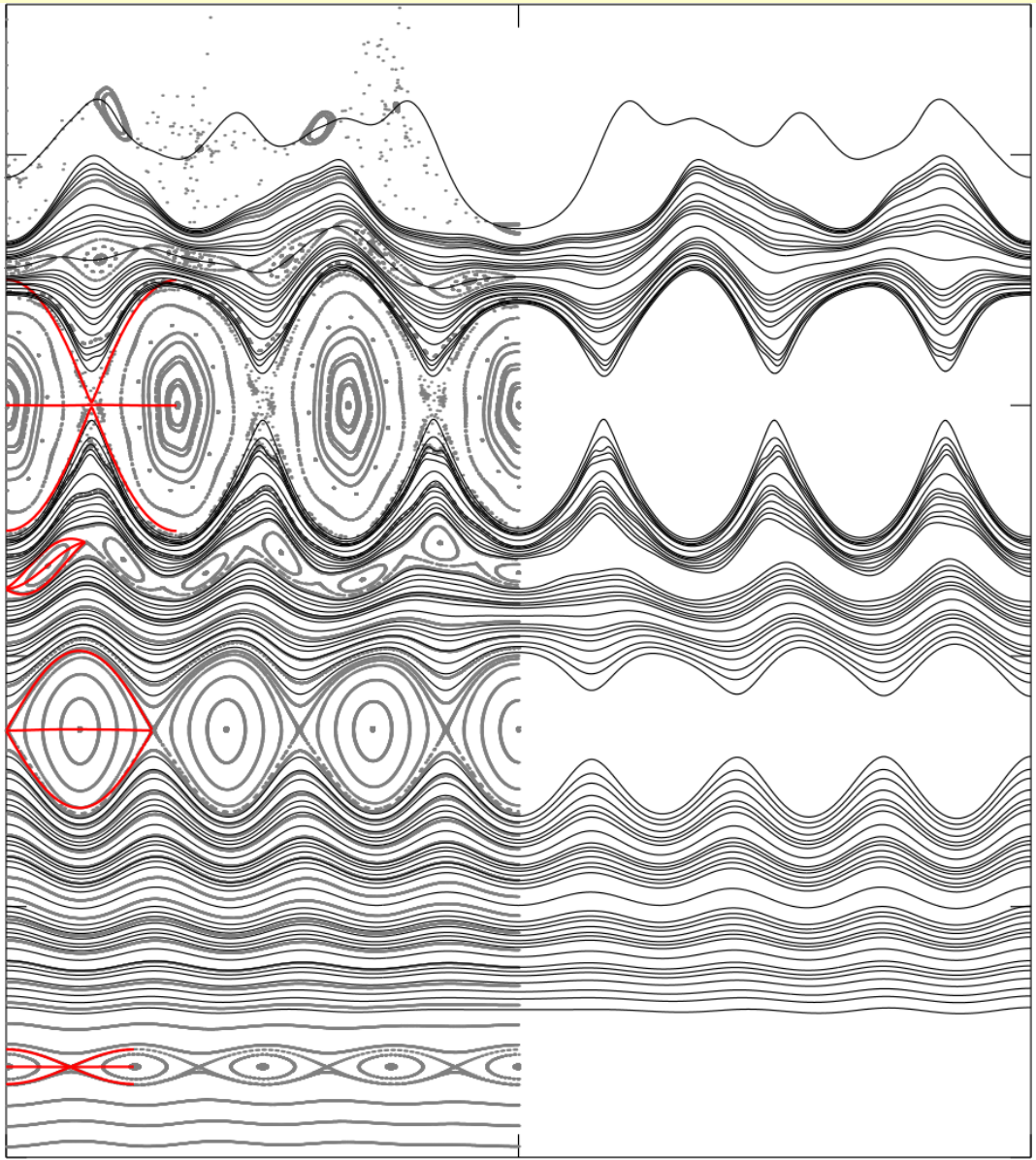

(10,6)

(30,19)

(20,13)

(30,20)

(10,7)

97 ghost surfaces

Poincaré plot.

Assuming no source in islands,
$T \approx T(\rho)$,
$p \approx p(\rho)$.

Numerical Solution to anisotropic transport

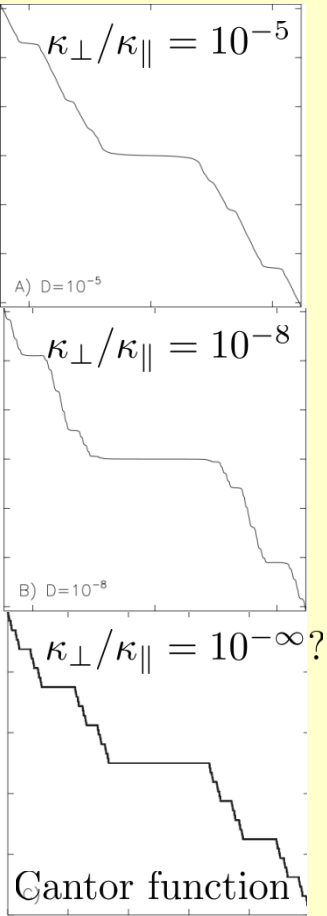

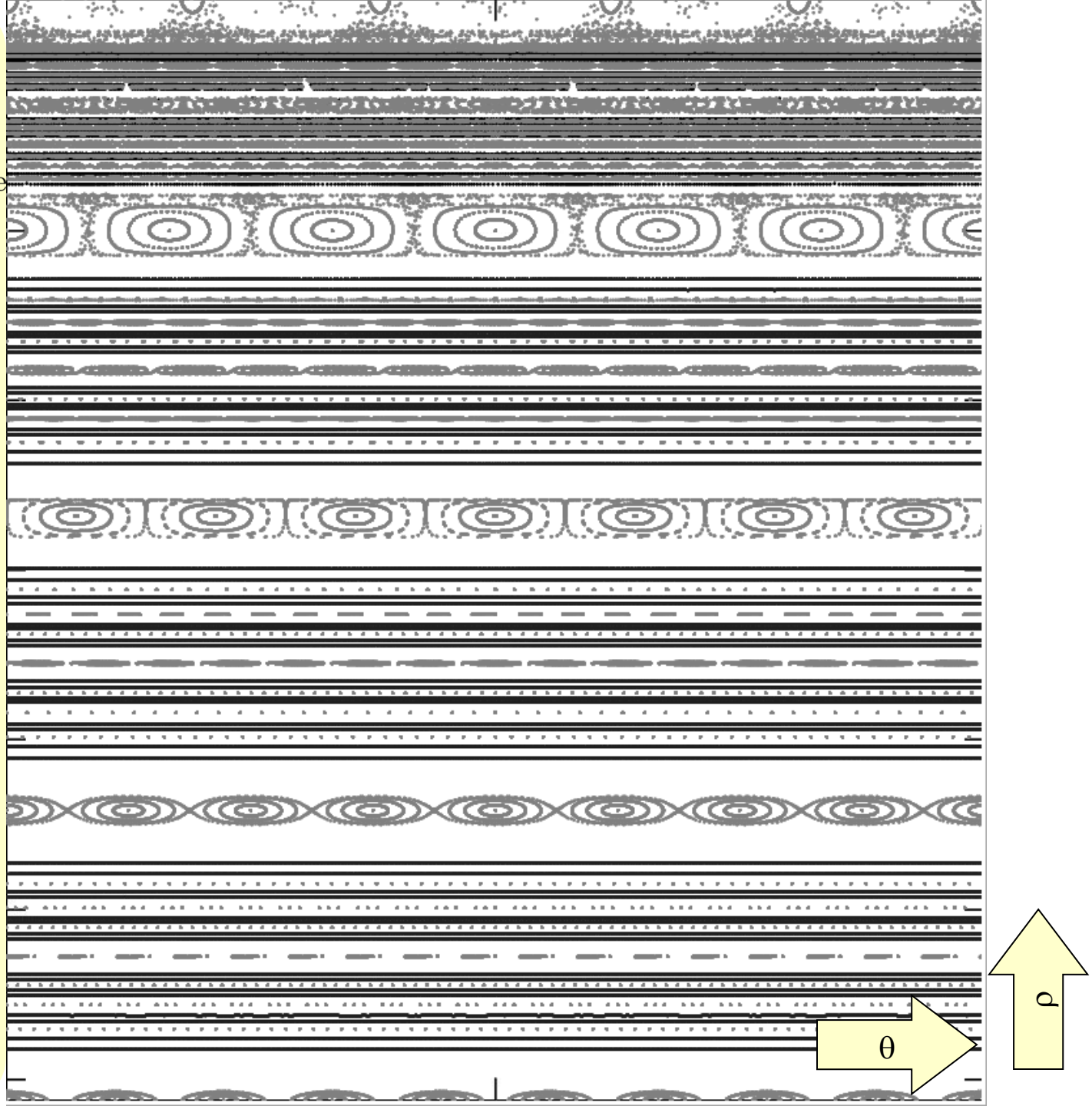

$\left(\frac{10}{5}\right)$

$\left(\frac{20}{11}\right)$

$\left(\frac{10}{6}\right)$

$\left(\frac{10}{7}\right)$

$\left(\frac{10}{8}\right)$

$\left(\frac{10}{9}\right)$

Poincaré plot.

Coordinates constructed by interpolation between QFM surfaces;

flux surfaces are straight.

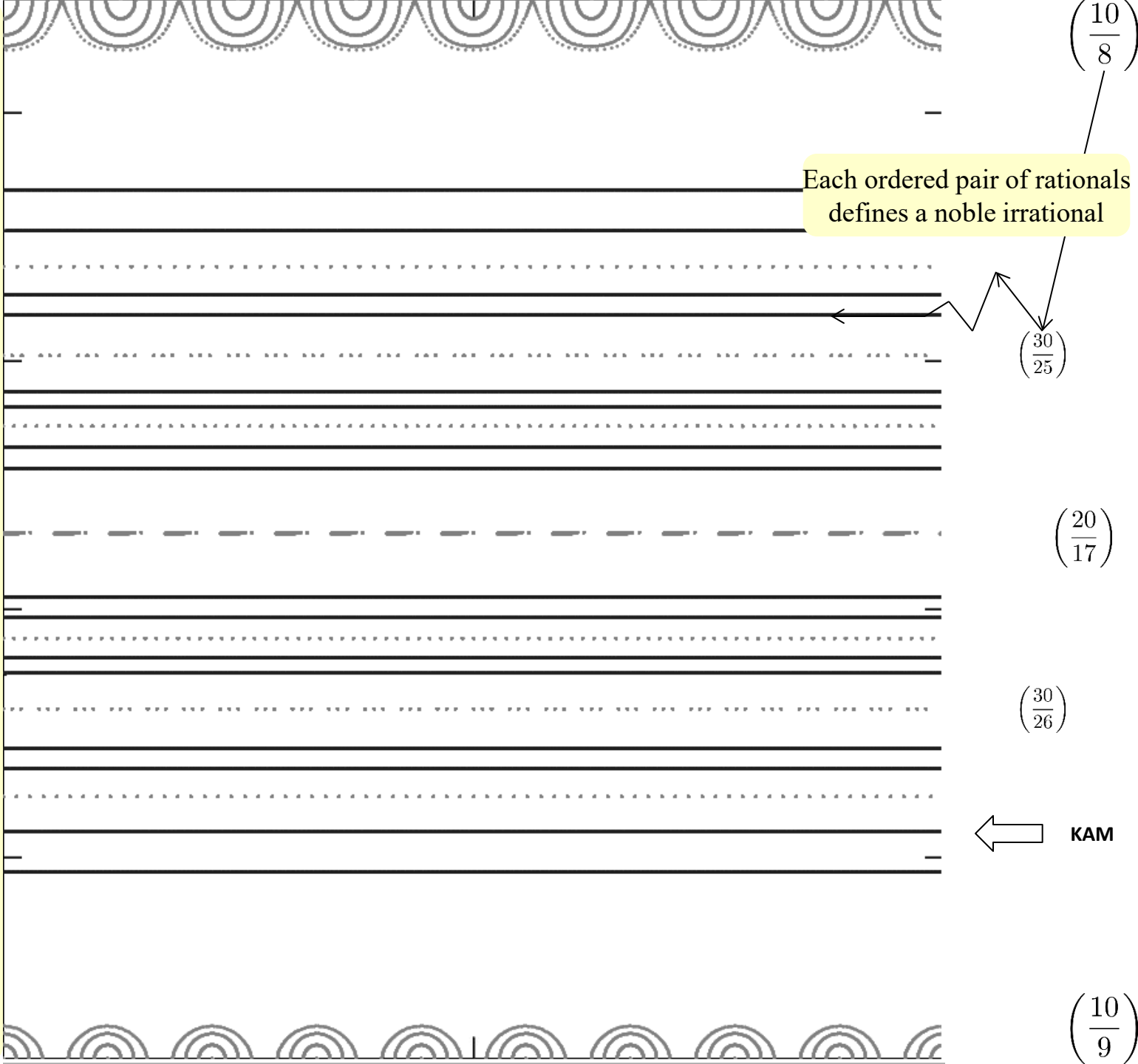

Poincaré plot.

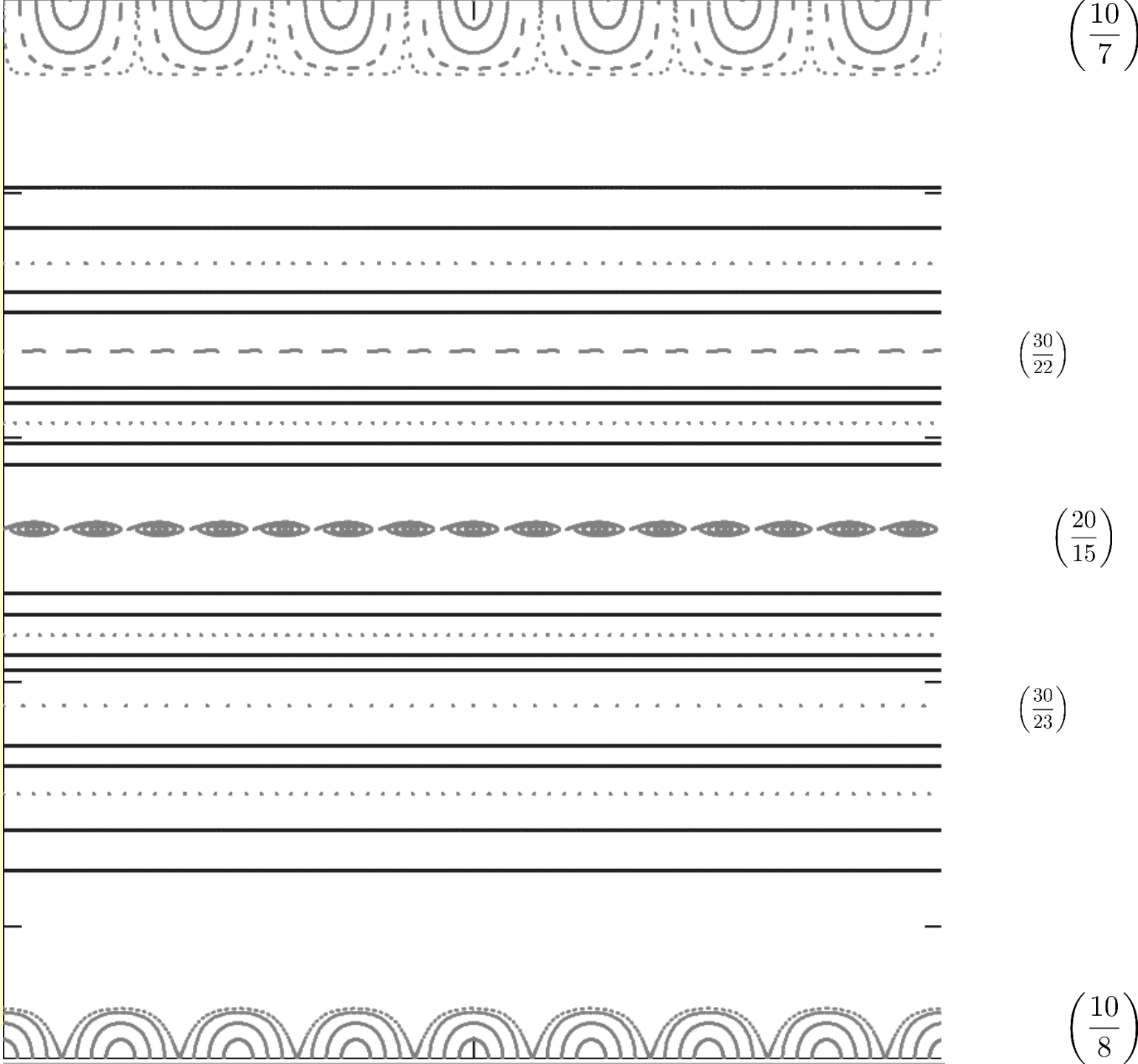

Poincaré plot.

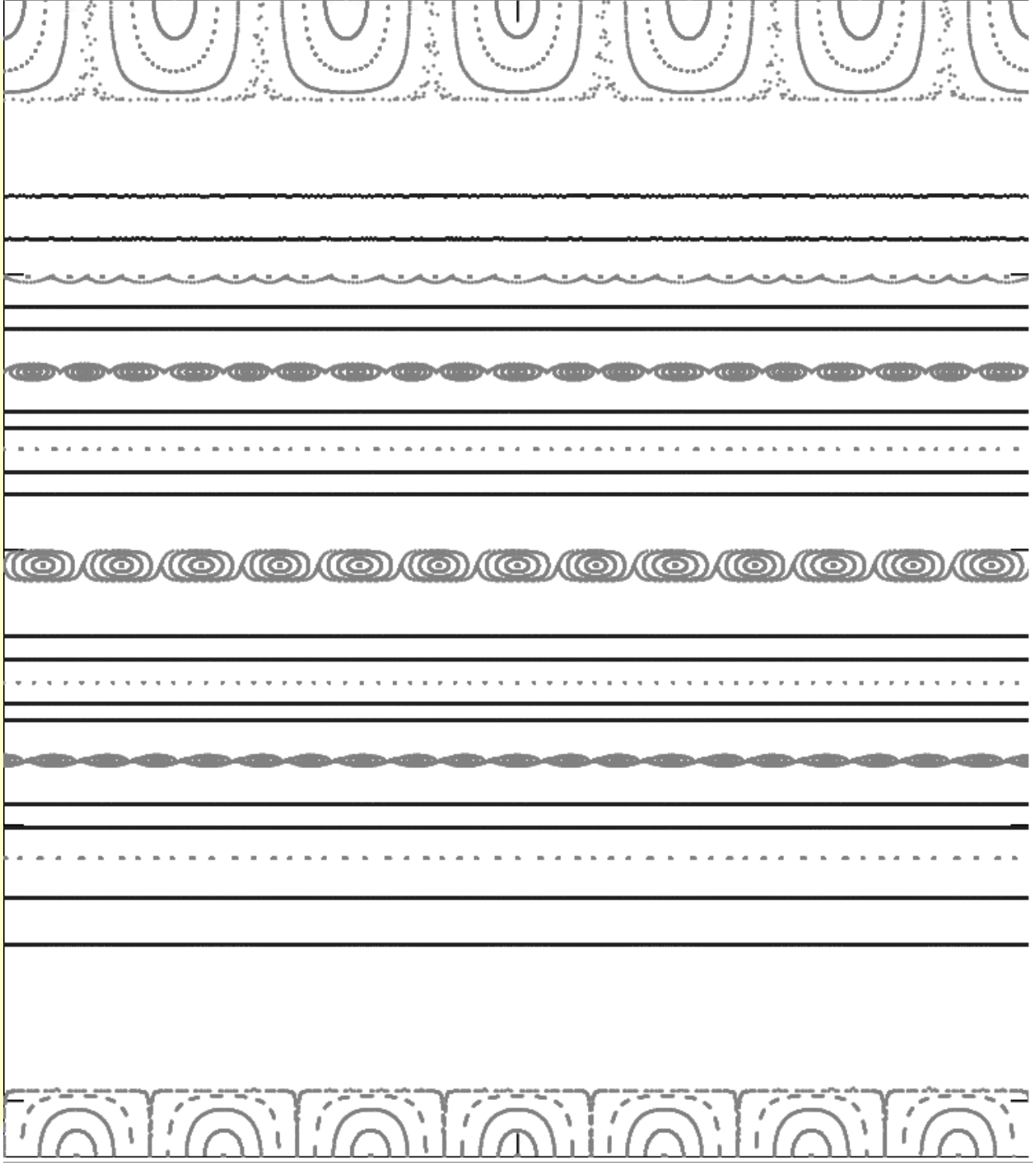

Islands become square.

Poincaré plot.

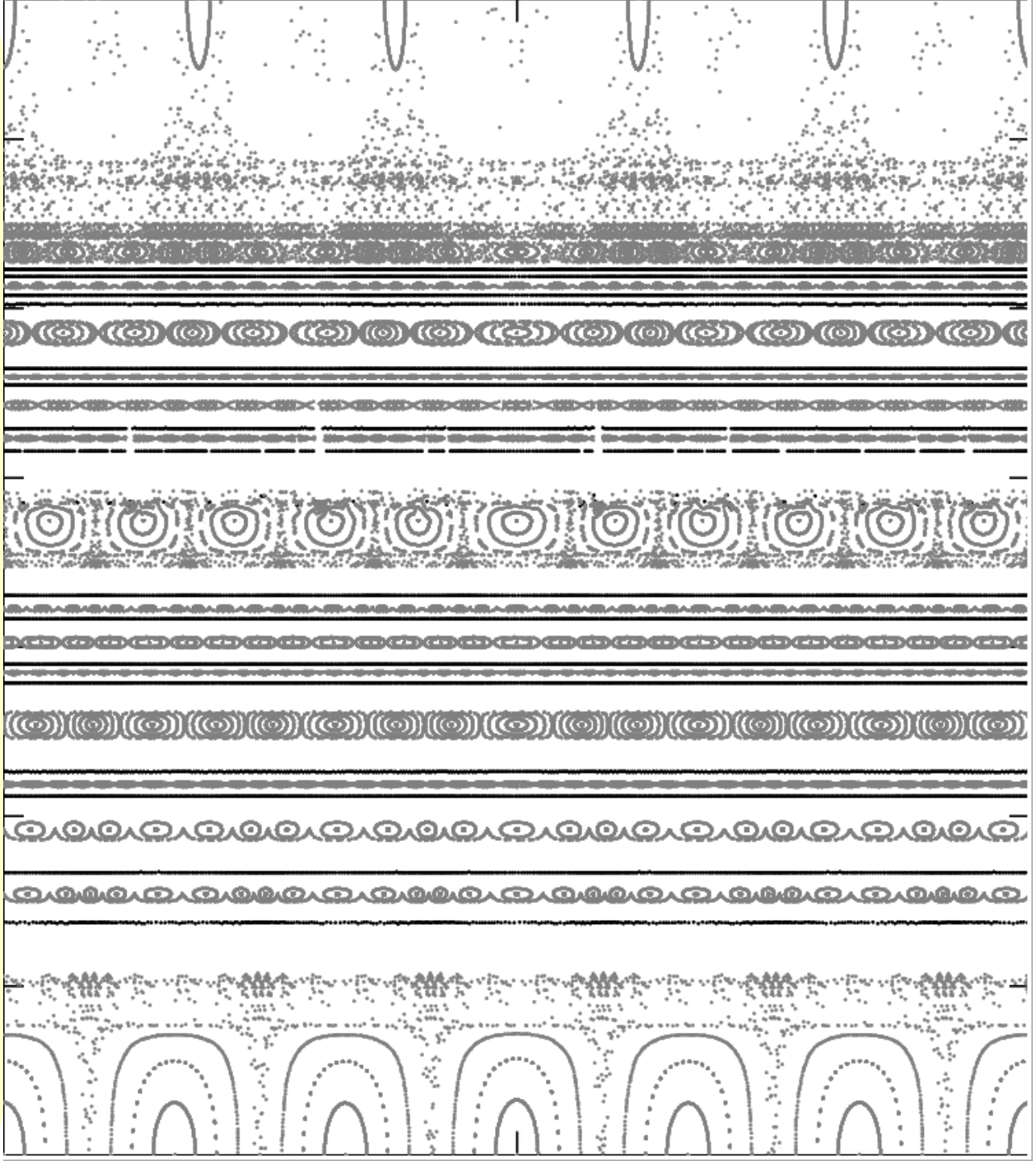

Poincaré plot.

Edge of confinement region is not a single, sharp barrier;

but instead a hierarchy of

i. islands,
ii. KAM, and
iii. cantori.

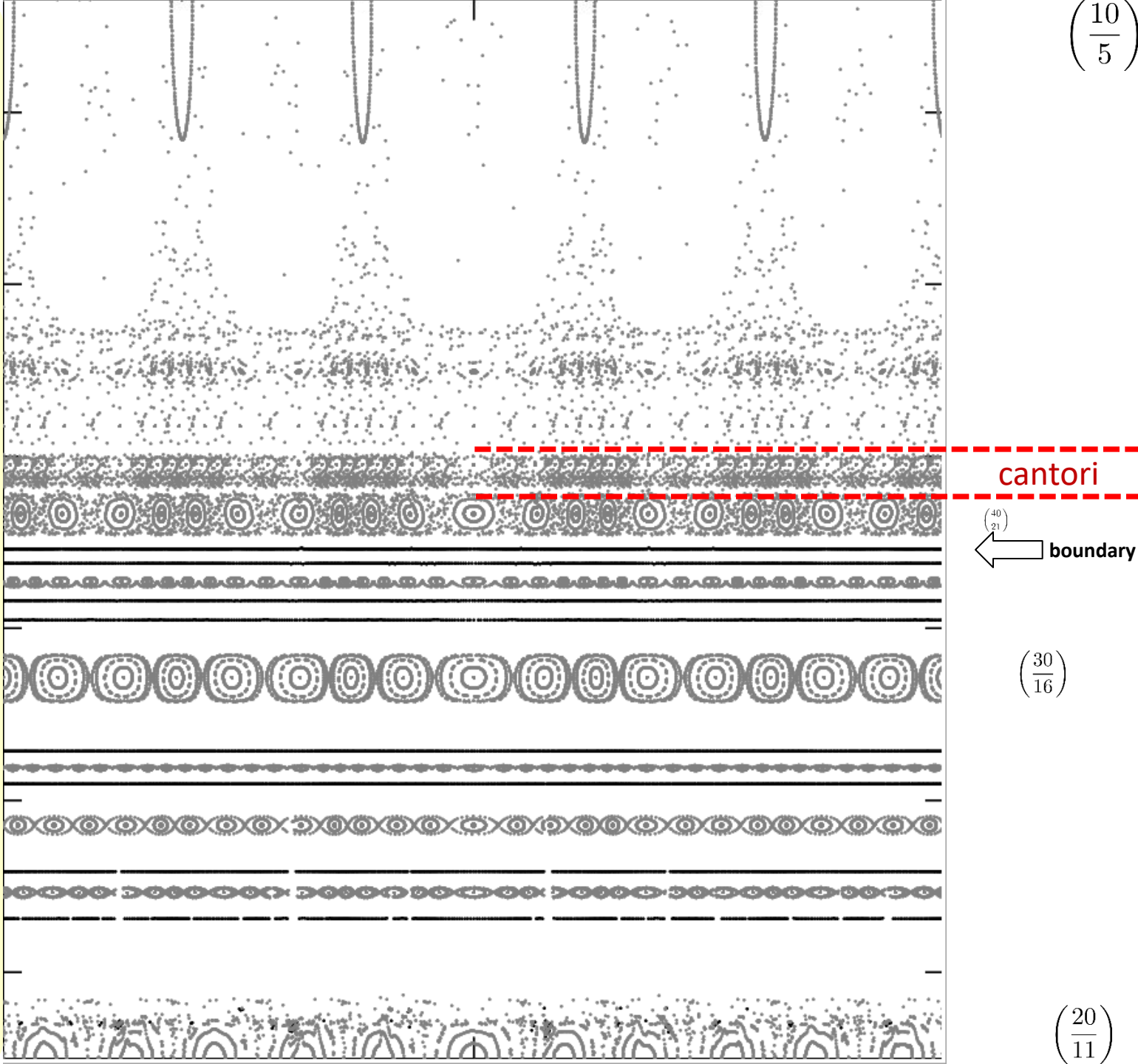

Anisotropic Heat Transport

Consider heat transport:
rapid transport along the magnetic field,
slow transport across the magnetic field.

1. Imagine that transport along $\mathbf{B}$ is unrestricted
   e.g. parallel random walk with long steps $\approx$ collisional mean free path.

2. Transport across the magnetic field is very small:
   e.g. perpendicular random walk with short steps $\approx$ Larmor radius.

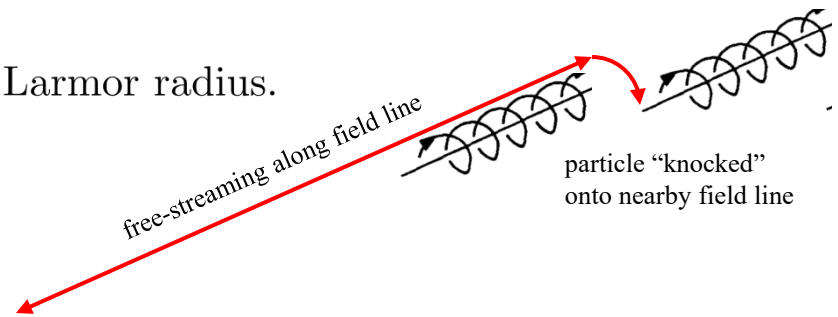

3. Simplest transport model: anisotropic diffusion,

$$\boxed{\frac{\partial T}{\partial t} = \nabla \cdot \left(\kappa_{\parallel} \nabla_{\parallel} T + \kappa_{\perp} \nabla_{\perp} T\right) + S}, \quad \kappa_{\perp}/\kappa_{\parallel} \sim 10^{-10},\ T \equiv \text{temperature};\ S \equiv \text{source};$$

4. Extreme anisotropy presents numerical challenges
   $\rightarrow$ extreme numerical resolution is required.

5. For computational efficiency, introduce "local fieldline coordinates".

   Construct coordinates (α, β, ζ) s.t. $\mathbf{B} \equiv \nabla\alpha \times \nabla\beta$, by local fieldline tracing;

   Parallel and perpendicular directions are treated separately, $\mathbf{B} \cdot \nabla \equiv B^{\phi}\partial_{\zeta}$, which reduces numerical diffusion.

   The parallel diffusion operator becomes $\nabla_{\parallel}^2 T = B^{\phi} \dfrac{\partial}{\partial \zeta}\left(\dfrac{B^{\phi}}{B^2}\dfrac{\partial T}{\partial \zeta}\right)$.

Numerical solution of anisotropic heat transport exploits field-aligned coordinates

1. Heat flux $\nabla \cdot \mathbf{q} = 0$, where $\mathbf{q} = \mathbf{b} \cdot \nabla T \, \kappa_{\|} \, \mathbf{b} + \kappa_{\perp} \nabla_{\perp} T$, strongly anisotropic.
2. Parallel relaxation employs field-alligned coordinates, $\mathbf{B} = \nabla\alpha \times \nabla\beta$, so parallel derivative is accurate, $\nabla_{\|}^2 T = \dfrac{\partial^2 T}{\partial \eta^2} = B^{\zeta} \dfrac{\partial}{\partial \zeta} \left(\dfrac{B^{\zeta}}{B^2} \dfrac{\partial T}{\partial \zeta} \right)$.
3. Perpendicular relaxation simply $\nabla_{\perp}^2 T = \dfrac{\partial^2 T}{\partial \alpha^2} + \dfrac{\partial^2 T}{\partial \beta^2}$.
4. Sparse linear system solved iteratively on numerical grid, resolution $= 2^{12} \times 2^{12}$.

Poincaré plot

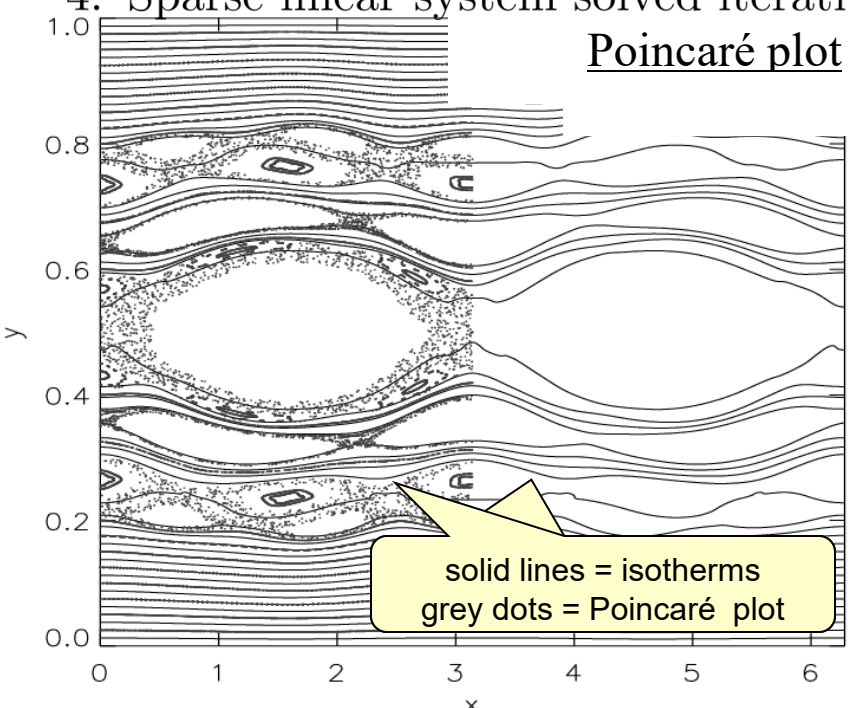

Error vs grid resolution

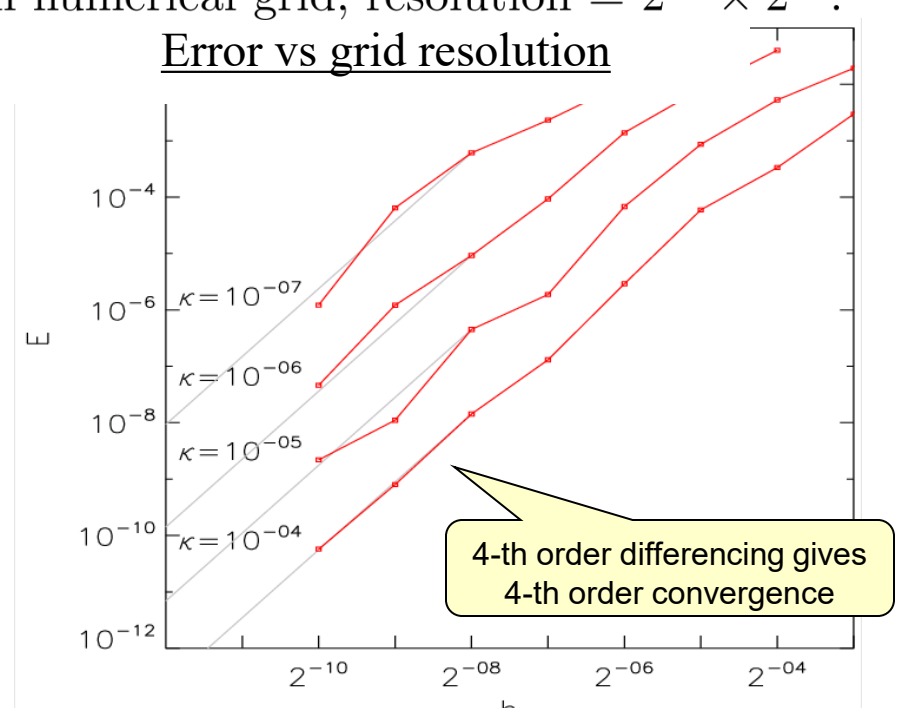

Isotherms of the steady state solution to the anisotropic diffusion coincide with ghost surfaces; analytic, 1-D solution is possible.

1. The temperature is constant on KAM surfaces, cantori, and ghost-surfaces, i.e. $T = T(\rho)$.

2. From $T = T(\rho, \theta, \zeta)$ to $T = T(\rho)$ allows

$$\boxed{\frac{dT}{d\rho} \propto \frac{1}{\kappa_{\parallel}\varphi_2 + \kappa_{\perp} G}},$$

where

$$\varphi_2 \equiv \underbrace{\int B_n^2 \, d\mathbf{s}}_{\text{quadratic flux}}, \quad \text{and}$$

$$G \equiv \underbrace{\int \nabla\rho \cdot \nabla\rho \, d\mathbf{s}}_{\text{metric}}.$$

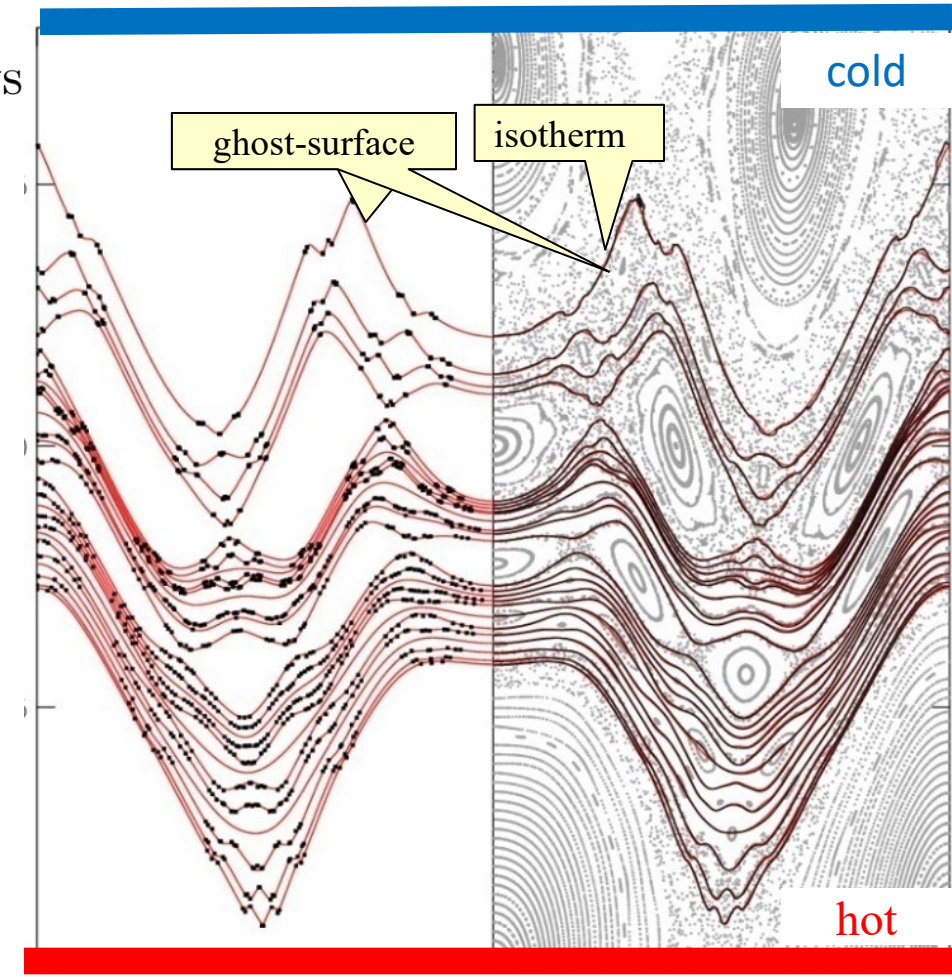

Chaotic coordinates simplify temperature profile to a smoothed Diophantine (fractal) staircase

1. From $0 = \frac{\partial}{\partial s}\int_V \nabla\cdot\mathbf{q}\,dv = \frac{\partial}{\partial s}\int_{\partial\mathcal{V}} \mathbf{q}\cdot\mathbf{n}\,d\sigma$, assume $T = T(s)$ to derive $T' = \frac{const.}{\kappa_\parallel \Omega + \kappa_\perp G}$ for quadratic-flux $\Omega = \int g^{ss}\frac{B_n^2}{B^2}\,d\sigma$, and metric $G = \int g^{ss} d\sigma$, $g^{ss} = \nabla s\cdot\nabla s$.
2. In the "ideal limit", $\kappa_\perp \to 0$, $T'(s) \to \infty$ on irrational KAM surfaces (where $\Omega = 0$).
3. Non-zero $\kappa_\perp$ ensures $T(s)$ is smooth; $T'(s)$ peaks on minimal Ω surfaces = noble cantori.

Temperature Profile

$$\frac{\kappa_\parallel}{\kappa_\perp} = 10^{10}$$

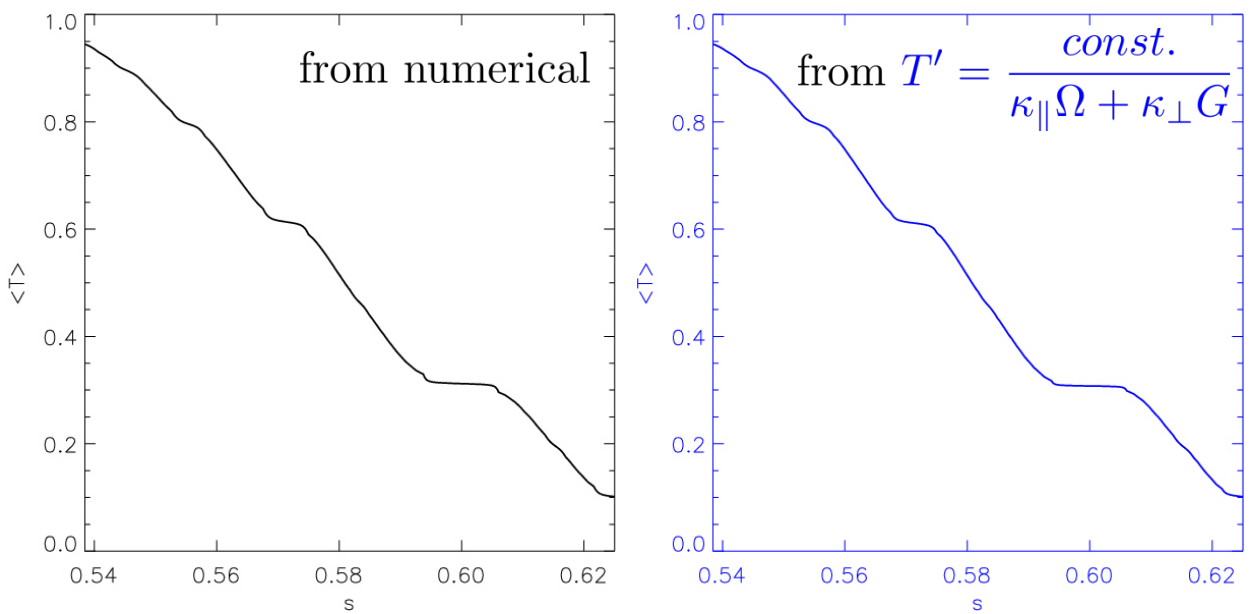

Comments

1. The "geometry" of integrable dynamics can be incorporated into the coordinates

   action-angle coordinates.

2. The geometry and "fractal-ness" of non-integrable dynamics can be incorporated into the coordinates

   "chaotic coordinates".

3. In the limit that all the regular dynamics is incorporated, the coordinates become pathological.

4. In practice, some "smoothing" diffusion-type effects

Unstable manifold

The magnetic axis is a "stable" fixed point (usually), and the X-point is "unstable". Consider the eigenvalues of tangent mapping:

1. Consider following a fieldline nearby a fixed point, $\mathbf{x}_0 + \delta\mathbf{x}$, around many toroidal periods:

$$\underbrace{\nabla\mathbf{M} \cdot \ldots \nabla\mathbf{M}}_{\text{tangent mapping}} \cdot \delta\mathbf{x} = (\nabla\mathbf{M})^n \cdot \delta\mathbf{x} = (\nabla\mathbf{M})^n \cdot \underbrace{(a\,\mathbf{v}_u + b\,\mathbf{v}_s)}_{\text{eigenvectors}} = a\,\lambda_u^n\,\mathbf{v}_u + b\,\lambda_s^n\,\mathbf{v}_s$$

2. The determinant, $|\nabla\mathbf{M}| = 1$ at fixed points (because $\nabla \cdot \mathbf{B} = 0$), so the eigenvalues are either:

i. complex congugates, $\lambda = \alpha + \beta\, i$, $\lambda = \alpha - \beta\, i$, and the fixed point is stable:
nearby trajectories <u>rotate</u>: rotational-transform on axis, $\tan \iota = \beta/\alpha$.

ii. real reciprocals, $\lambda_u > 1$ and $\lambda_s = 1/\lambda_u$, and the fixed point is unstable:
nearby trajectories <u>diverge</u>: $\lambda_u^n \to \infty$ as $n \to \infty$, $\lambda_s^n \to 0$ as $n \to \infty$;
$\mathbf{v}_u$ indicates unstable direction, $\mathbf{v}_s$ indicates stable direction.

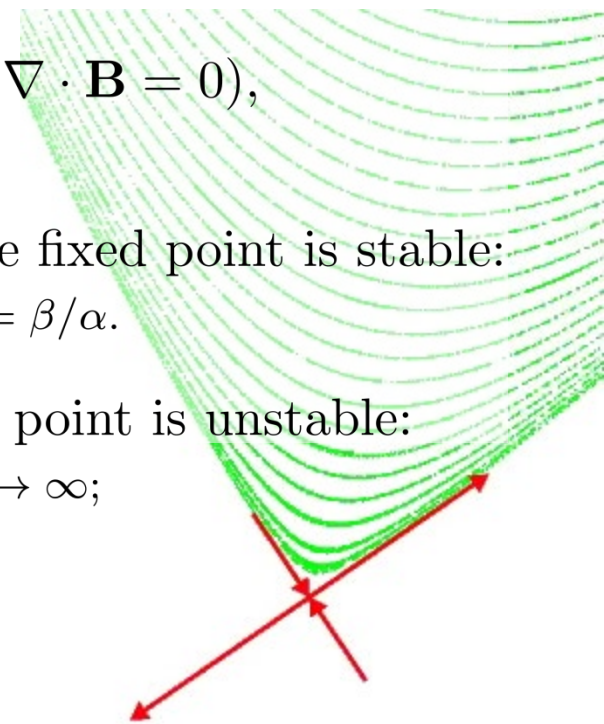

The stable/unstable direction forwards in ϕ is the unstable/stable direction backwards in ϕ.

1. $\mathbf{x} \in$ " stable manifold " if $\mathbf{M}^n(\mathbf{x}) \to \mathbf{x}_0$ as $n \to +\infty$.

   all magnetic fieldlines with "starting point" $\mathbf{x} = \mathbf{x}_0 + d\,\mathbf{v}_s$, where $d \in [\epsilon\lambda_s, \epsilon]$, and follow *backwards* in ϕ.

2. $\mathbf{x} \in$ "unstable manifold" if $\mathbf{M}^n(\mathbf{x}) \to \mathbf{x}_0$ as $n \to -\infty$.

   all magnetic fieldlines with "starting point" $\mathbf{x} = \mathbf{x}_0 + d\,\mathbf{v}_u$, where $d \in [\epsilon/\lambda_u, \epsilon]$, and follow *forwards* in ϕ.

3. For the integrable case, the unstable manifold leads into the stable manifold, and there is a "clean" separatrix.

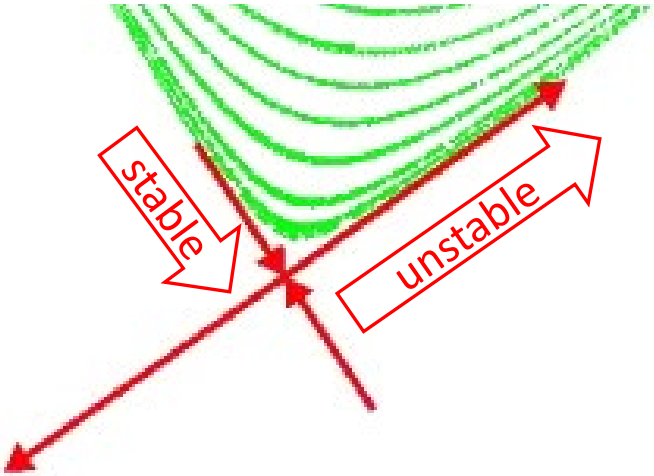

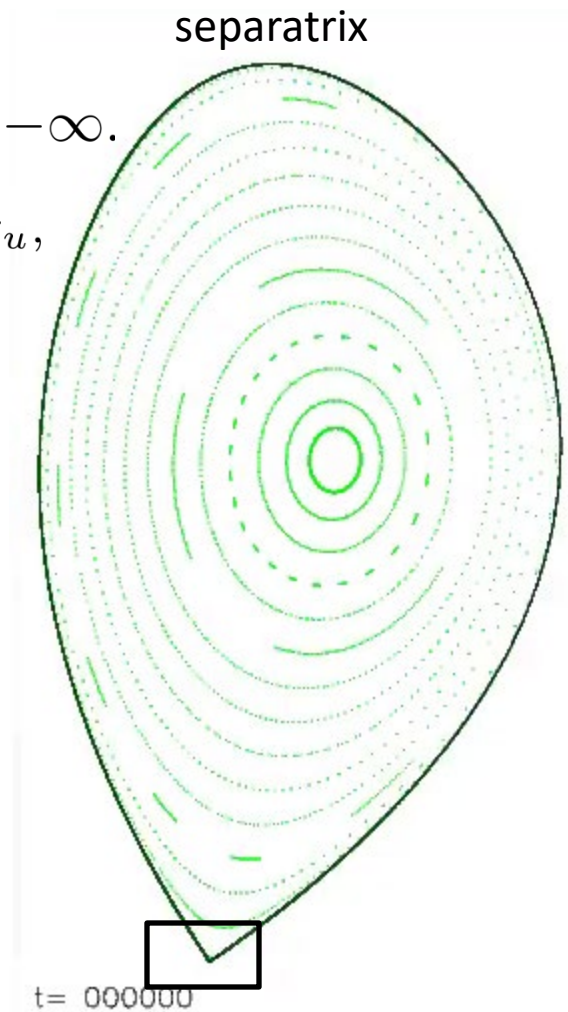

For perturbed magnetic fields, the separatrix splits. A "partial" separatrix can be constructed.

1. "Homoclinic" points, $\mathbf{x}_h \equiv$ intersection of stable, unstable manifolds, $\mathbf{M}^n(\mathbf{x}_h) \to \mathbf{x}_0$ as $n \to \pm\infty$.

2. To locate $\mathbf{x}_h$, find (d_u, d_s),
$$\mathbf{M}^{+i}(\mathbf{x}_0 + d_u\,\mathbf{v}_u) = \mathbf{M}^{-j}(\mathbf{x}_0 + d_s\,\mathbf{v}_s),$$
if $\mathbf{x}_h$ is homoclinic,
so is $\mathbf{M}^k(\mathbf{x}_h), \forall k$.

3. Partial separatrix
= "smooth" part of unstable manifold
+ "smooth" part of stable manifold.

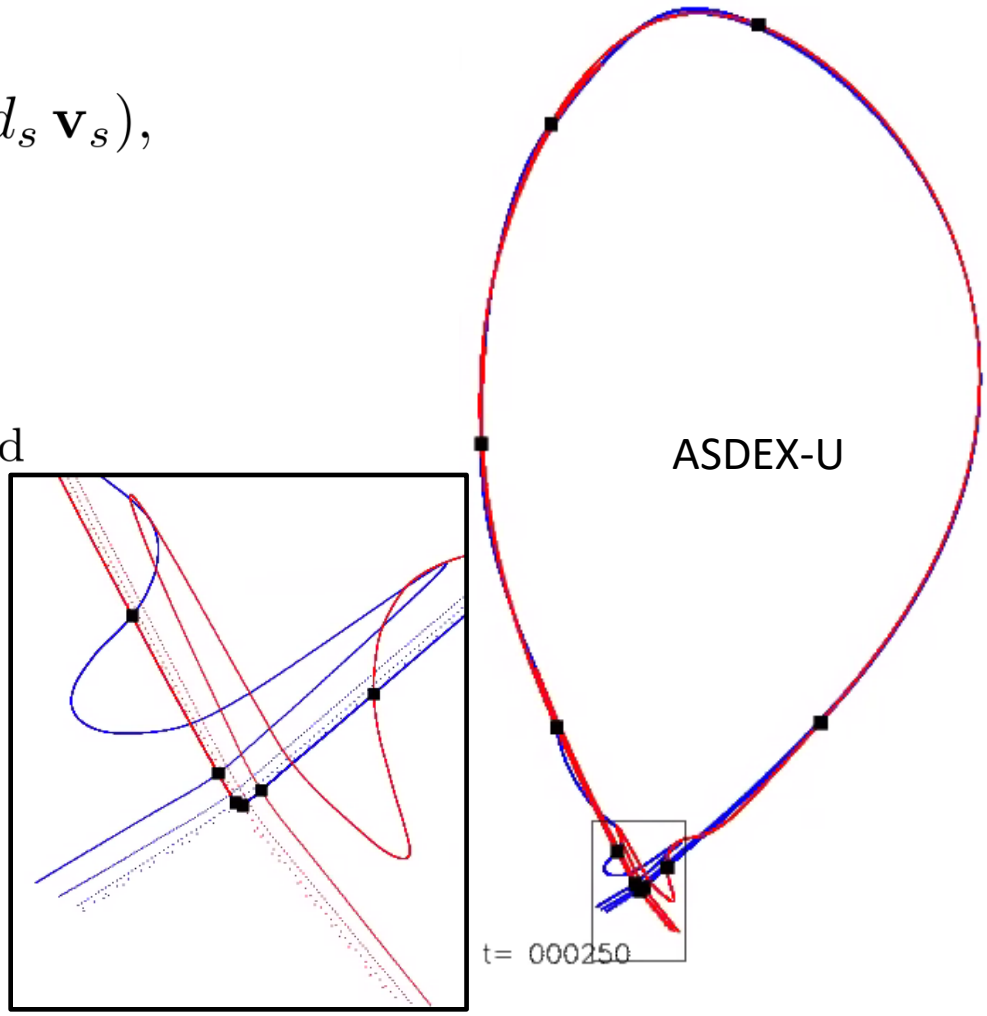

Anisotropic heat transport + unstable manifold = ?
What is the temperature in the “chaotic edge” ?

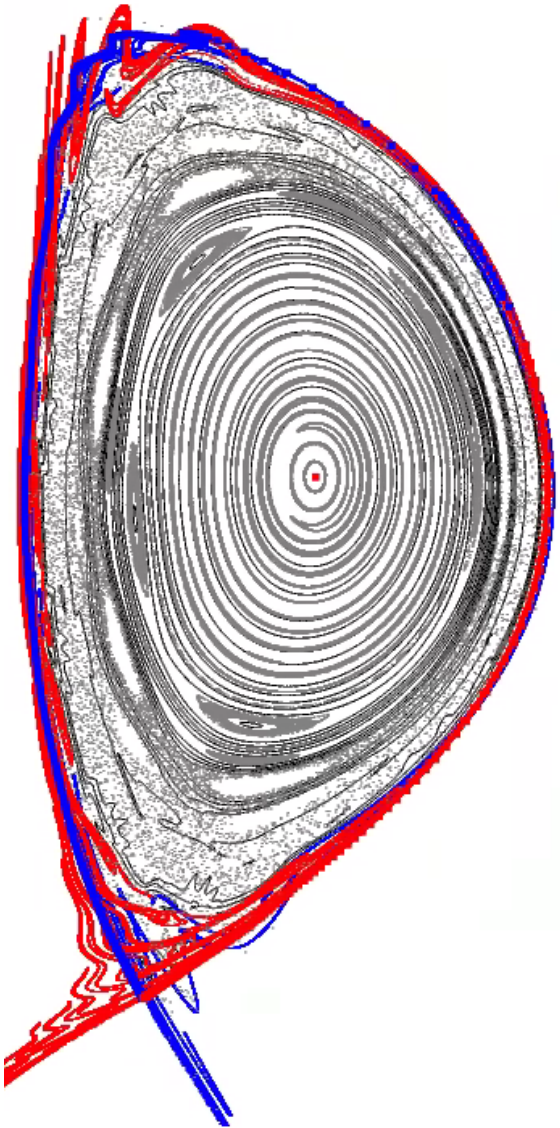

Anisotropic heat transport + unstable manifold = ?

What is the temperature in the “chaotic edge” ?

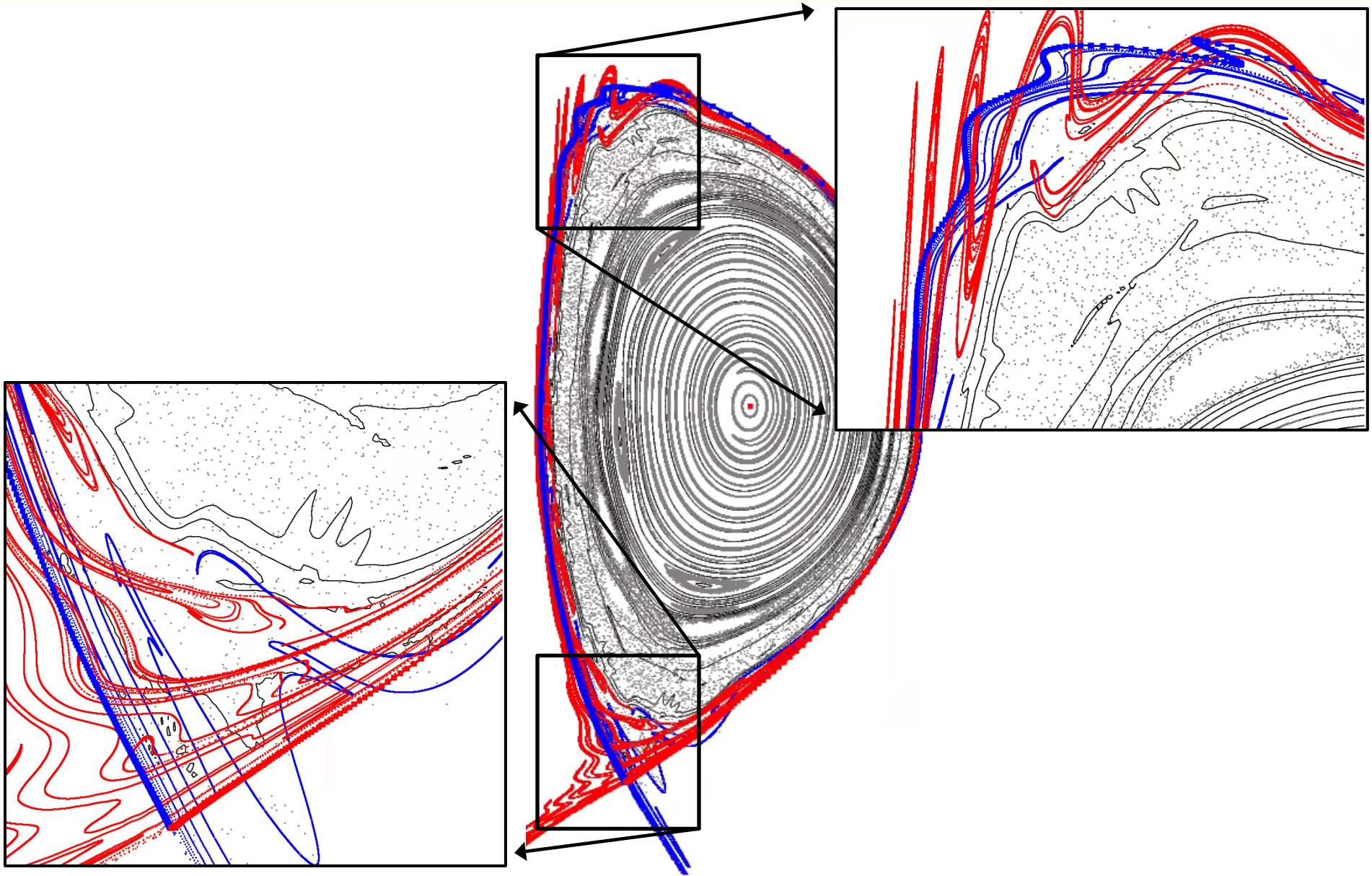

Practical construction

To illustrate, we examine the standard configuration of LHD

The initial coordinates are axisymmetric, circular cross section,

$R = 3.63 + \rho\, 0.9 \cos\vartheta$

$Z = \rho\, 0.9 \sin\vartheta$ which are not a good approximation to flux coordinates!

Poincaré plot in cylindrical coordinates

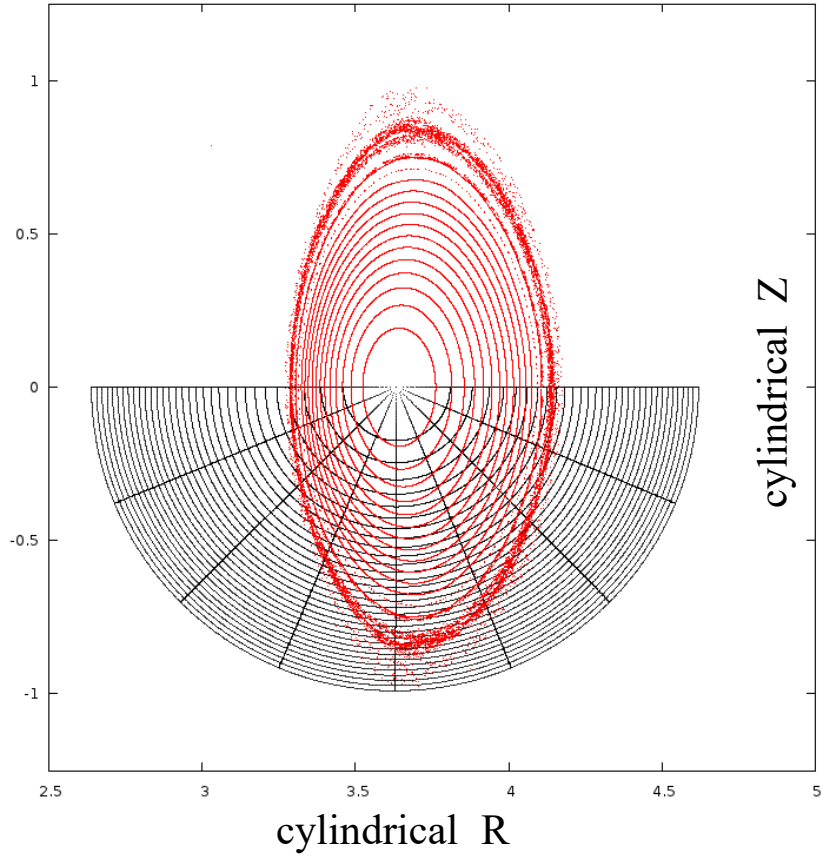

Poincaré plot in toroidal coordinates

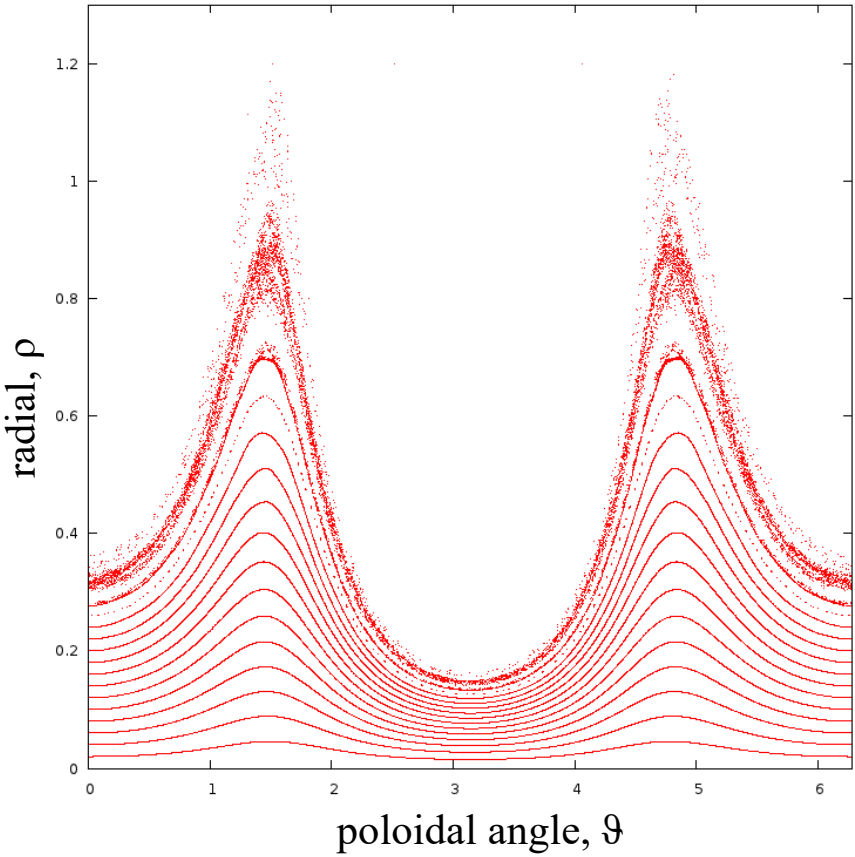

We construct coordinates that better approximate straight-field line flux coordinates,

by constructing a set of rational, almost-invariant surfaces, e.g. the (1,1), (1,2) surfaces

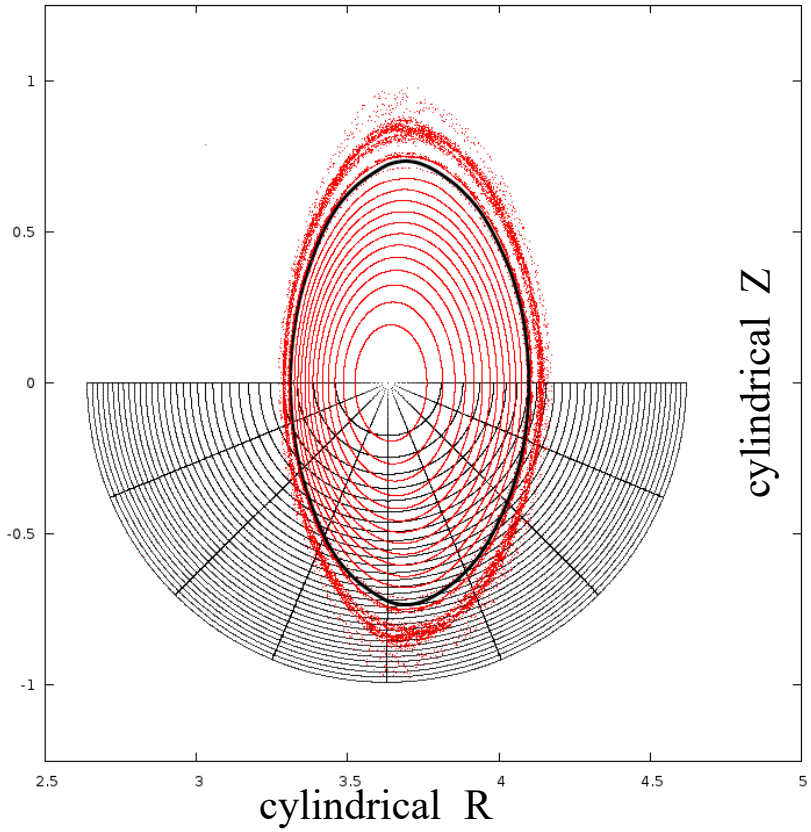

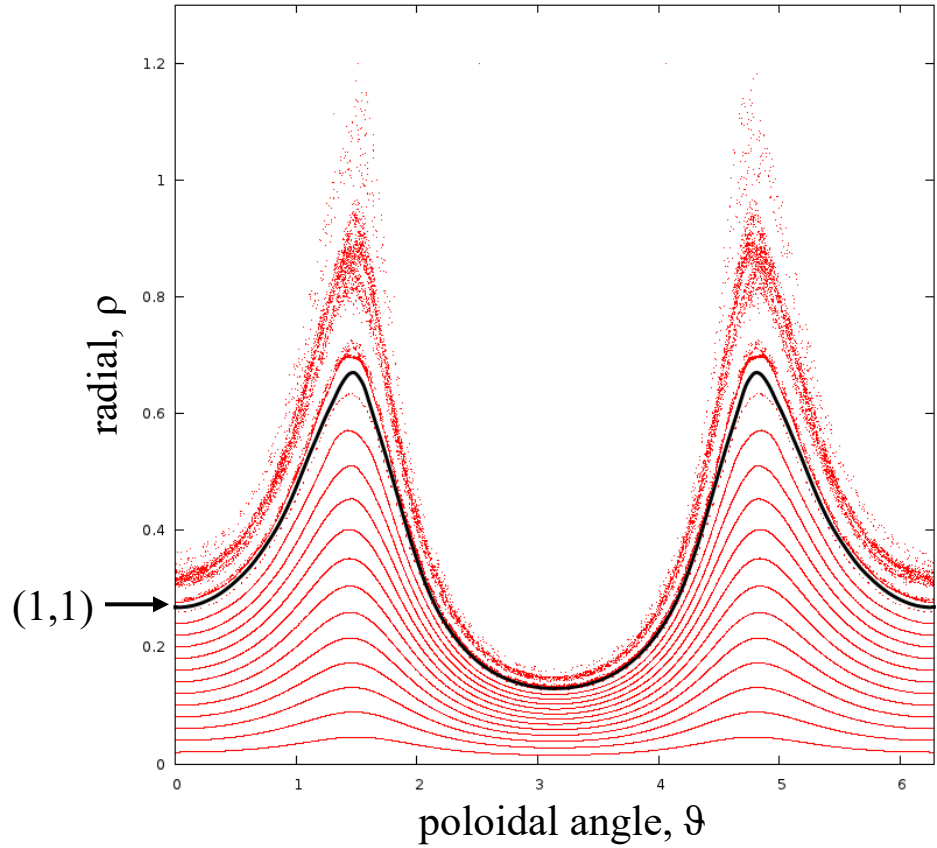

A Fourier representation of the (1,1) rational surface is constructed,

$R = R(\alpha,\zeta) = \sum R_{m,n} \cos(m\,\alpha - n\,\zeta)$

$Z = Z(\alpha,\zeta) = \sum Z_{m,n} \sin(m\,\alpha - n\,\zeta)$, where α is a straight field line angle

Updated coordinates:
the (1,1) surface is used as a coordinate surface.

The updated coordinates are a better approximation to straight-field line flux coordinates, and the flux surfaces are (almost) flat

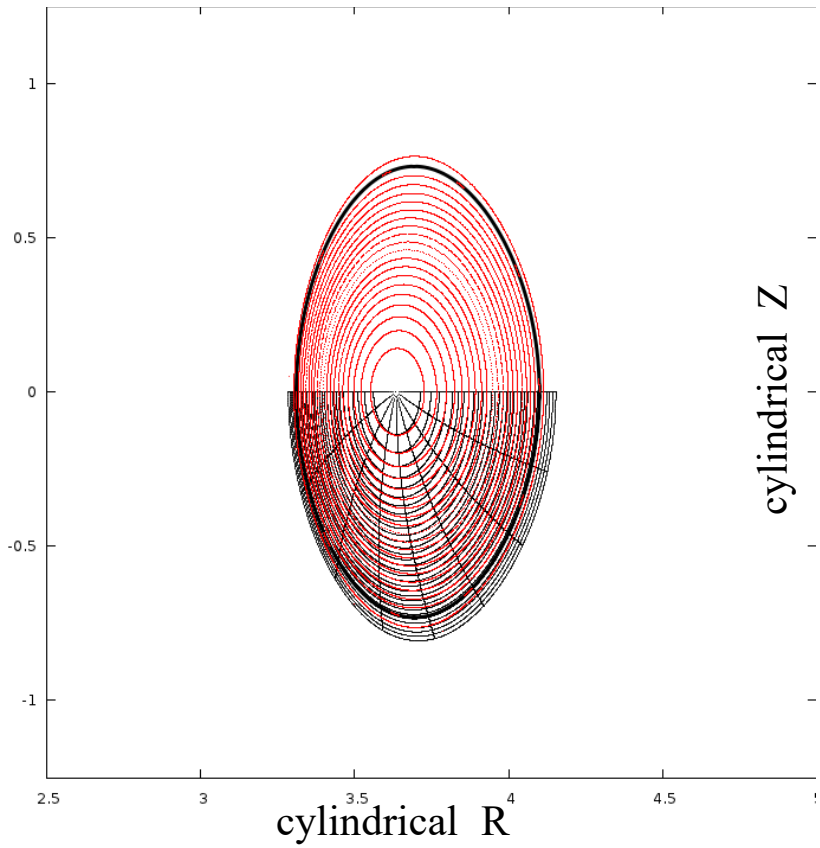

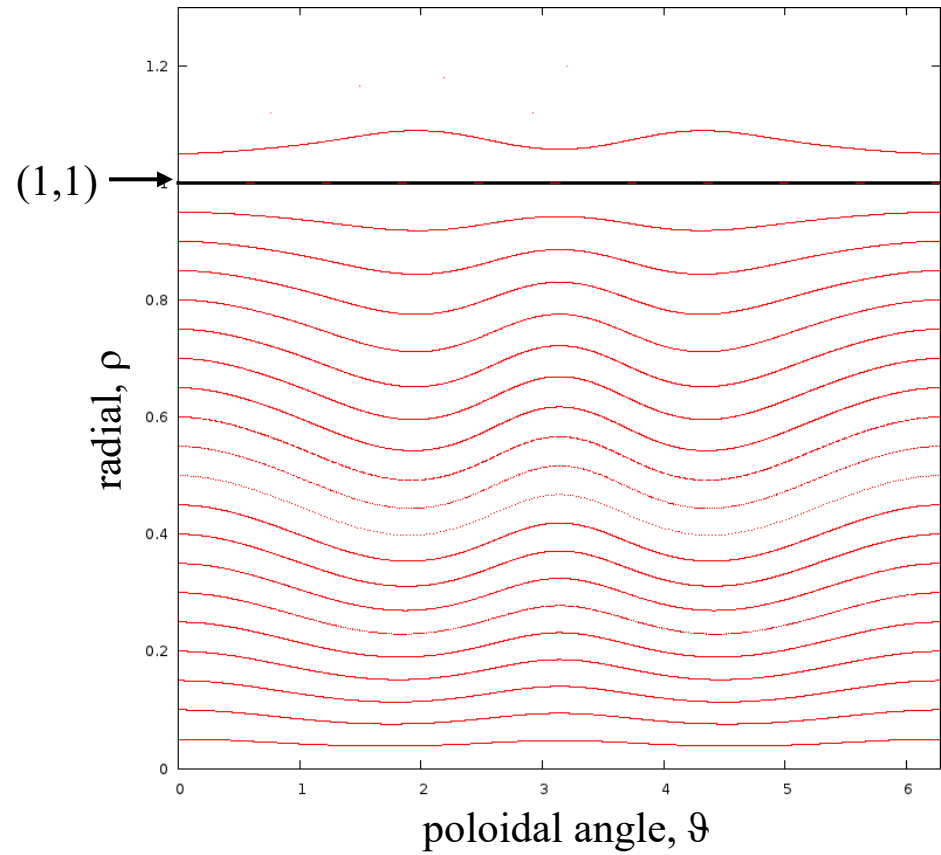

Now include the (1,2) rational surface

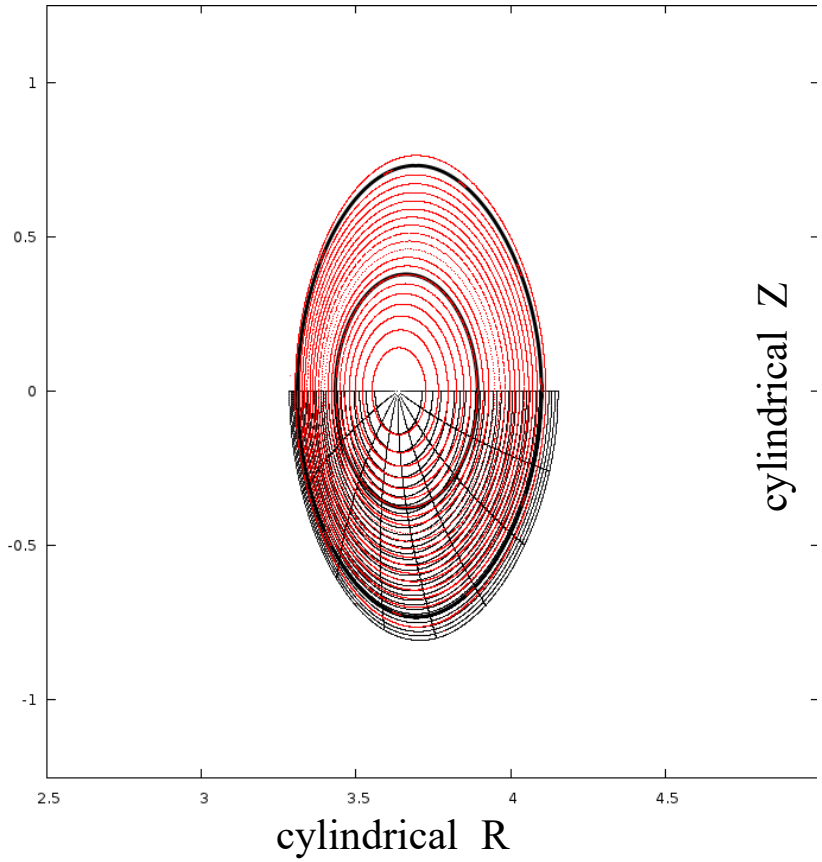

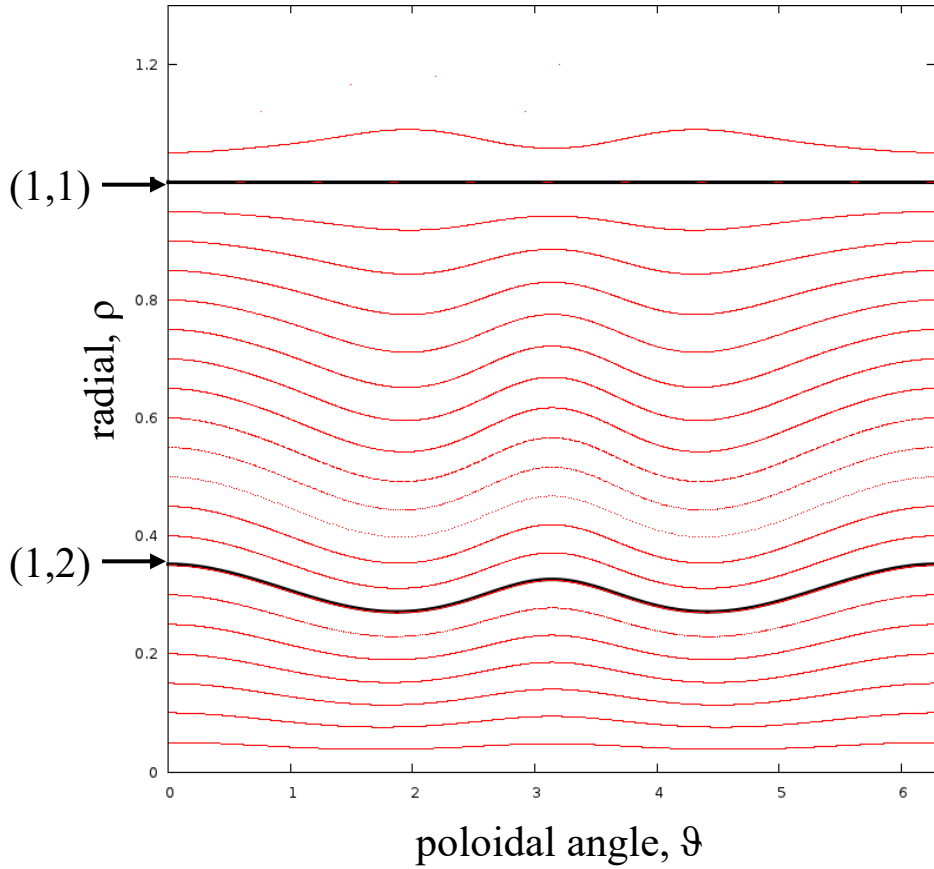

Updated coordinates:
the (1,1) surface is used as a coordinate surface
the (1,2) surface is used as a coordinate surface

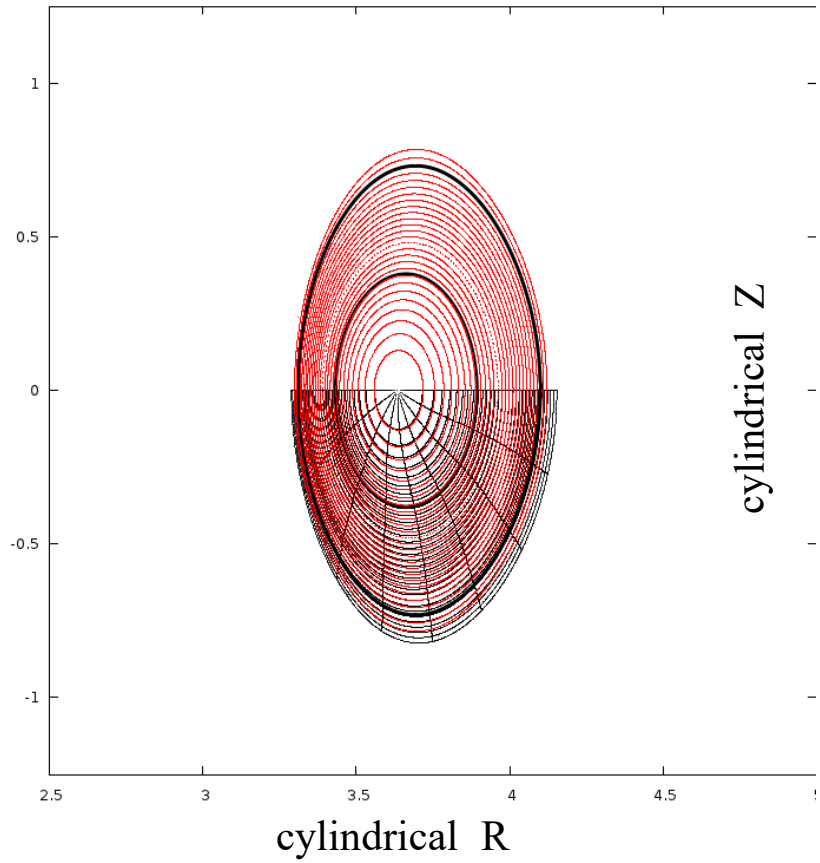

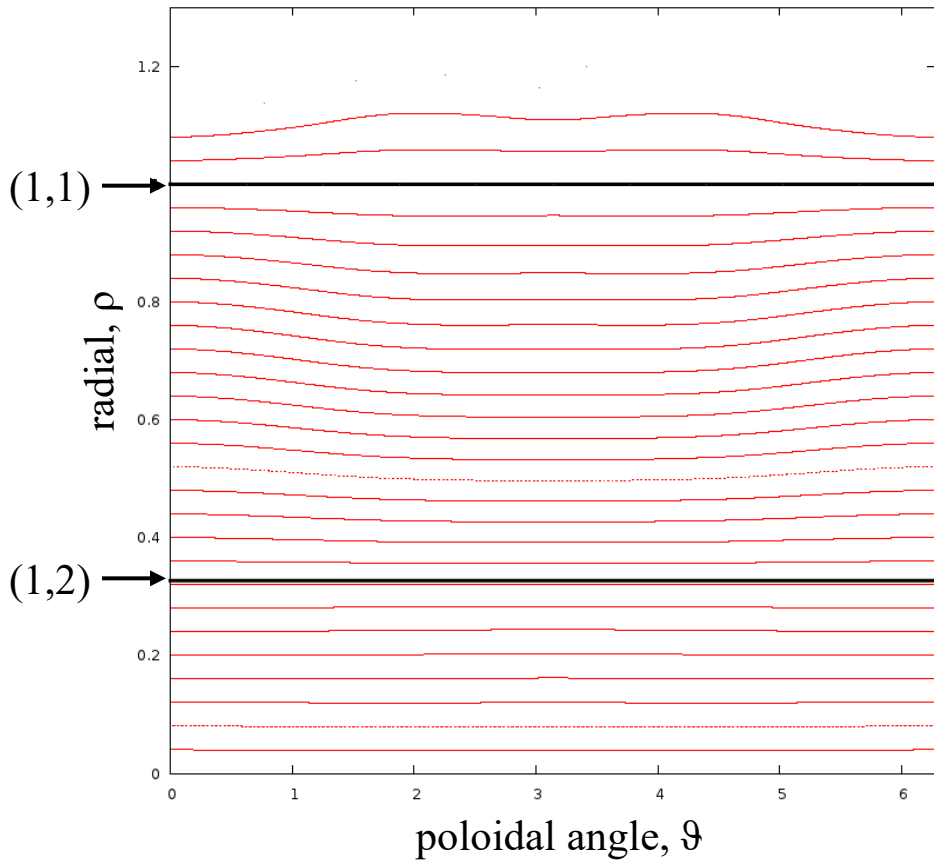

Now include the (2,3) rational surface

Note that the (1,1) and (1,2) surfaces have previously been constructed and are used as coordinate surfaces, and so these surfaces are flat.

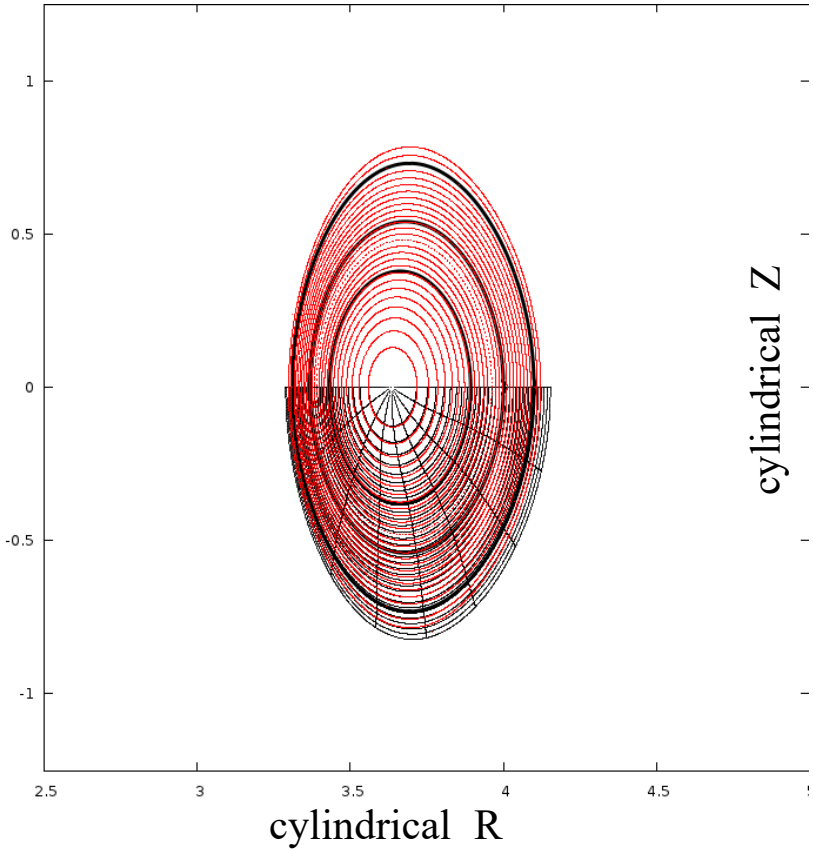

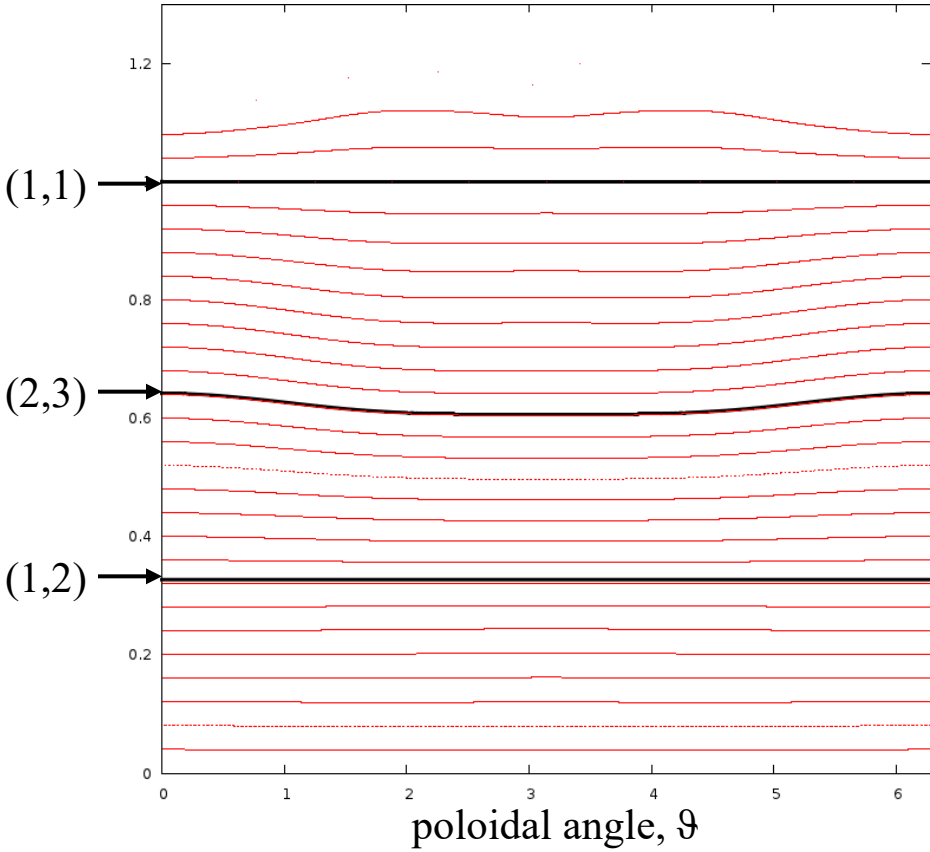

Updated Coordinates:

the (1,1), (2,3) & (1,2) surfaces are used as coordinate surfaces

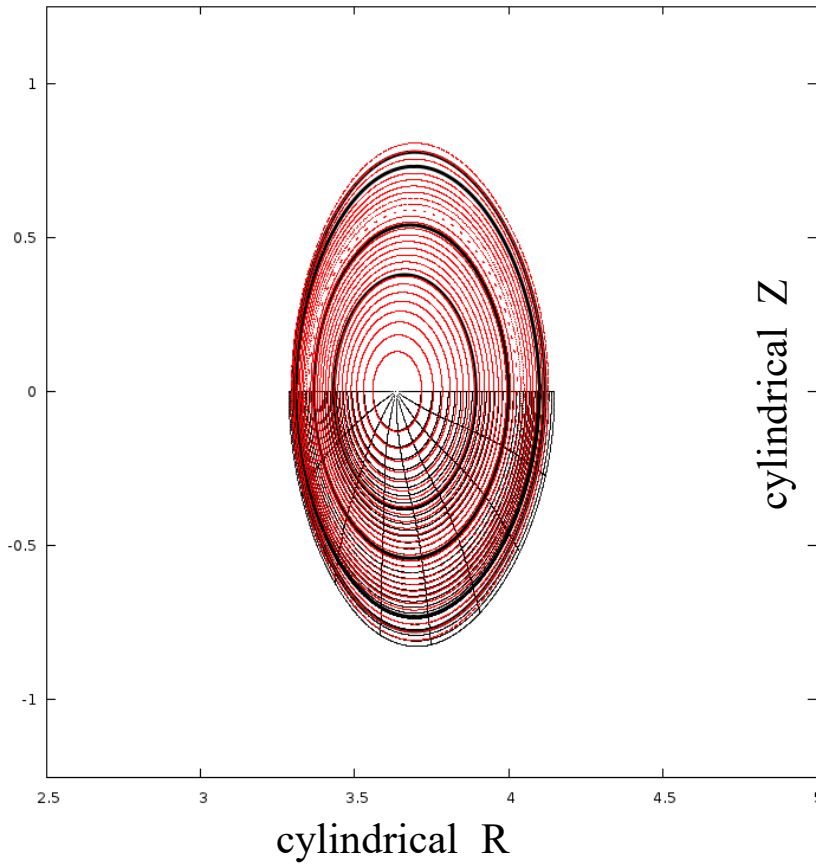

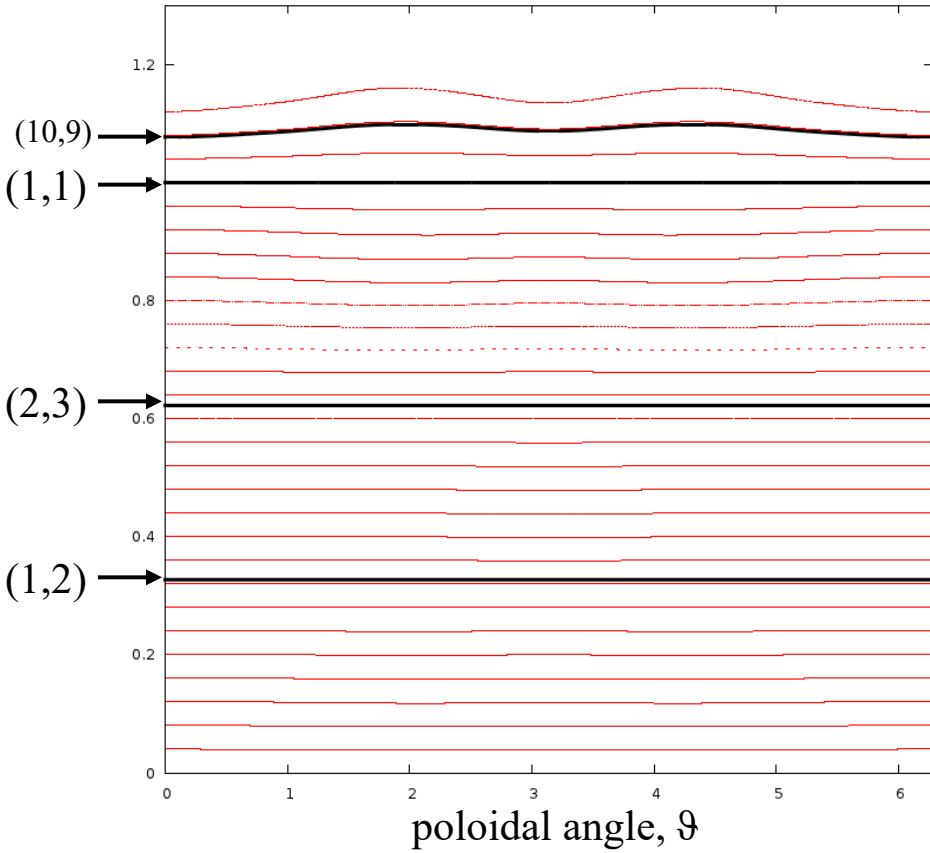

New Coordinates, the (10,9) surface is used as the coordinate boundary
the (1,1) surface is used as a coordinate surface
the (2,3) surface is used as a coordinate surface
the (1,2) surface is used as a coordinate surface

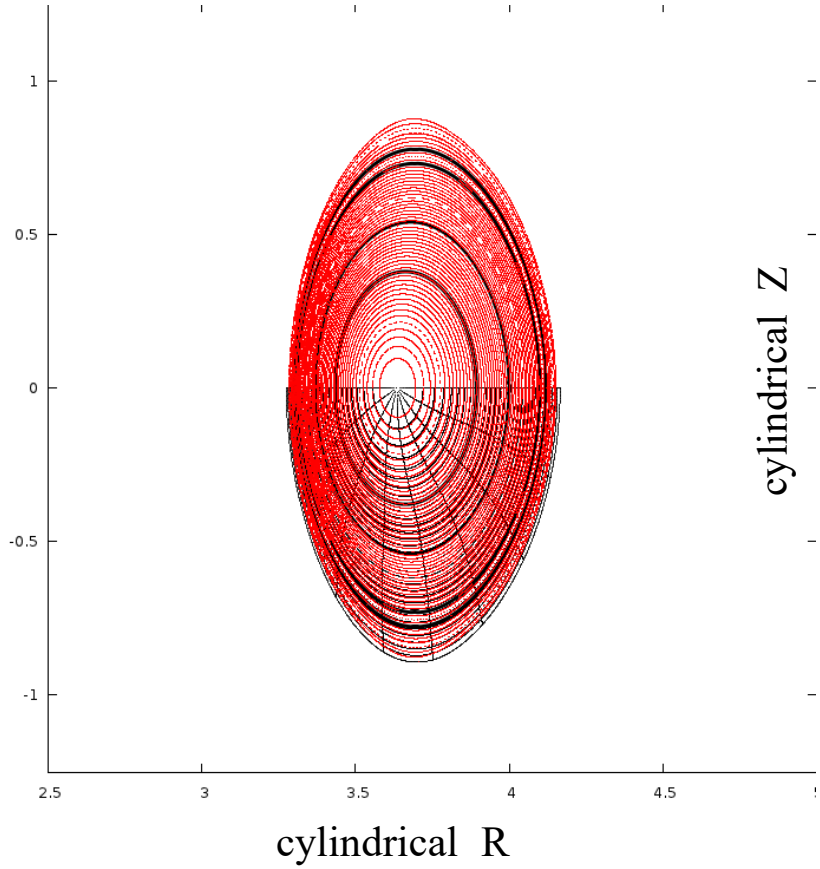

Poincare plot

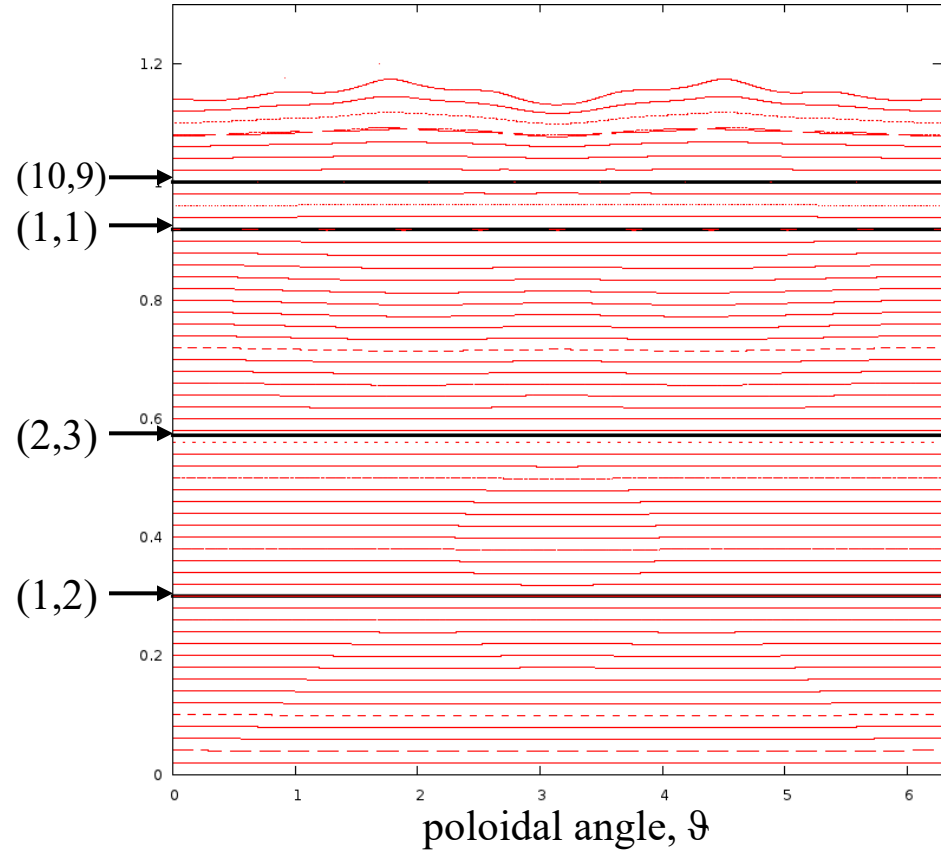

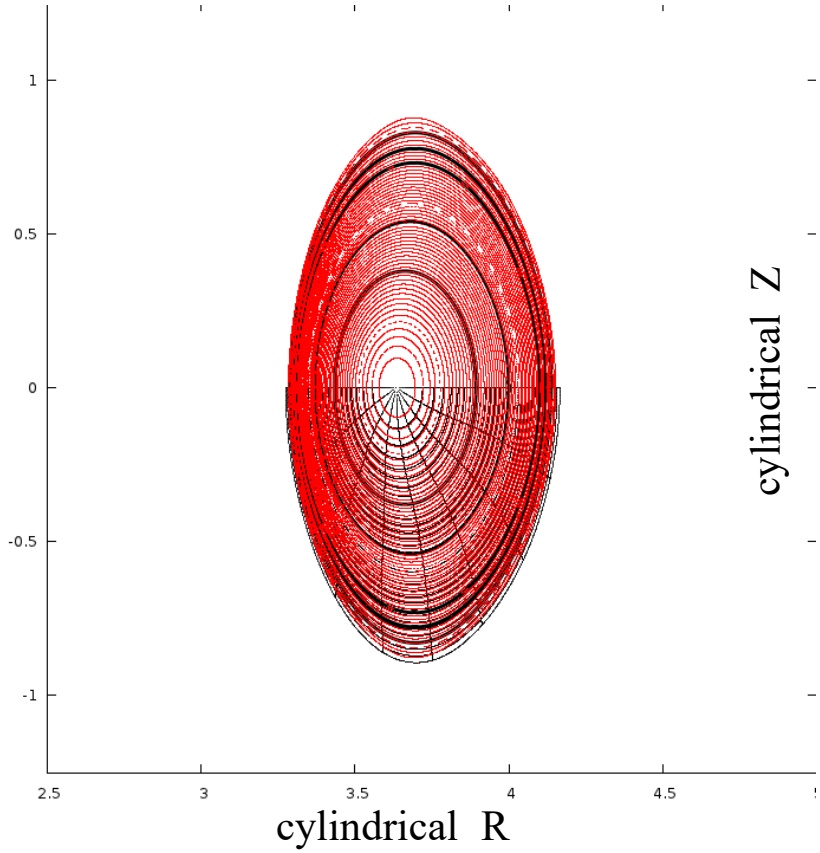
1
0.5
0
-0.5
-1
2.5
3
3.5
4
4.5
cylindrical Z
cylindrical R

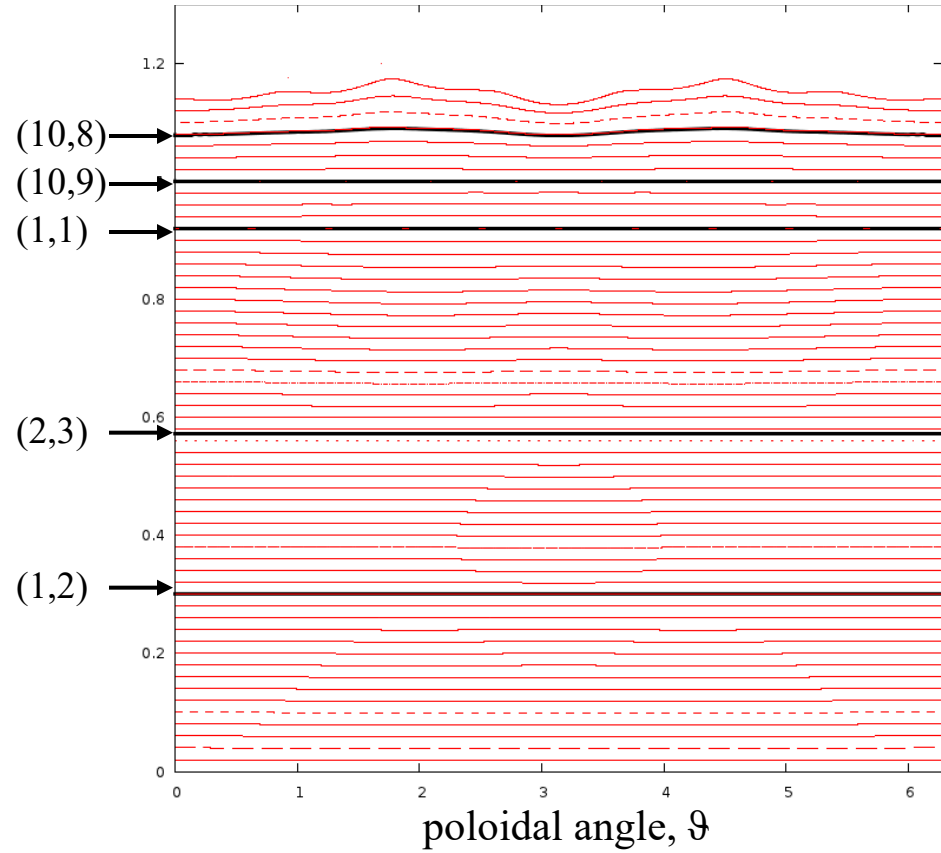
(10,8)
(10,9)
(1,1)
(2,3)
(1,2)
1.2
0.8
0.6
0.4
0.2
0
0
1
2
3
4
5
6
poloidal angle, ϑ

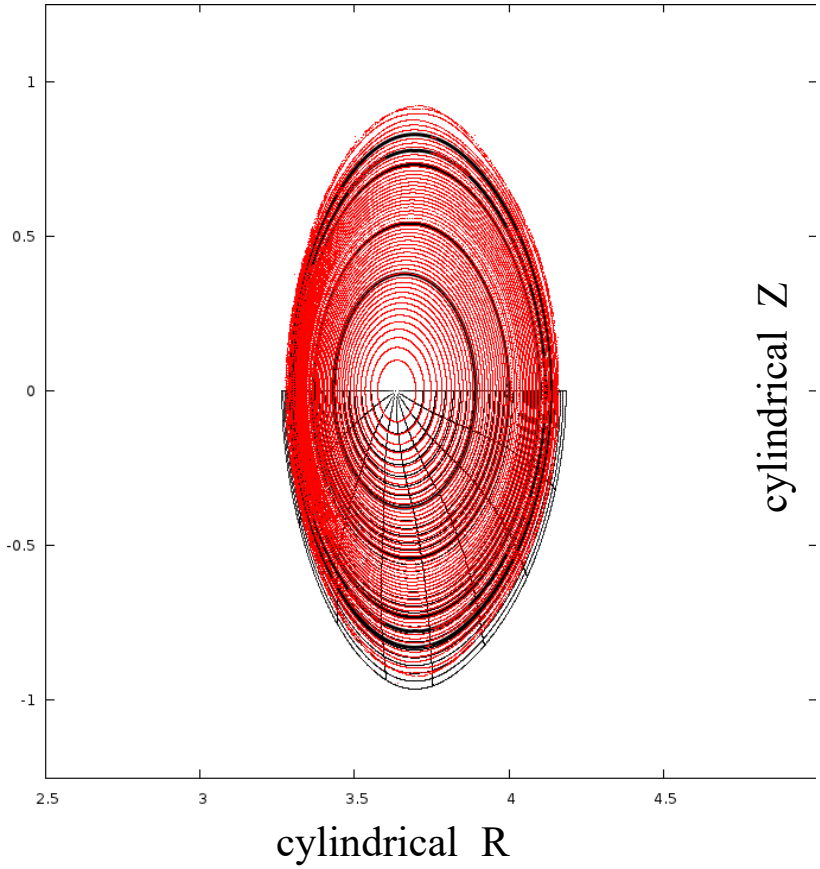
1
0.5
0
-0.5
-1
2.5
3
3.5
4
4.5
cylindrical Z
cylindrical R

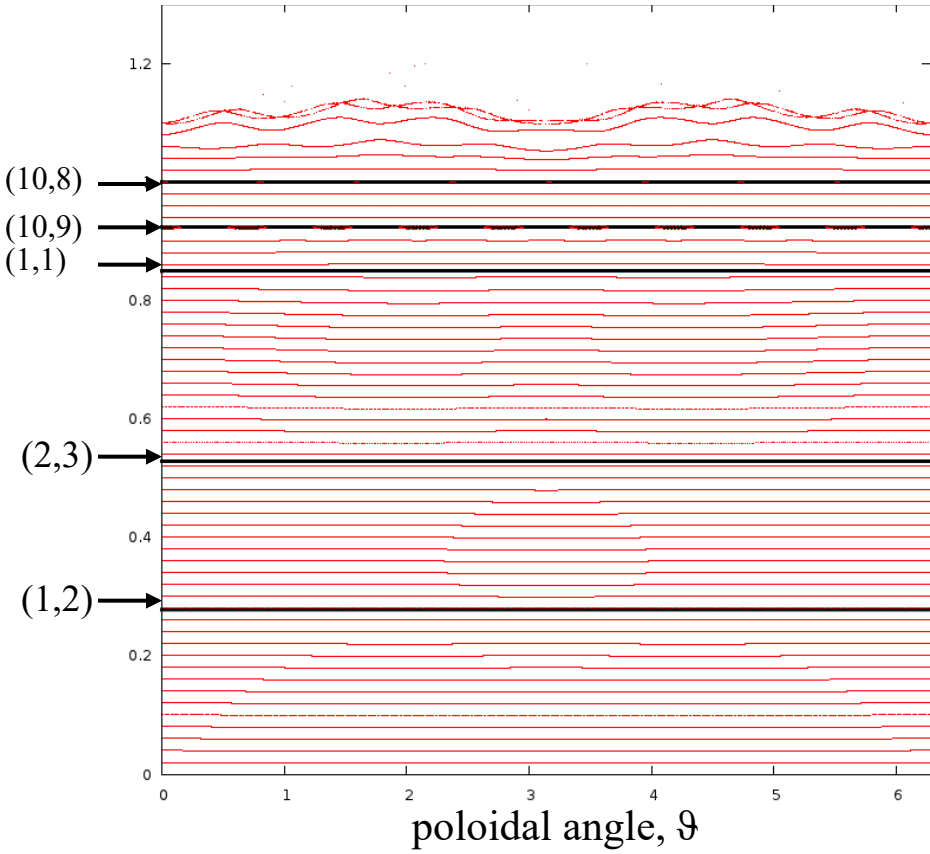
1.2
0.8
0.6
0.4
0.2
0
0
1
2
3
4
5
6
(10,8)
(10,9)
(1,1)
(2,3)
(1,2)
poloidal angle, ϑ

Straight field line coordinates can be constructed over the domain where invariant flux surfaces exist

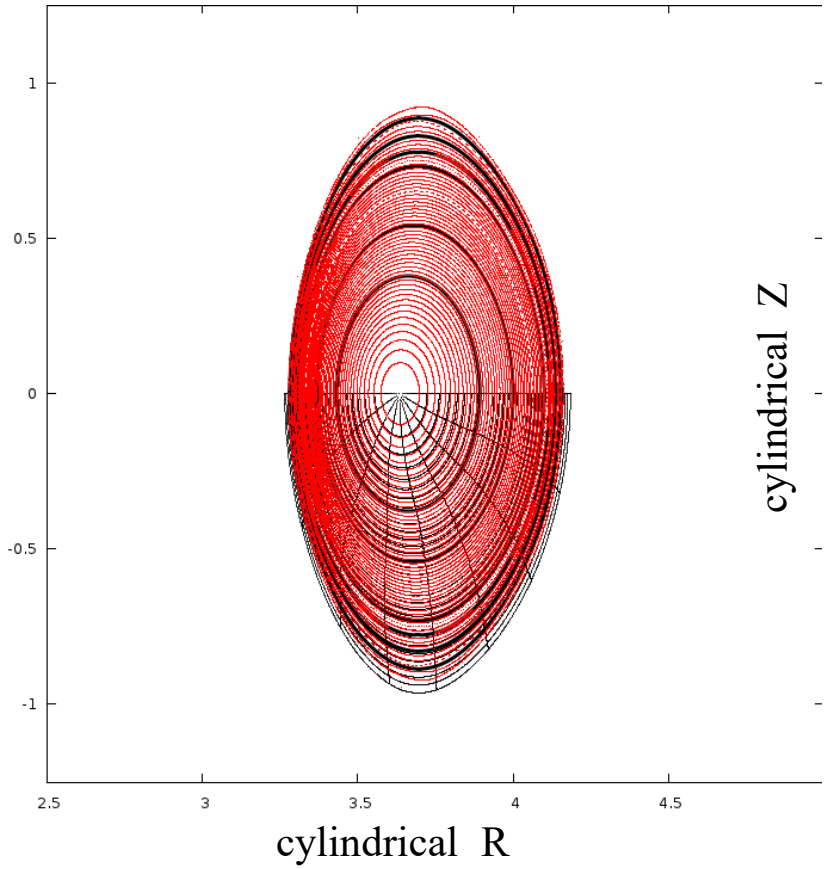

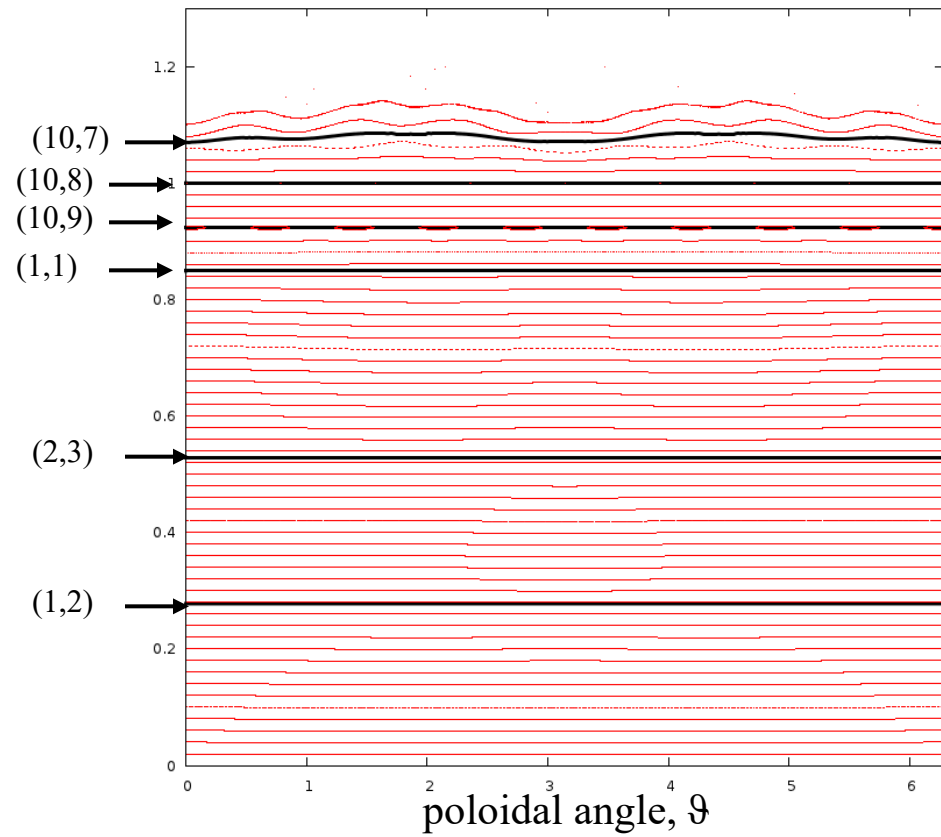

Straight field line coordinates can be constructed over the domain where invariant flux surfaces exist

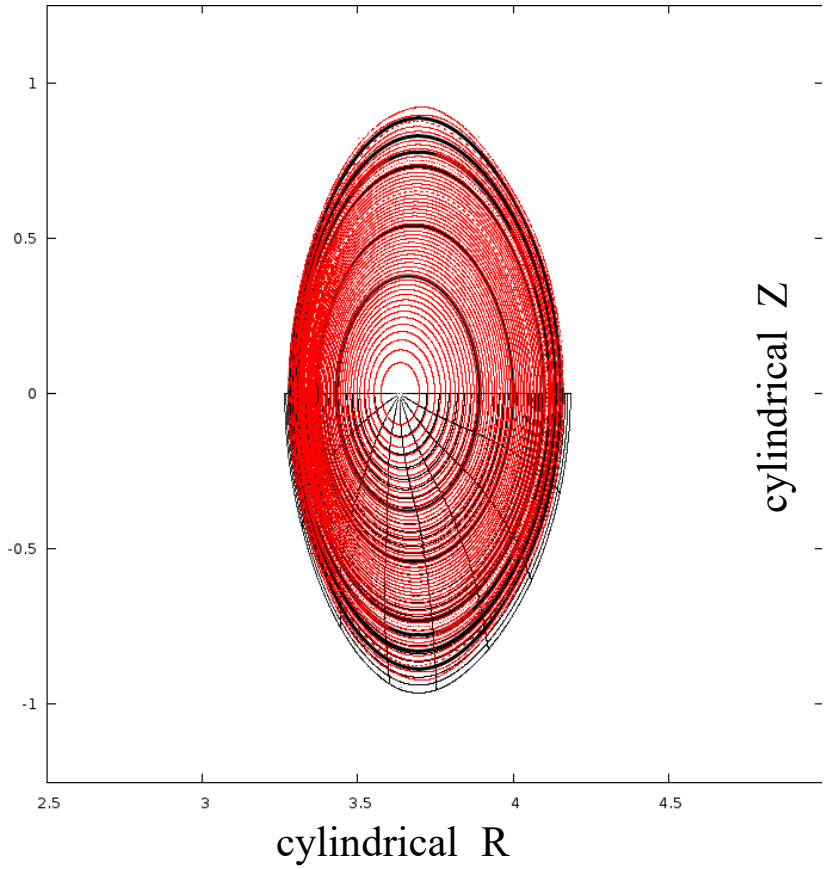

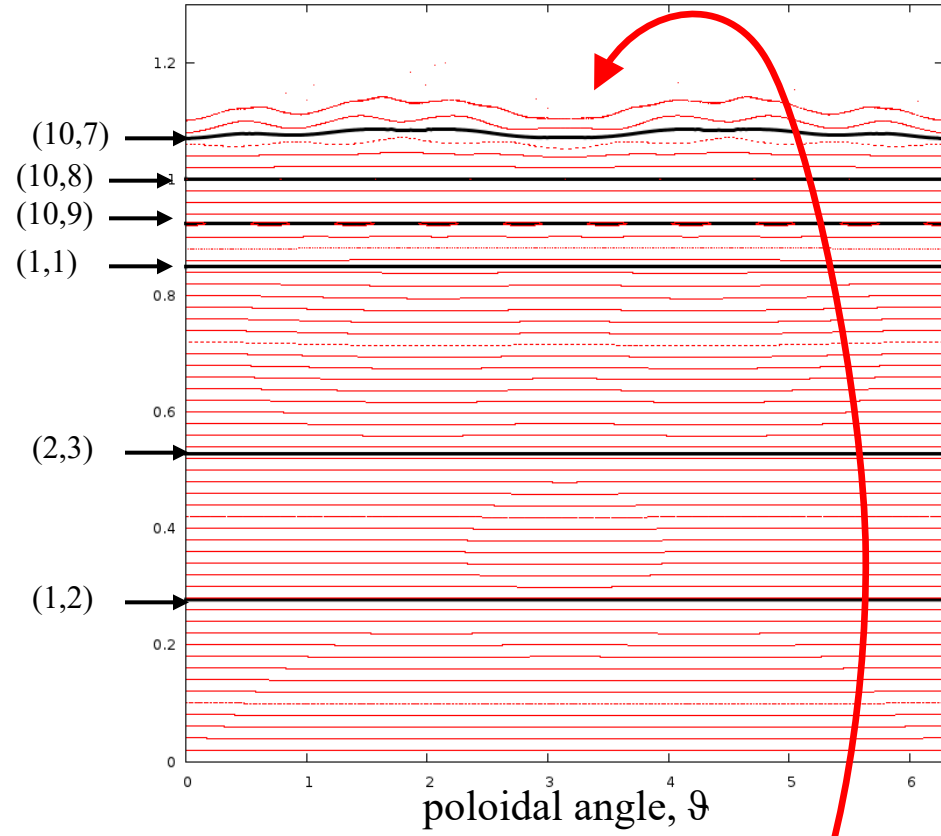

Near the plasma edge, there are magnetic islands, chaotic field lines.
Lets take a closer look . . . . .

Now, examine the "edge" . . . .

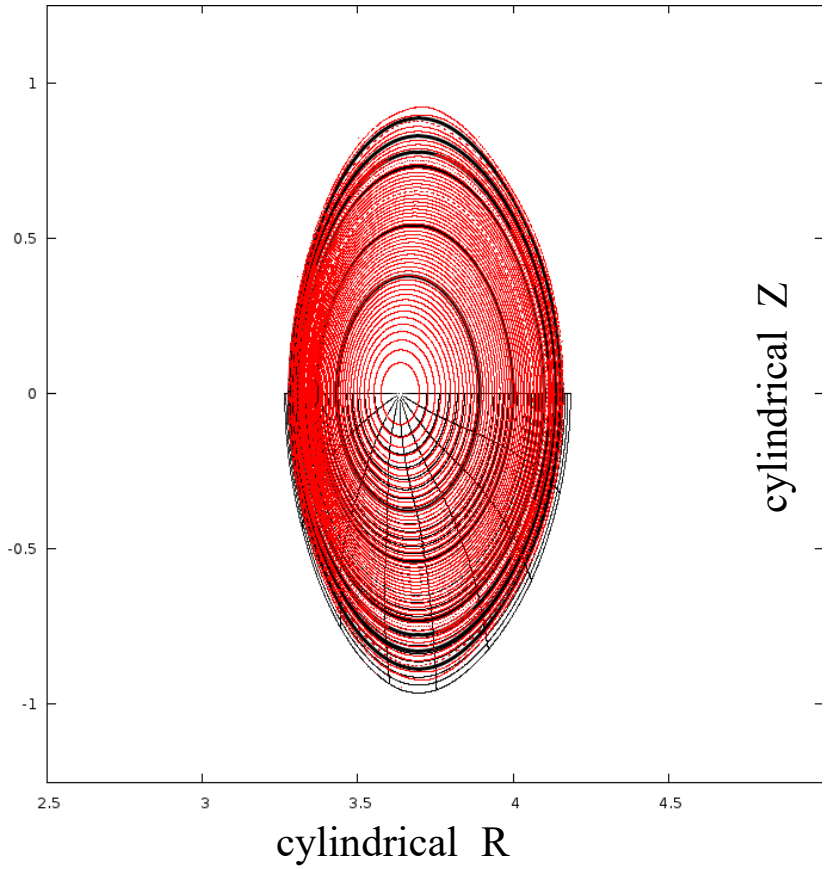

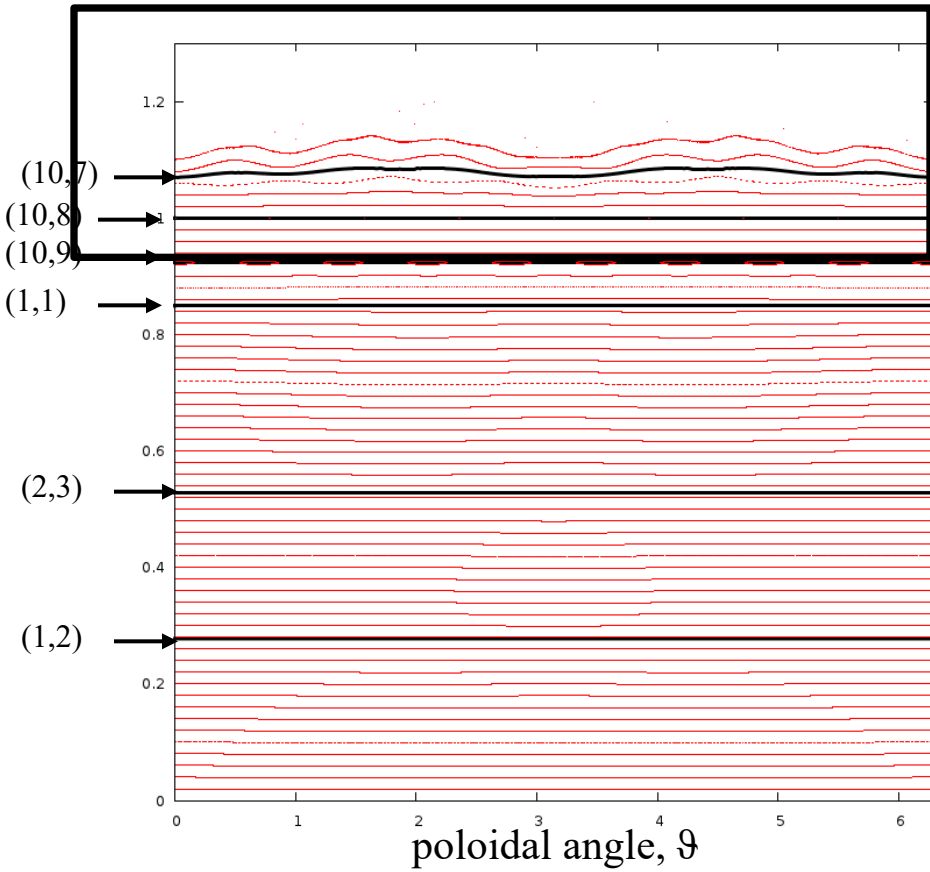

Near the plasma edge, there are magnetic islands and field-line chaos

But this is no problem. There is no change to the algorithm!
The rational, almost-invariant surfaces can still be constructed.
The quadratic-flux minimizing surfaces ≈ ghost-surfaces pass through the island chains,

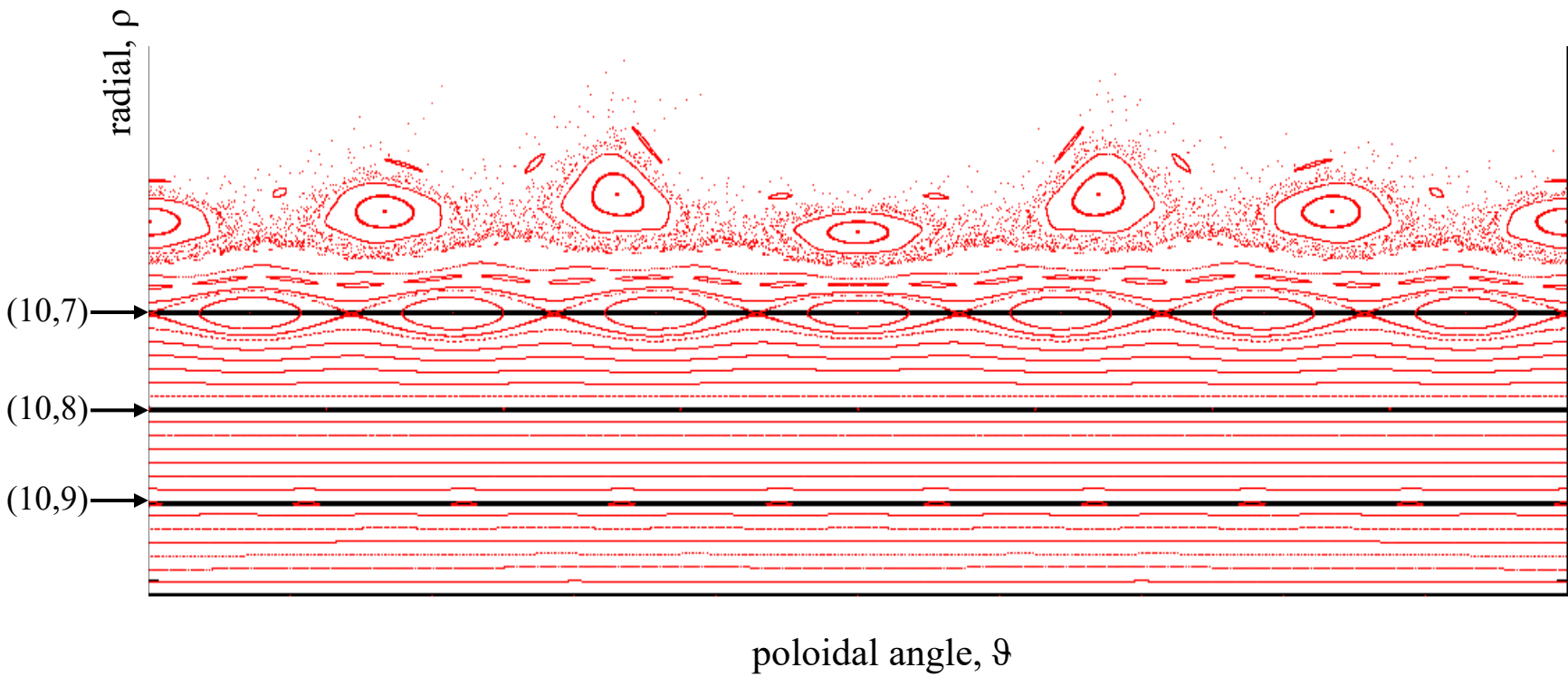

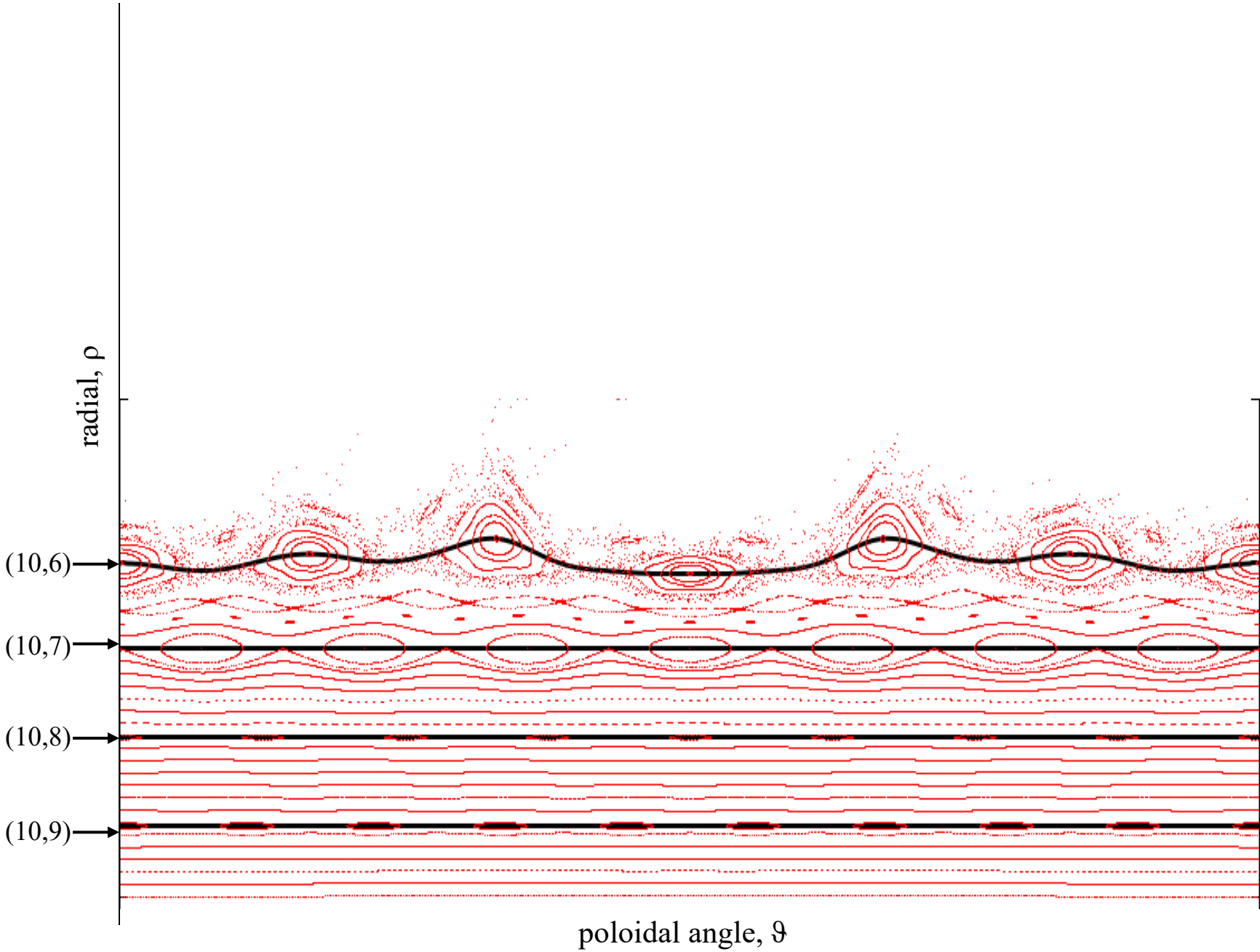
radial, ρ
(10,6)
(10,7)
(10,8)
(10,9)
poloidal angle, ϑ

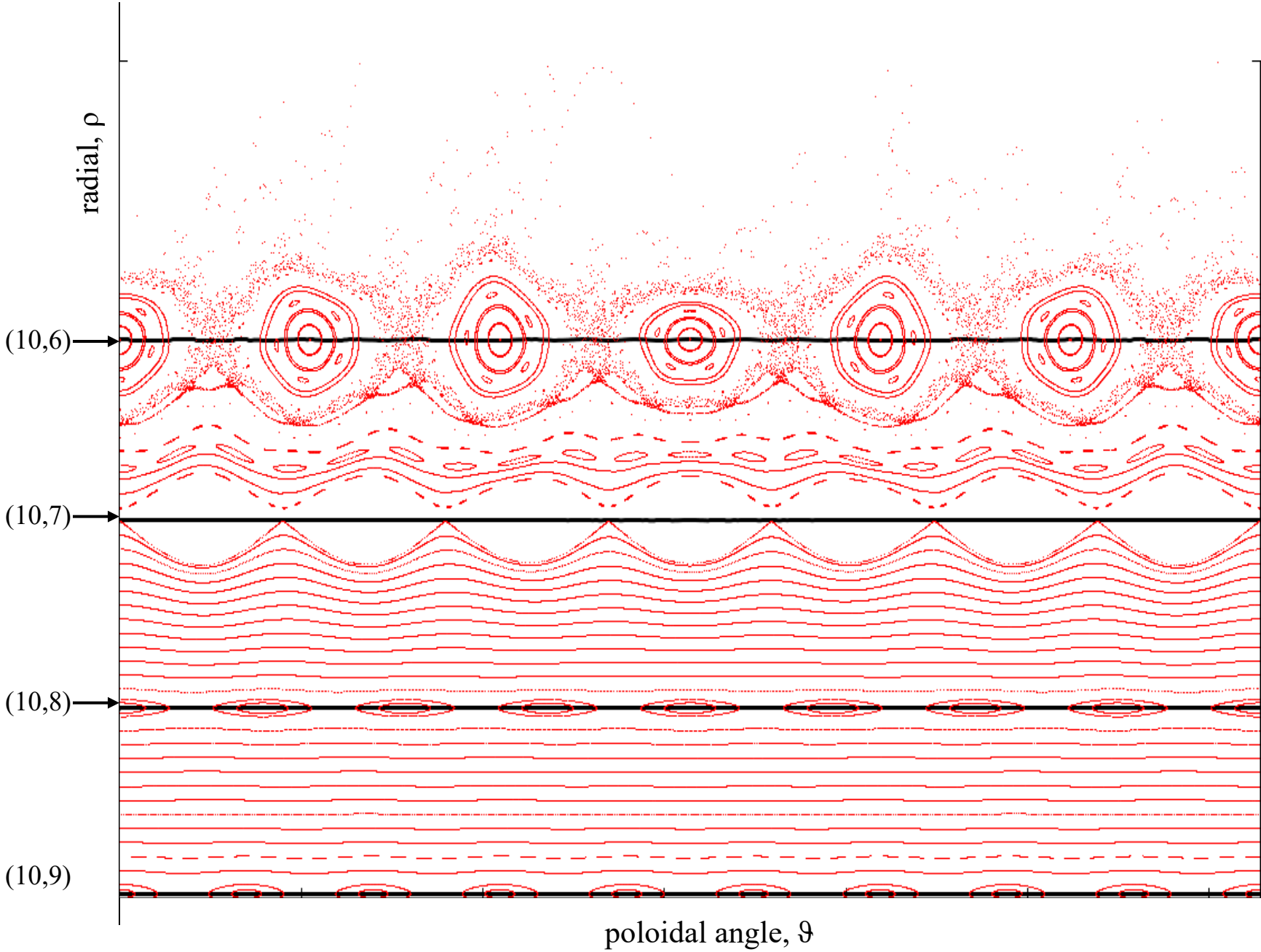
radial, ρ
(10,6)
(10,7)
(10,8)
(10,9)
poloidal angle, ϑ

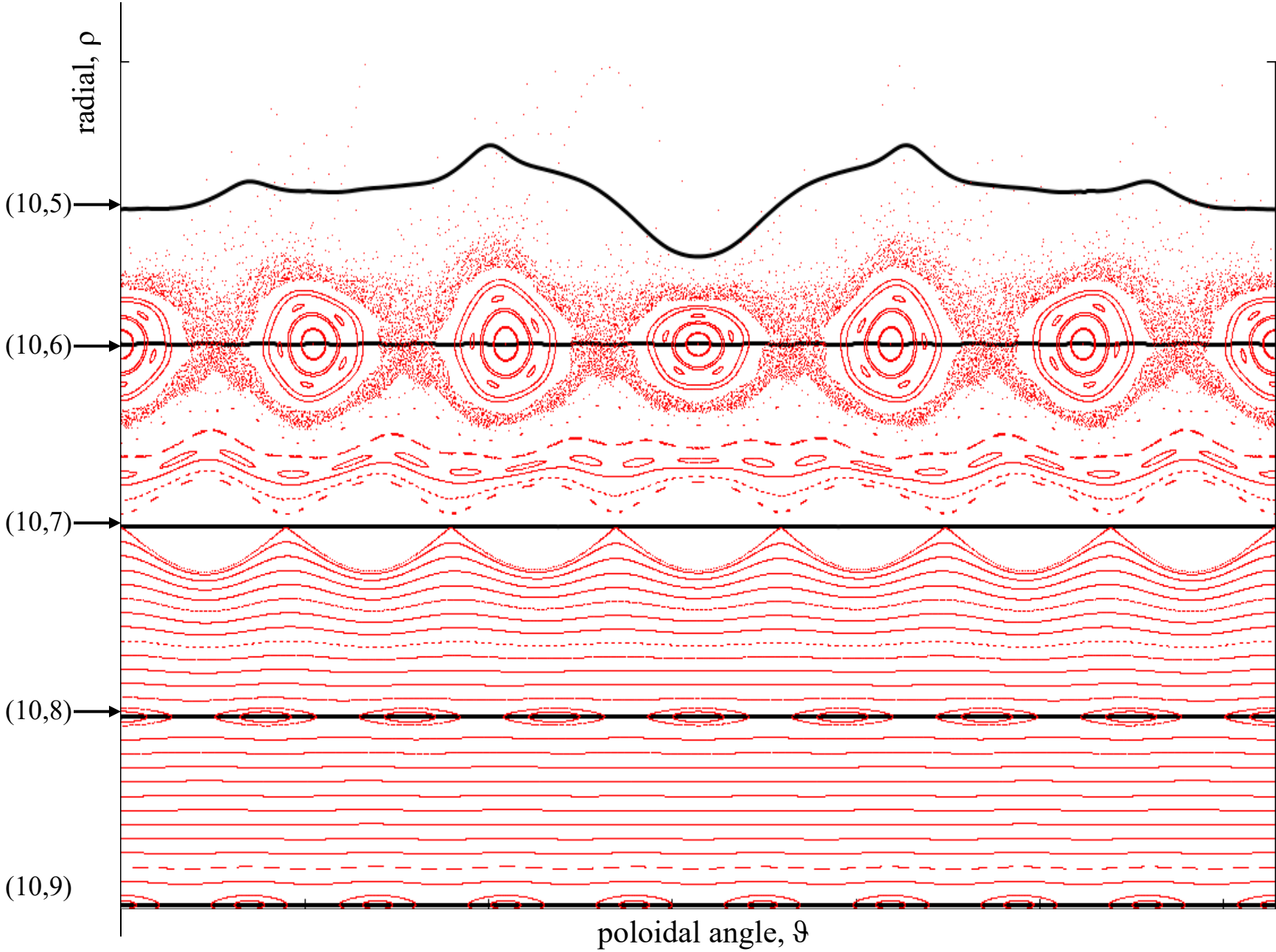
radial, ρ
(10,5)
(10,6)
(10,7)
(10,8)
(10,9)
poloidal angle, ϑ

Now, lets look for the ethereal, last closed flux surface.

(from dictionary.reference.com)
e·the·re·al [ih-**theer**-ee-uhl]
Adjective
1.light, airy, or **tenuous**: an ethereal world created through the poetic imagination.
2.extremely delicate or refined: ethereal beauty.
3.heavenly or celestial: gone to his ethereal home.
4.of or pertaining to **the upper regions of space**.

Perhaps the last flux surface is in here

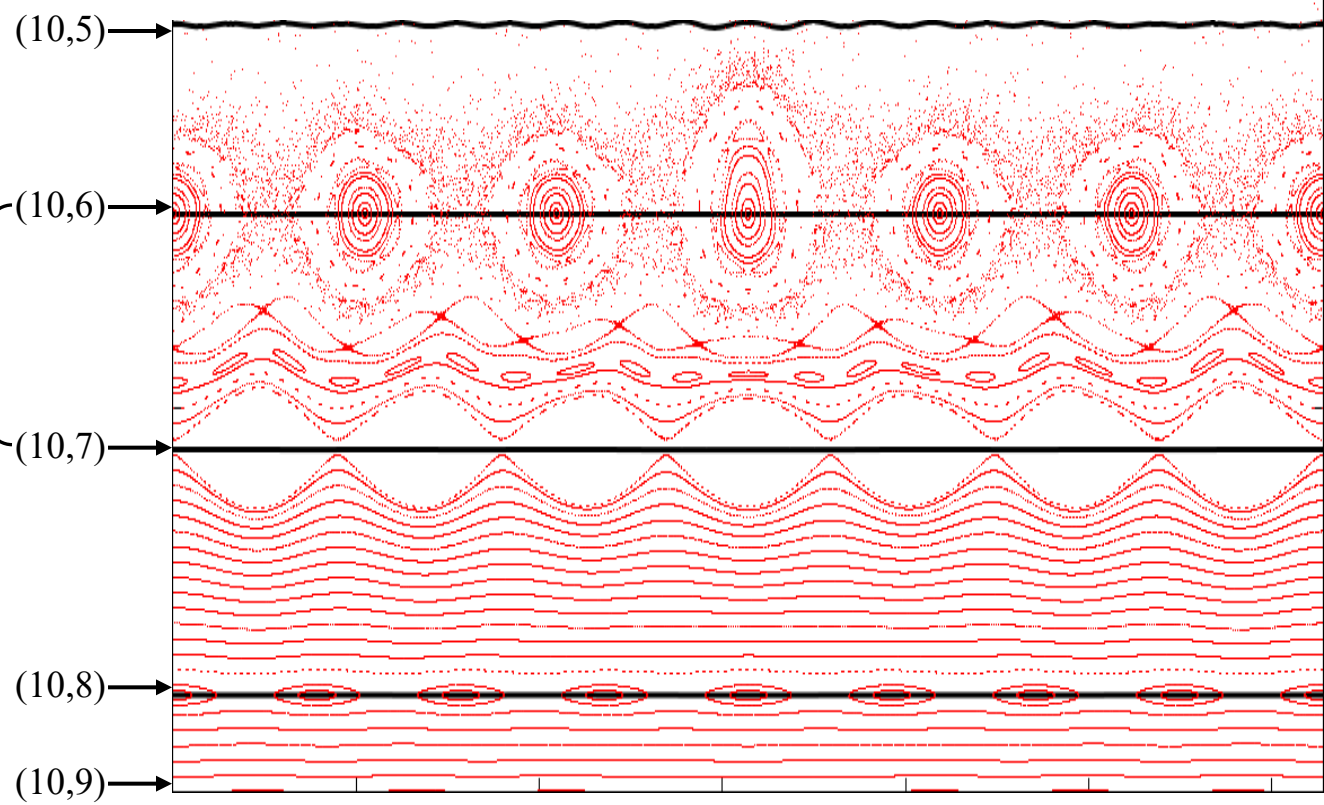

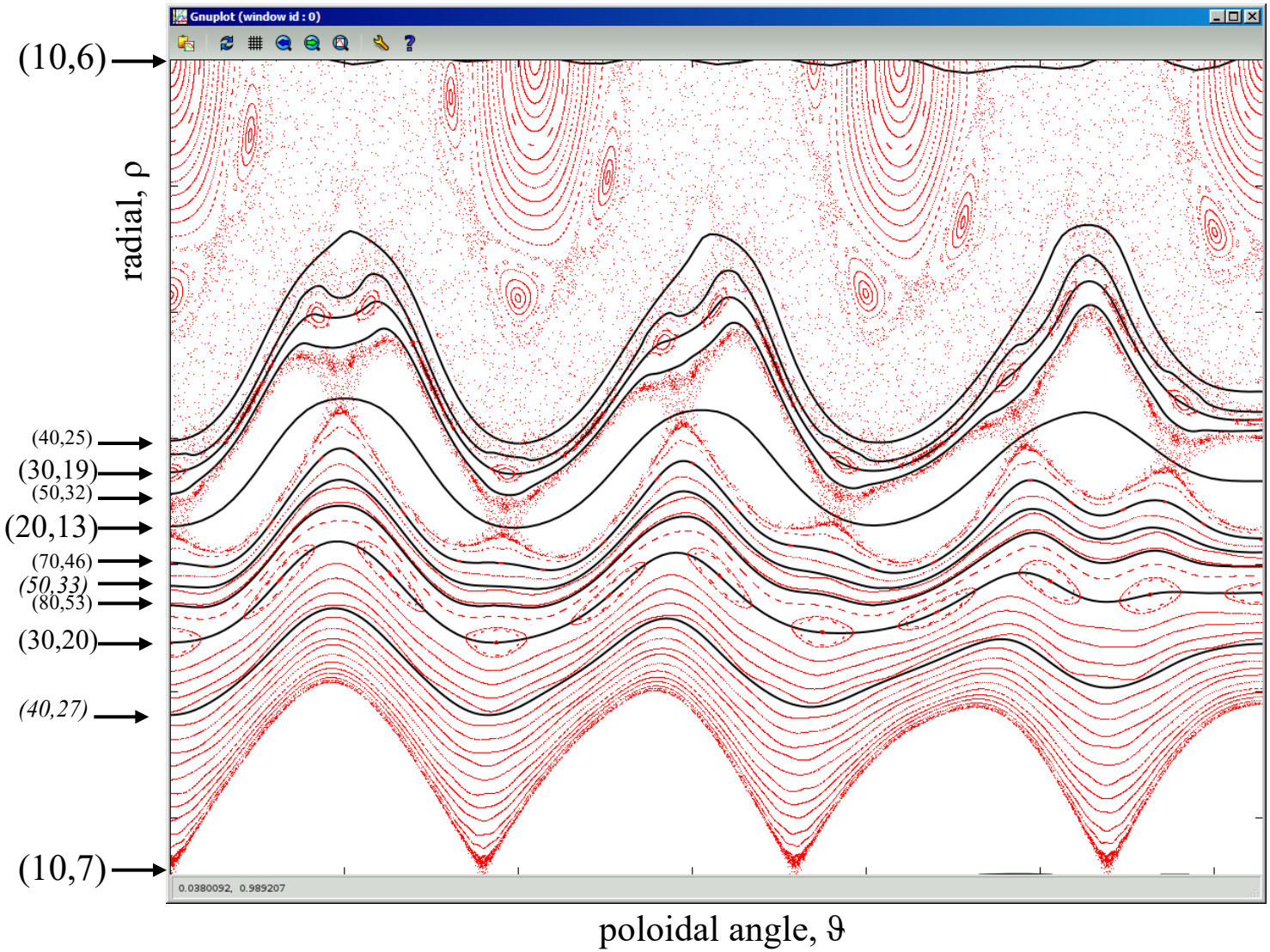

Hereafter, will not Fourier decompose the almost-invariant surfaces and use them as coordinate surfaces.
This is because they become quite deformed and can be very close together,
and the simple-minded piecewise cubic method fails to provide interpolated coordinate surfaces that do not intersect.

(20,13)

radial, ρ

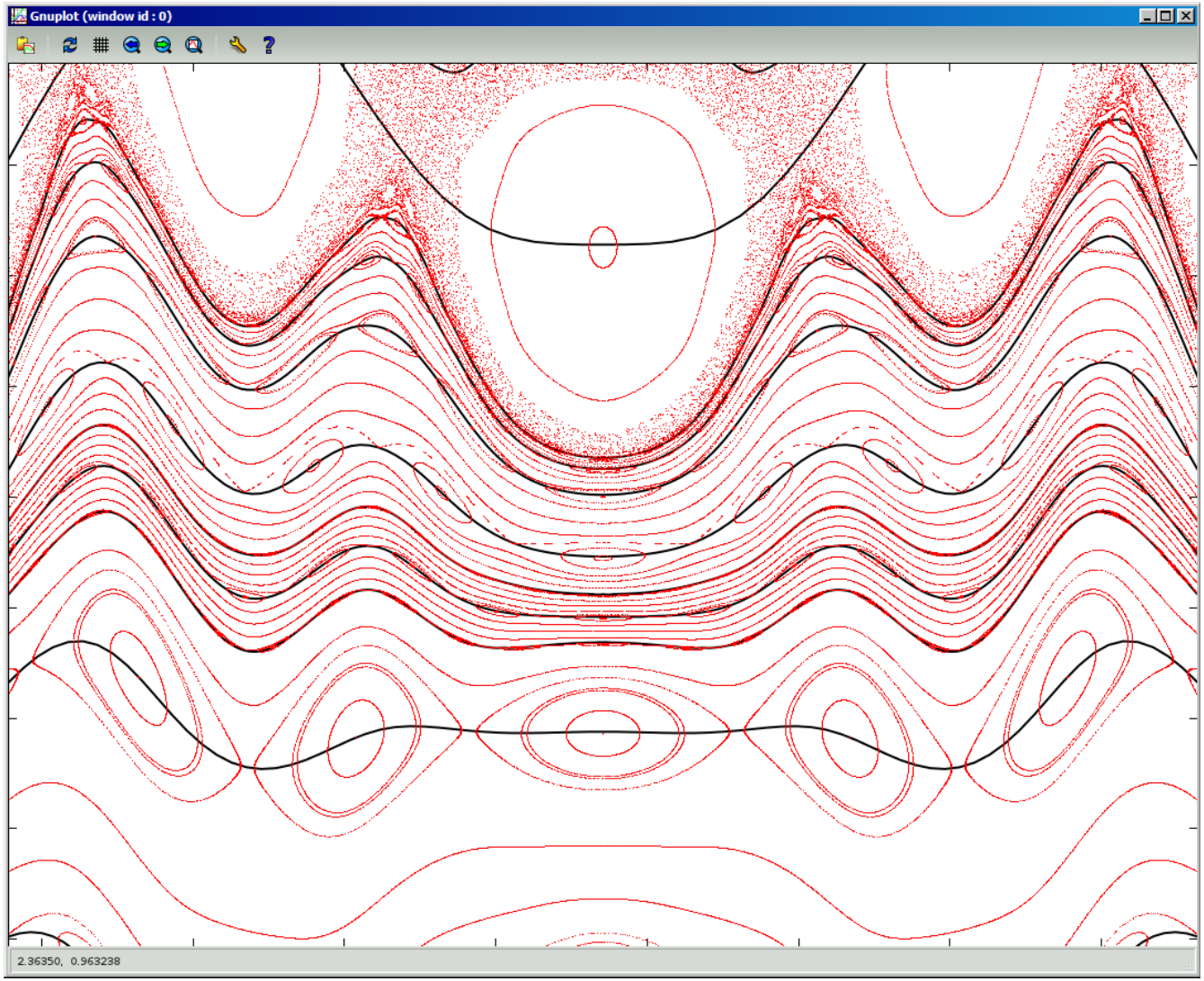

poloidal angle, ϑ

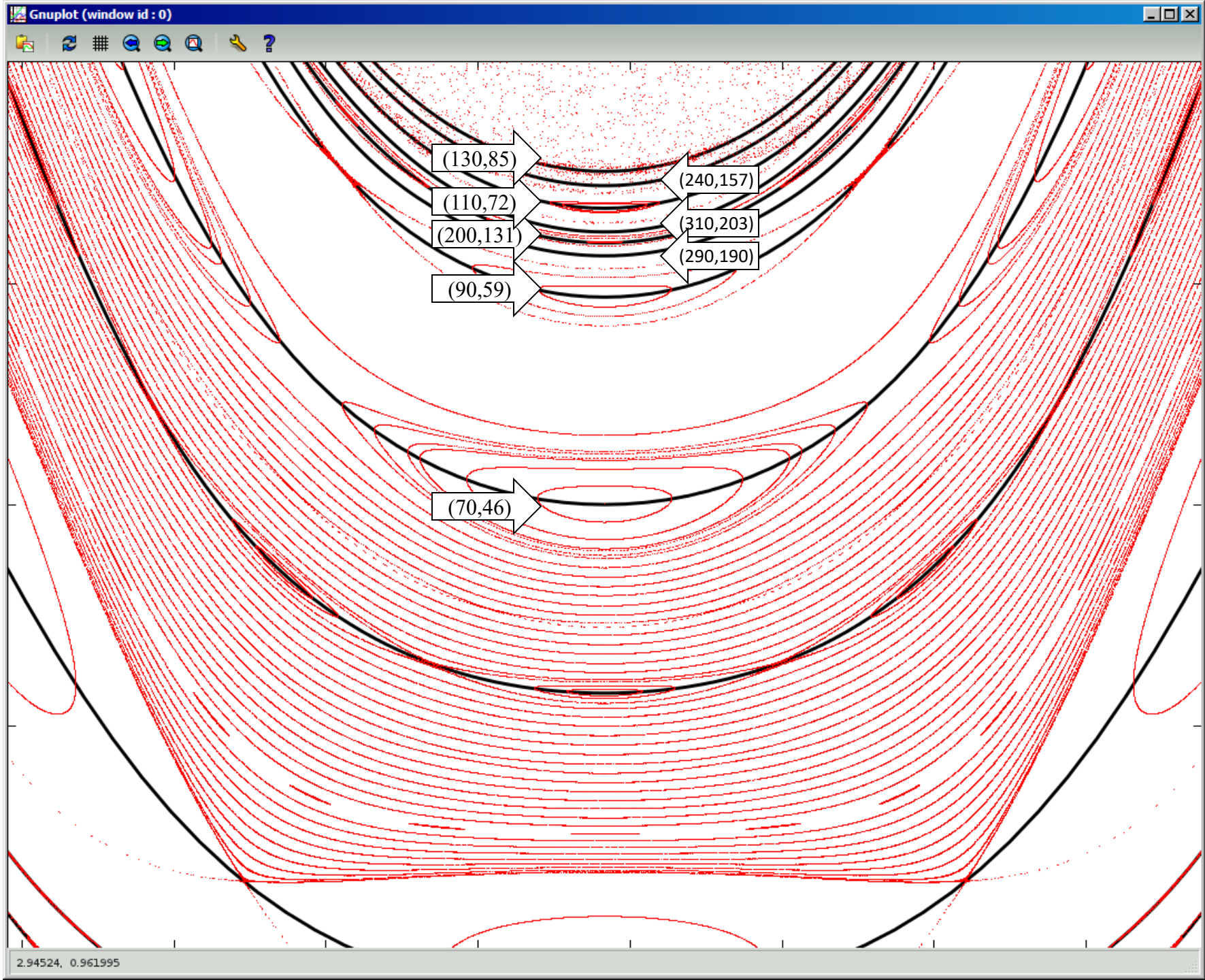
Gnuplot (window id : 0)
(130,85)
(110,72)
(200,131)
(90,59)
(240,157)
(310,203)
(290,190)
(70,46)
2.94524, 0.961995

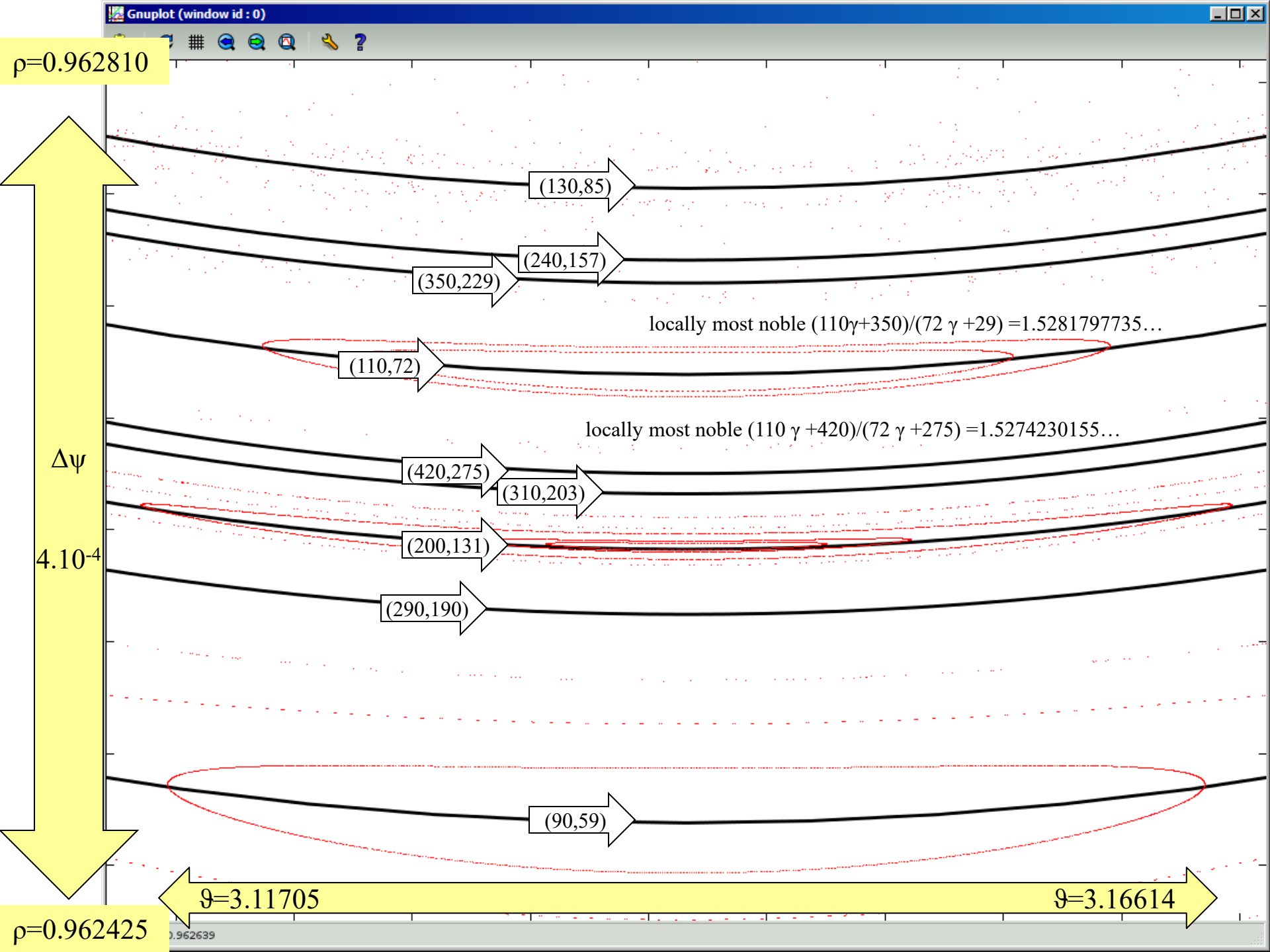
Gnuplot (window id : 0)
ρ=0.962810
(130,85)
(240,157)
(350,229)
locally most noble (110γ+350)/(72 γ +29) =1.5281797735…
(110,72)
locally most noble (110 γ +420)/(72 γ +275) =1.5274230155…
(420,275)
(310,203)
(200,131)
(290,190)
(90,59)
Δψ
4.10-4
ϑ=3.11705
ϑ=3.16614
ρ=0.962425

To find the significant barriers to field line transport, construct a hierarchy of high-order surfaces, and compute the upward flux

$\Psi_{10/7}$	7.50156×10^{-04}
$\Psi_{40/27}$	5.35875×10^{-06}
$\Psi_{30/20}$	2.17100×10^{-05}
$\Psi_{110/73}$	5.76470×10^{-08}
$\Psi_{80/53}$	3.18777×10^{-07}
$\Psi_{290/192}$	2.90328×10^{-11}
$\Psi_{210/139}$	5.10028×10^{-10}
$\Psi_{340/225}$	4.32721×10^{-12}
$\Psi_{130/86}$	2.10427×10^{-08}
$\Psi_{180/119}$	2.95639×10^{-09}
$\Psi_{230/152}$	2.23672×10^{-09}
$\Psi_{50/33}$	3.67232×10^{-06}
$\Psi_{120/79}$	7.86600×10^{-08}
$\Psi_{70/46}$	1.37526×10^{-06}
$\Psi_{90/59}$	8.35105×10^{-07}
$\Psi_{290/190}$	6.50293×10^{-08}
$\Psi_{200/131}$	7.07049×10^{-08}
$\Psi_{310/203}$	3.85707×10^{-07}
$\Psi_{420/275}$	3.73482×10^{-07}
$\Psi_{110/72}$	8.62439×10^{-07}
$\Psi_{350/229}$	1.29837×10^{-07}
$\Psi_{240/157}$	4.27556×10^{-07}
$\Psi_{130/85}$	6.22742×10^{-07}
$\Psi_{20/13}$	1.87579×10^{-04}
$\Psi_{90/58}$	4.90660×10^{-06}
$\Psi_{70/45}$	7.79506×10^{-06}
$\Psi_{50/32}$	1.89412×10^{-05}
$\Psi_{80/51}$	7.84026×10^{-06}
$\Psi_{30/19}$	9.25352×10^{-05}
$\Psi_{10/6}$	3.71570×10^{-03}

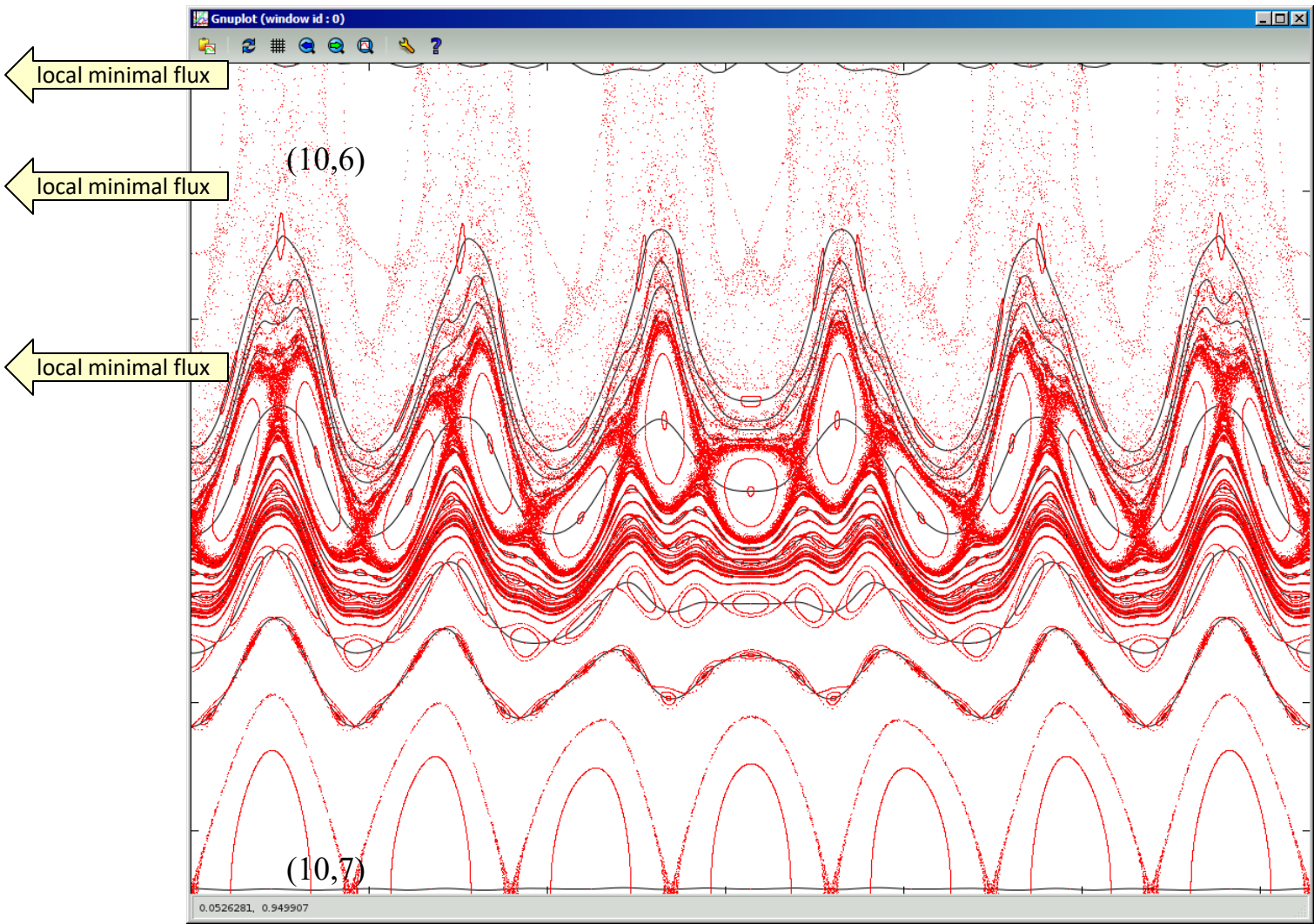

ASDEX Upgrade:
work in progress, preliminary results,
with S. Jardin, I. Krebs, . .

The magnetic field is provided by M3D-C1

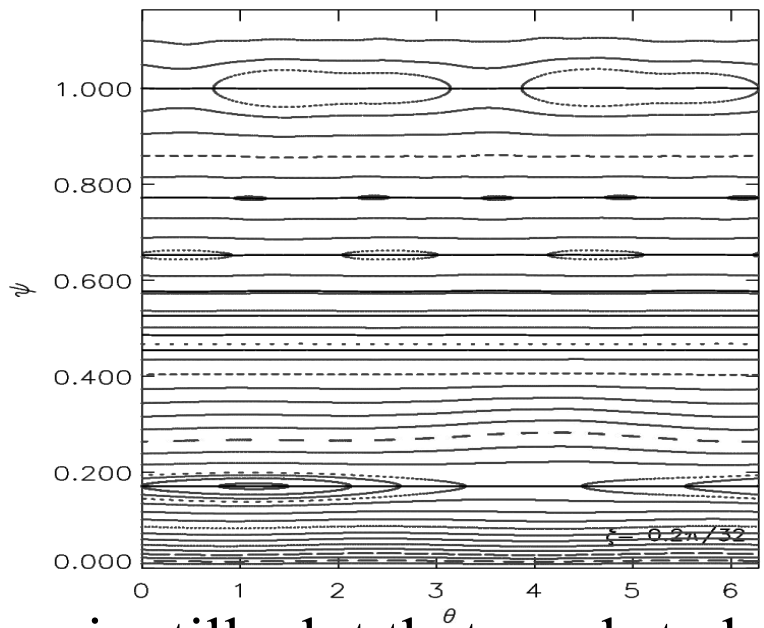

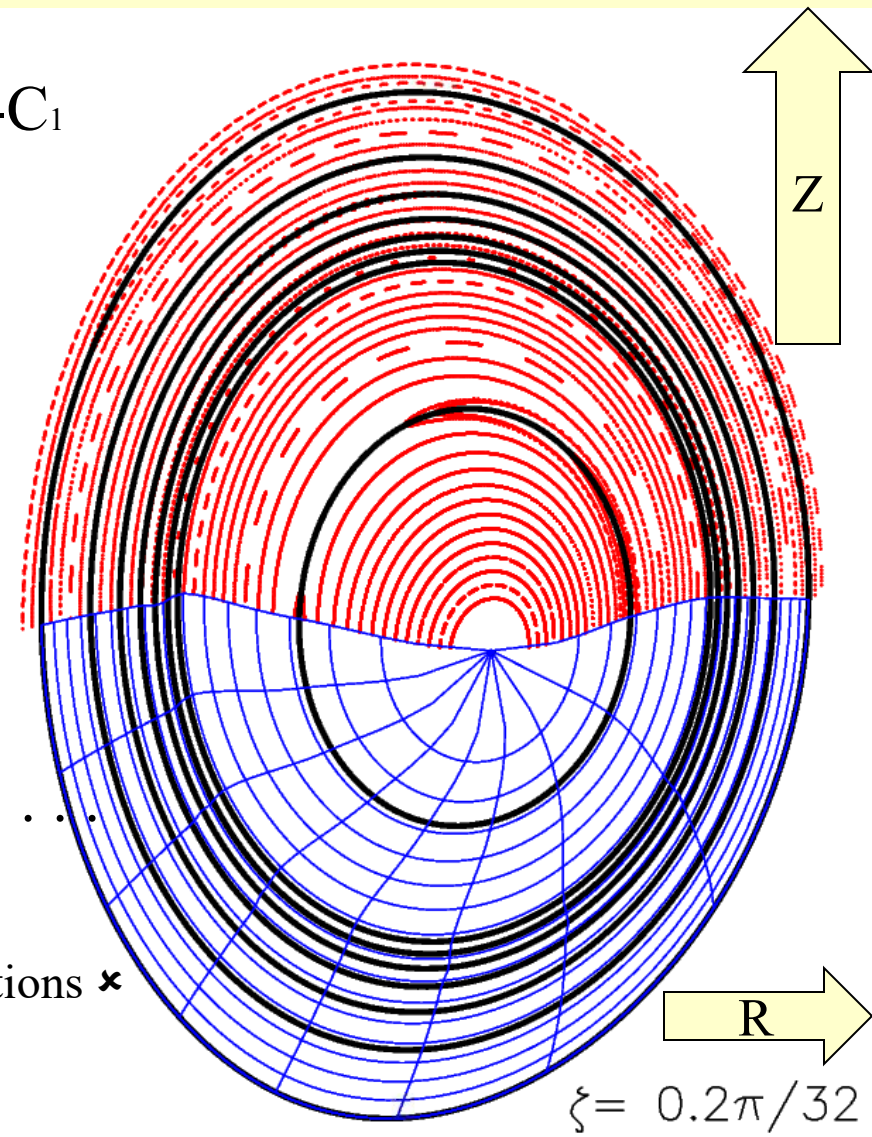

There is still a lot that needs to be done . . . .

i. Allow for non-stellarator-symmety ✓
ii. Constrain poloidal angle ✗
iii. Interpolate coordinate surfaces without intersections ✗
iv. Extrapolate into separatrix ✗
v. Coordinate axis = magnetic axis ✗

In chaotic-coordinates™, the flux surfaces are straight, and the islands are square.

These coordinates can simplify many calculations, e.g.

pressure = p(s)

temperature = T(s)

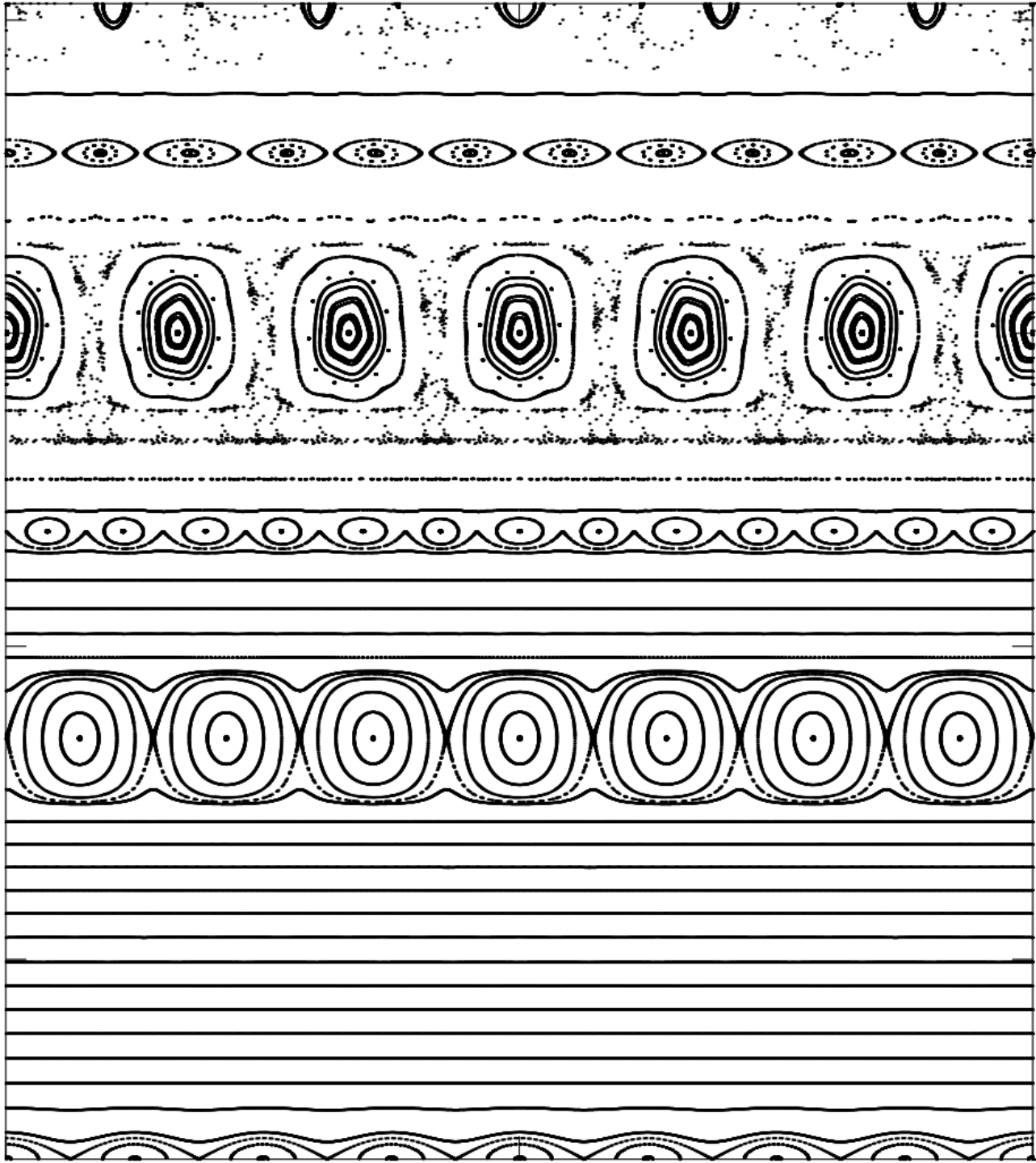

Mathematical Preliminary: Vector Potential

A magnetic vector potential, in a suitable gauge, is quickly determined by radial integration.

1. Generally, gauge freedom allows $\mathbf{A} = A_\theta(\rho,\theta,\zeta)\nabla\theta + A_\zeta(\rho,\theta,\zeta)\nabla\zeta$.

2. $\nabla \times \mathbf{B} = \mathbf{A}$ gives

$$\begin{aligned}
\sqrt{g}B^\rho &= \partial_\theta A_\zeta - \partial_\zeta A_\theta, \\
\sqrt{g}B^\theta &= - \partial_\rho A_\zeta, \\
\sqrt{g}B^\zeta &= \partial_\rho A_\theta.
\end{aligned}$$

3. Given the magnetic field, $\mathbf{A}$ is quickly determined by radial integration in Fourier space:

$$\begin{aligned}
\partial_\rho A_{\theta,m,n} &= +(\sqrt{g}B^\zeta)_{m,n}, \\
\partial_\rho A_{\zeta,m,n} &= -(\sqrt{g}B^\theta)_{m,n},
\end{aligned}$$

and the remaining equation, $\sqrt{g}B^\rho = \partial_\theta A_\zeta - \partial_\zeta A_\theta$, is satisfied if $\nabla \cdot \mathbf{B} = 0$.

4. Hereafter, use notation $\mathbf{A} = \psi\nabla\theta - \chi\nabla\zeta$.

Physics Preliminary: Magnetic Fieldline Action

The action is the line integral, along an arbitrary curve, of the vector potential.

$$S[\mathcal{C}] \equiv \int_{\mathcal{C}} \mathbf{A}\cdot d\mathbf{l}, \quad \text{along trial curve,} \quad \mathcal{C} : \rho = \rho(\zeta), \theta = \theta(\zeta).$$

$$\mathbf{A} = \psi\nabla\theta - \chi\nabla\zeta, \quad d\mathbf{l} \equiv d\rho\, e_\rho + d\theta\, e_\theta + d\zeta\, e_\zeta, \quad \mathbf{A}\cdot d\mathbf{l} = \Big(\psi\,\dot\theta - \chi\Big)\, d\zeta.$$

$$\text{e.g.} \quad \psi = \sum_{m,n} \psi_{m,n}(\rho)\cos(m\theta - n\zeta), \quad \chi = \sum_{m,n} \chi_{m,n}(\rho)\cos(m\theta - n\zeta).$$

Numerically, a curve is represented as piecewise-constant, piecewise-linear.

For $\zeta \in (\zeta_{i-1}, \zeta_i)$,
$\rho(\zeta) = \rho_i$,
$\theta(\zeta) = \theta_{i-1} + \dot\theta\,(\zeta - \zeta_{i-1})$,
where $\dot\theta \equiv (\theta_i - \theta_{i-1})/\Delta\zeta$.

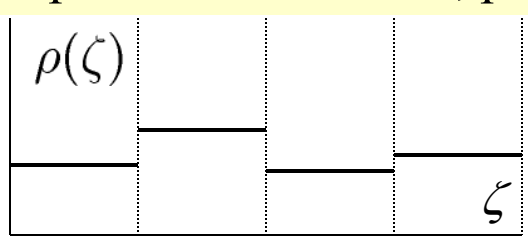

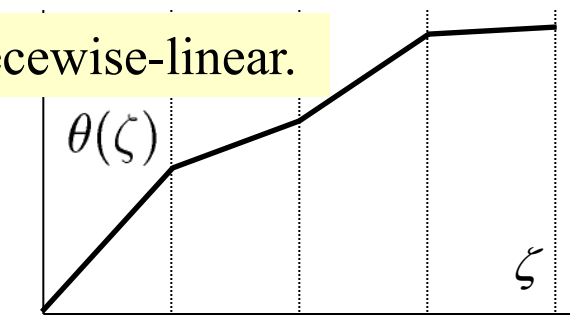

The $\{\rho_i : i = 1, N\}$ and $\{\theta_i : i = 0, N\}$ describe the curve. N is resolution. Periodicity: $\zeta_N = 2\pi q$, $\theta_N = \theta_0 + 2\pi p$.

Seems crude; but, the trigonometric integrals are computed analytically, i.e. fast;

$$S = \sum_{i=1}^{N} \int_{\zeta_{i-1}}^{\zeta_i} d\zeta \Big(\psi\,\dot\theta - \chi\Big) = \sum_{i=1}^{N}\sum_{m,n} \Big[\psi_{m,n}(\rho_i)\,\dot\theta - \chi_{m,n}(\rho_i)\Big] \int_{\zeta_{i-1}}^{\zeta_i} d\zeta\, \cos(m\theta - n\zeta)$$

$$\int_{\zeta_{i-1}}^{\zeta_i} d\zeta\, \cos(m\theta - n\zeta) = \frac{\sin(m\theta_i - n\zeta_i) - \sin(m\theta_{i-1} - n\zeta_{i-1})}{m\dot\theta - n}$$

and, coordinates will be constructed in which the periodic fieldlines are straight.

Ghost Surfaces

Summary: Timeline of topics addressed in talk

(*not* a comprehensive history of Hamiltonian chaos!)

•	Poincaré	unstable manifold (i.e. chaos)
• 1954	Kolmogorov	KAM theorem
• 1962	Moser	
• 1963	Arnold	
• 1979	Chirikov	island overlap criterion
• 1979	Greene	residue criterion [see also 1991 MacKay]
• 1979	Percival	can(tor + tor)us = cantorus
• 1982	Mather	Aubry-Mather theorem (showing existence of cantori)
• 1983	Aubry	
• 1991	Angenent & Golé	ghost-circles
• 1991	Meiss & Dewar	quadratic-flux minimizing curves
• 2008	Hudson & Breslau	isotherms = ghost-surfaces
• 2009	Hudson & Dewar	ghost-surfaces = quadratic-flux minimizing surfaces

and texts:

• 1983	Lichtenberg & Lieberman	[Regular and Stochastic Motion]
• 1992	Meiss	[Reviews of Modern Physics]

Relevant publications:

http://w3.pppl.gov/~shudson/bibliography.html

Chaotic coordinates for the Large Helical Device , S.R.Hudson & Y. Suzuki
Physics of Plasmas, 21:102505, 2014

Generalized action-angle coordinates defined on island chains, R.L.Dewar, S.R.Hudson & A.M.Gibson
Plasma Physics and Controlled Fusion, 55:014004, 2013

Unified theory of Ghost and Quadratic-Flux-Minimizing Surfaces, R. L.Dewar, S. R.Hudson & A. M.Gibson
Journal of Plasma and Fusion Research SERIES, 9:487, 2010

Are ghost surfaces quadratic-flux-minimizing?, S.R.Hudson & R.L.Dewar
Physics Letters A, 373(48):4409, 2009

An expression for the temperature gradient in chaotic fields, S.R.Hudson
Physics of Plasmas, 16:010701, 2009

Temperature contours and ghost-surfaces for chaotic magnetic fields, S.R.Hudson & J.Breslau
Physical Review Letters, 100:095001, 2008

Calculation of cantori for Hamiltonian flows, S.R.Hudson
Physical Review E, 74:056203, 2006

Almost invariant manifolds for divergence free fields, R.L.Dewar, S.R.Hudson & P.Price
Physics Letters A, 194(1-2):49, 1994

List of publications, http://w3.pppl.gov/~shudson/

Generalized action-angle coordinates defined on island chains
R.L.Dewar, S.R.Hudson and A.M.Gibson
Plasma Physics and Controlled Fusion, 55:014004, 2013

Unified theory of Ghost and Quadratic-Flux-Minimizing Surfaces
Robert L.Dewar, Stuart R.Hudson and Ashley M.Gibson
Journal of Plasma and Fusion Research SERIES, 9:487, 2010

Are ghost surfaces quadratic-flux-minimizing?
S.R.Hudson and R.L.Dewar
Physics Letters A, 373(48):4409, 2009

An expression for the temperature gradient in chaotic fields
S.R.Hudson
Physics of Plasmas, 16:010701, 2009

Temperature contours and ghost-surfaces for chaotic magnetic fields
S.R.Hudson and J.Breslau
Physical Review Letters, 100:095001, 2008

Calculation of cantori for Hamiltonian flows
S.R.Hudson
Physical Review E, 74:056203, 2006

Almost invariant manifolds for divergence free fields
R.L.Dewar, S.R.Hudson and P.Price
Physics Letters A, 194(1-2):49, 1994

Ghost Surfaces

The standard map is a simple and widely-used model of chaotic dynamics . . .

1. Standard map: (sometimes also called Chirikov-Taylor map);

$$\begin{aligned} r_{n+1} &= r_n + k\sin\theta_n, \quad \text{where } k \text{ is perturbation} \\ \theta_{n+1} &= \theta_n + r_{n+1} \end{aligned}$$

   i. For $k = 0$, motion is <u>integrable</u>: $r = const.$, $\theta = \theta_0 + n\, r$;
   ii. For $k \neq 0$, islands and "chaotic" $\equiv$ irregular trajectories emerge;
   iii. For $k > k_c$, no invariant surfaces (except inside islands);
   iv. Definition : (m, n)-periodic orbit: $r_m = r_0 \quad \theta_m = \theta_0 + n$.

2. Linearized motion: $\delta z_{n+1} \equiv \begin{pmatrix} \delta r \\ \delta\theta \end{pmatrix}_{n+1} = \underbrace{\begin{pmatrix} 1, & k\sin\theta_n \\ 1, & 1 + k\sin\theta_n \end{pmatrix}}_{\text{tangent map, } M_n} \begin{pmatrix} \delta r \\ \delta\theta \end{pmatrix}_n$

   i. mapping is area preserving, therefore $det|M_n| = 1$.

3. Linearized motion of (m, n)-periodic orbits, $\delta z_m = M_m \ldots M_1 M_0, \delta z_0$

   i. "stability" of periodic orbits determined by eigenvalues, λ_i, of $M^m \equiv M_m \ldots M_1 M_0$;
      X: hyperbolic: $\lambda_2 = 1/\lambda_1$; λ_i real; $|\lambda_1| > 1$; unstable;
      O: elliptic: λ_i complex congugates; $|\lambda_i| = 1$; stable;
   ii. As k increases, eventually all periodic orbits become unstable.

4. For given k, which flux surfaces exist? What is k_c?

$k = 0.2$

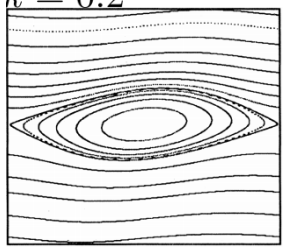

$k = 0.5$

$k = 0.8$

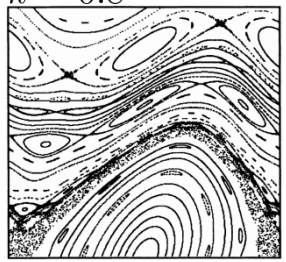

$k_c = 0.9716354$

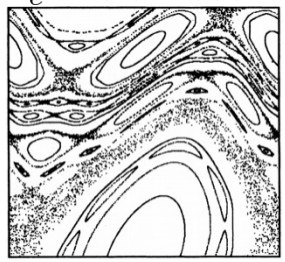

The standard map is very simple, but the trajectories are very complicated.

There are islands around islands around islands . . .

Birkhoff (1935) “It is clear that not only do general elliptic periodic solutions possess neighboring elliptic and hyperbolic periodic solutions, but also, beginning again with the neighboring elliptic solutions, who are, as it were, satellites of these solutions, one can obtain other elliptic and hyperbolic solutions which are secondary satellites.”

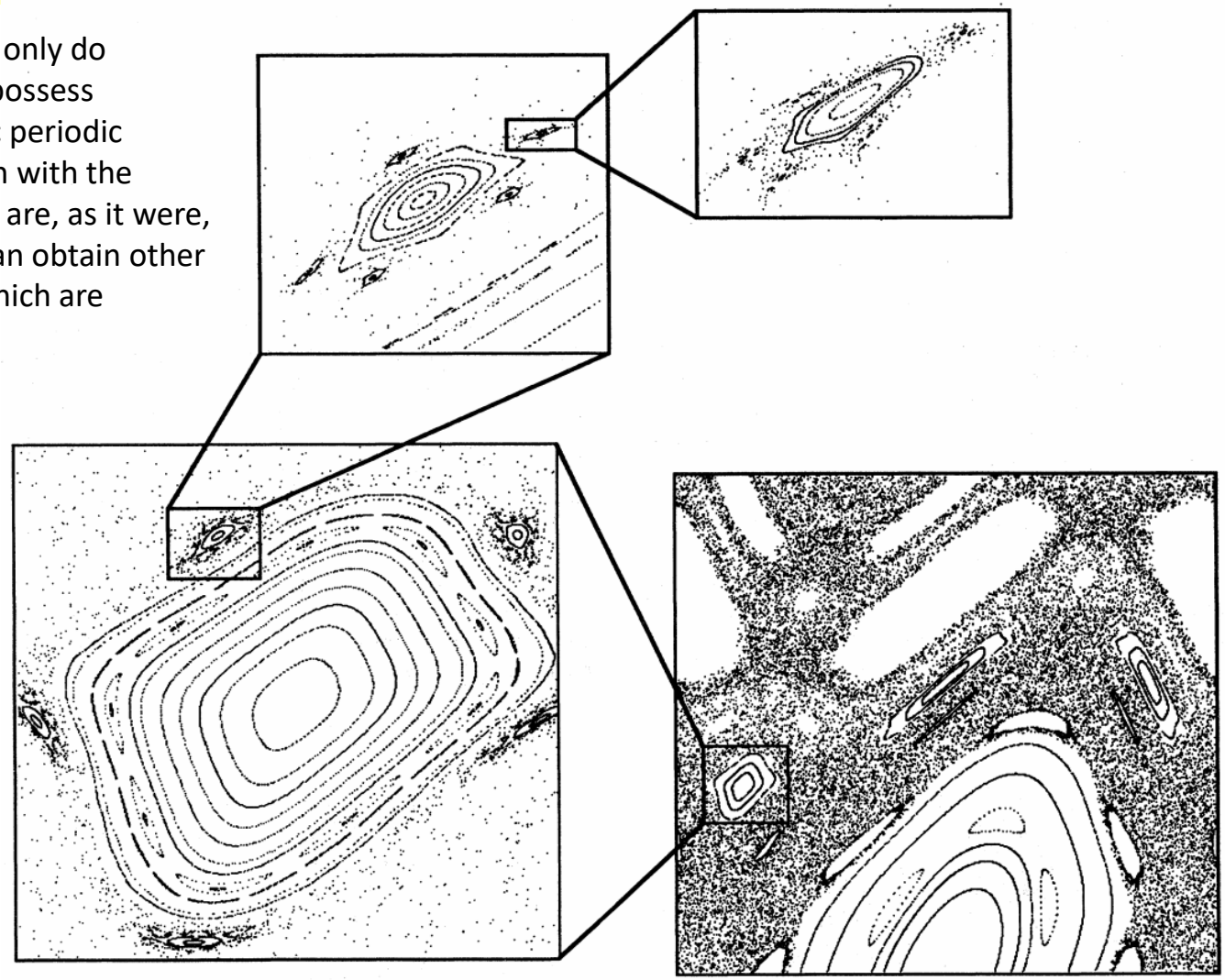

[“Symplectic maps, variational principles, and transport”, J. D. Meiss, Reviews of Modern Physics, 64(3):795 (1992)]

1979 : Chirikov's Island-Overlap Criterion

PHYSICS REPORTS 52, 5(1979)263-37

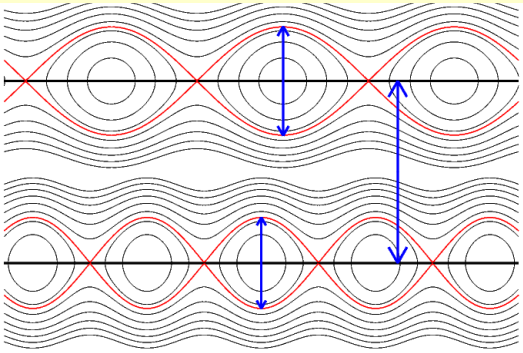

1. Can estimate resonance $\equiv$ "island" width
   i. single resonance Hamiltonian $H = \frac{1}{2}\psi^2 + \epsilon\cos(m\theta) = E = const.$
   ii. $\psi = \pm\sqrt{2[E - \epsilon\cos(m\theta)]}$
   iii. for separatrix, choose $E = \epsilon$; island width $w = 4\sqrt{\epsilon}$

2. Introduce <u>island overlap</u> criterion: if $\boxed{\frac{w_1}{2} + \frac{w_2}{2} > \Delta\psi}$, then chaos.
   i. for standard map, predicted $k_c \approx 2.5$.

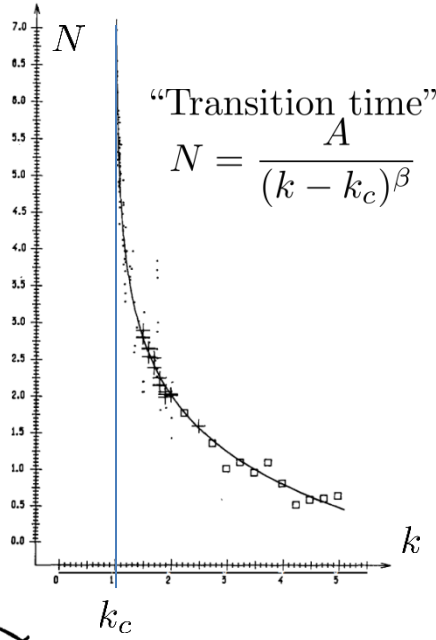

3. However, numerical experiments show $k_c \approx 0.989$
   i. plot $N \equiv$ # iterations to leave given domain against k;
   ii. two free parameters, k_c and β;

4. "The overlap is not only provided by integer resonances, but also by higher harmonic resonances."
   i. If additional resonances are considered, the predicted k_c chang
   e.g. $k_{1,1} = 2.5$, $k_{1,2} = 1.46$, $k_{1,3} = 0.90$, $k_{2,3} = 1.35$, . .

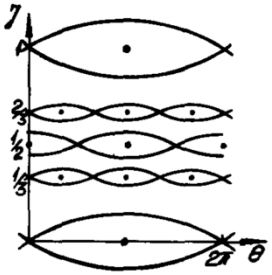

Greene's residue criterion: the existence of an irrational flux surface is determined by the stability of closely-approximating periodic orbits.

1. The tangent map is defined $\begin{pmatrix} \delta\theta_q \\ \delta\rho_q \end{pmatrix} = \nabla M^q \begin{pmatrix} \delta\theta_0 \\ \delta\rho_0 \end{pmatrix}$.

2. The eigenvalues of ∇M^q at periodic fieldlines determine stability:
   $|\nabla M^q| = 1$; $\lambda_1 = 1/\lambda_2$; if $|\lambda| > 1$, unstable, exponential; if $|\lambda| = 1$, stable, sinusoidal.

3. The residue is defined $R_{p/q} \equiv (2 - \lambda - \lambda^{-1})/4$.

4. Consider sequence of rationals that approach an irrational, i.e. $p_i/q_i \to \iota$ as $i \to \infty$.
   (the "best" approximations called the convergents, given by continued fractions).
   If $R_{p/q} \to 0$, surface$_\iota$ exists;
   if $R_{p/q} \to \frac{1}{4}$, surface$_\iota$ critical; and
   if $R_{p/q} \to \infty$, surface$_\iota$ destroyed.

5. By cleverly searching Farey tree
   [following Greene, MacKay]
   can find "boundary surface"
   $\equiv$ last, closed, flux surface.

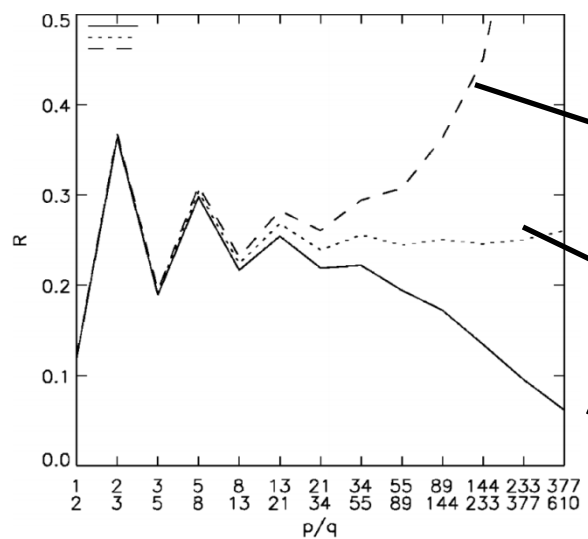

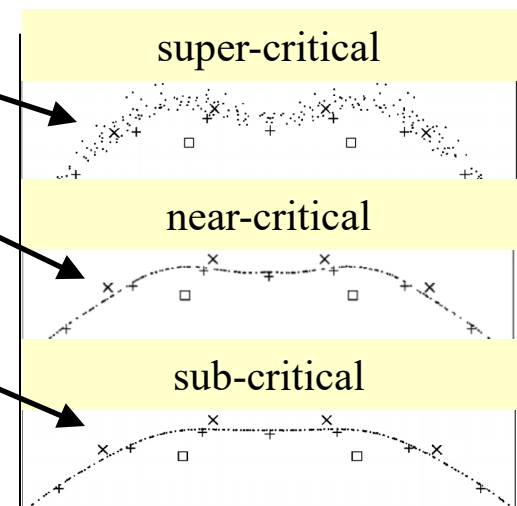

1979 : Greene's Residue Criterion

J. Math. Phys. 20(6), 1979, 1183 (1979)

1. The existence of an irrational flux surface is related to the stability of nearby periodic orbits!

   i. periodic orbits are convenient because they have finite length

   and ii. because they are guaranteed to exist [Poincaré-Birkhoff theorem]

2. Construct a sequence of rationals that converge to the irrational, $\lim_{i\to\infty} \frac{n_i}{m_i} = \iota$

$$\text{e.g. } \frac{1}{1}, \frac{2}{1}, \frac{3}{2}, \frac{5}{3}, \frac{8}{5}, \frac{13}{8}, \frac{21}{13}, \frac{34}{21}, \frac{55}{34}, \frac{89}{55}, \frac{144}{89}, \frac{233}{144}, \frac{377}{233} \cdots \to \frac{1+\sqrt{5}}{2} = \text{golden mean}$$

3. Introduce the residue, $R_{n/m}$, defined on the periodic orbits, which measures stability:

$$\boxed{R_{n/m} \equiv \frac{1}{4}\left[2 - \lambda_1 - \lambda_2\right]}$$, where λ_i are eigenvalues of tangent map, M^m.

   i. if $R_{n_i/m_i} \to 0$, surface exists

   ii. if $R_{n_i/m_i} \to \frac{1}{4}$, surface is critical

   iii. if $R_{n_i/m_i} \to \infty$, surface destroyed

4. $k_c = 0.971635406...$

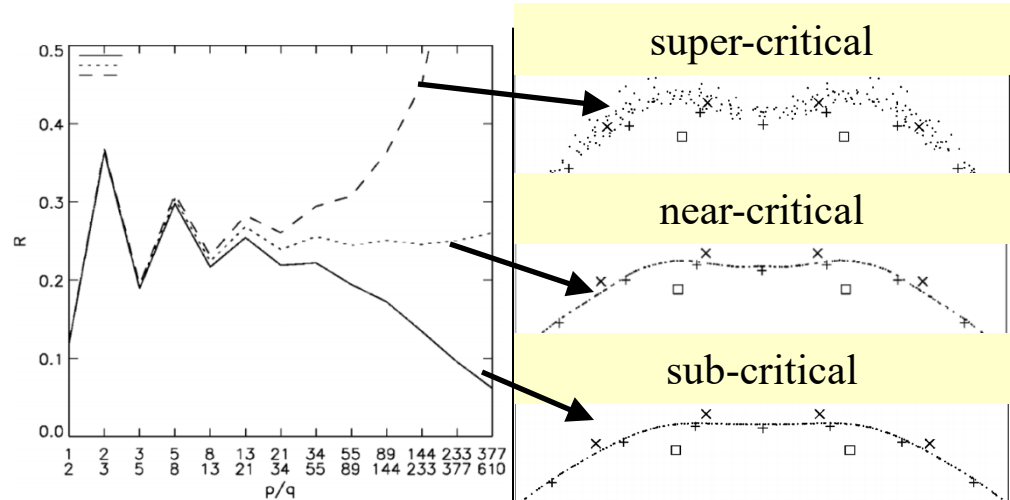

Standard Map critical function is similar to the Bruno function

1. Define $k_c(t)$ as the largest value of k for which an t invariant curve exists;

   i. the critical function peaks on strongly irrationals: $k_c(t) > 0$ if t is irrational;

   ii. rational surfaces do not exist: $k_c(t) = 0$ if $t = n/m$.

   iii. k_c is everywhere discontinuous.

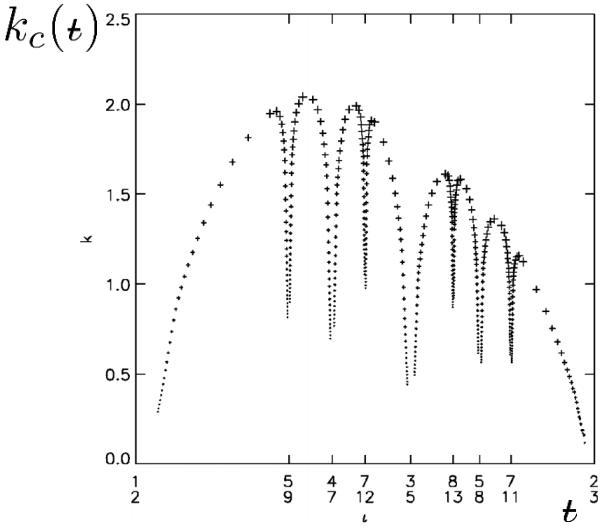

2. The critical function has a form very similar to the Bruno function,

$$B(\omega) = -\log\omega + \omega B(\omega^{-1}), \quad B(\omega) = B(\omega+1) = B(-\omega).$$

   i. $B(\omega)$ is more simply calculated as a function of the continued fraction representation.

3. Marmi & Stark [Nonlinearity, 1992] gave evidence that

$$C_\beta \equiv \log(\, k_c(\omega)\,) + \beta B(\omega)$$

   is continuous.

   i. i.e., that the critical function and the Bruno function have the same fractal structure.

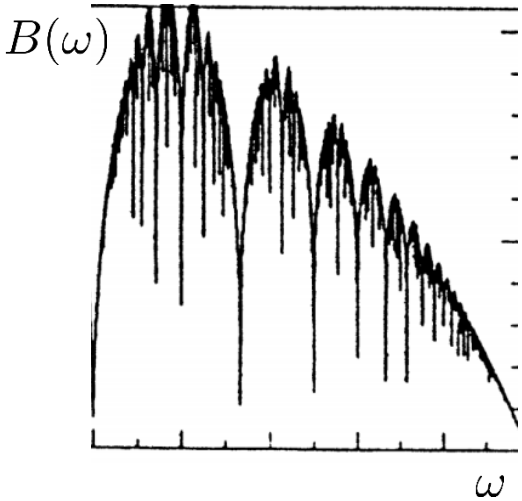

The action gradient, ν, is constant along the pseudo fieldlines; construct Quadratic Flux Minimzing (QFM) surfaces by pseudo fieldline (local) integration.

1. The *true* fieldline flow along $\mathbf{B}$ around q toroidal periods from (θ_0, ρ_0) produces a mapping, $\begin{pmatrix} \theta_q \\ \rho_q \end{pmatrix} = M^q \begin{pmatrix} \theta_0 \\ \rho_0 \end{pmatrix}$.

2. Periodic fieldlines are fixed points of M^q, i.e. $\theta_q = \theta_0 + 2\pi p,\ \rho_q = \rho_0$.

3. In integrable case: given θ_0, a one-dimensional search in ρ is required to find the *true* periodic fieldline.

4. In non-integrable case, only the
   (i) "stable" (action-minimax), O, (which is not always stable), and the
   (ii) unstable (action minimizing), X, periodic fieldlines are guaranteed to survive.

5. The *pseudo* fieldline flow along $\mathbf{B}_\nu = \mathbf{B} - \dfrac{\nu}{\sqrt{g}}\mathbf{e}_\rho$ around q periods from (θ_0, ρ_0) produces a mapping, $\begin{pmatrix} \theta_q \\ \rho_q \end{pmatrix} = P^q \begin{pmatrix} \nu \\ \rho_0 \end{pmatrix}$, but ν is not yet known.

6. In general case: given θ_0, a two-dimensional search in (ν, ρ) is required to find the periodic *pseudo* fieldline.

Alternative Lagrangian integration construction: QFM surfaces are families of extremal curves of the constrained-area action integral.

1. Introduce $F(\boldsymbol{\rho},\boldsymbol{\theta}) \equiv \int_{\mathcal{C}} \mathbf{A}\cdot d\mathbf{l} - \nu\left(\int_{\mathcal{C}} \theta\nabla\zeta\cdot d\mathbf{l} - a\right)$, where $\boldsymbol{\rho}\equiv\{\rho_i\}$, $\boldsymbol{\theta}\equiv\{\theta_i\}$;
   where ν is a Lagrange multiplier, and a is the required "area", $\int_0^{2\pi q}\theta(\zeta)\,d\zeta$.

2. An identity of vector calculus gives $\delta F = \int_{\mathcal{C}} d\mathbf{l}\times(\nabla\times\mathbf{A} - \nu\nabla\theta\times\nabla\zeta)\cdot\delta\mathbf{l}$,
   extremizing curves are tangential to $\mathbf{B} - \nu\nabla\theta\times\nabla\zeta = \mathbf{B} - \frac{\nu}{\sqrt{g}}\mathbf{e}_\rho = \mathbf{B}_\nu$.

3. Constrained-area action-extremizing curves satisfy $\frac{\partial F}{\partial\rho_i} = 0$ and $\frac{\partial F}{\partial\theta_i} = 0$.

4. The piecewise-constant representation for $\rho(\zeta)$ and $\partial_{\rho_i}F = 0$ yields $\rho_i = \rho_i(\theta_{i-1},\theta_i)$, so the trial curve is completely described by θ_i, i.e. $F\equiv F(\boldsymbol{\theta})$.

5. The piecewise-linear representation for $\theta(\zeta)$ gives $\frac{\partial F}{\partial\theta_i} = \partial_2 F_i(\theta_{i-1},\theta_i) + \partial_1 F_{i+1}(\theta_i,\theta_{i+1})$,
   so the Hessian, $\nabla^2 F(\boldsymbol{\theta})$, is tridiagonal (assuming ν is given) and is easily inverted.

6. Multi-dimensional Newton method: $\delta\boldsymbol{\theta} = -\left(\nabla^2 F\right)^{-1}\cdot\nabla F(\boldsymbol{\theta})$;
   global integration, <u>much</u> less sensitive to "Lyapunov" integration errors.

Magnetic flux surfaces are required for good confinement; but 3D effects create "magnetic islands", and island overlap creates chaos.

1. $\mathbf{A} = \psi(\rho,\theta,\zeta)\nabla\theta - \chi(\rho,\theta,\zeta)\nabla\zeta = \psi\nabla\theta - \chi(\psi,\theta,\zeta)\nabla\zeta, \quad \underbrace{\text{if } \rho \equiv \rho(\psi,\theta,\zeta)}_{coordinate\ transformation}$

2. $\mathbf{B} = \nabla\psi \times \nabla\theta - \nabla\chi(\psi,\theta,\zeta) \times \nabla\zeta$

3. Toroidal flux: $\displaystyle\int_{\mathcal{S}} \mathbf{B}\cdot d\mathbf{s} = \int_0^{2\pi} d\theta \int_0^{\psi} d\bar{\psi}\ \mathbf{B}\cdot\mathbf{e}_\psi \times \mathbf{e}_\theta = 2\pi\psi,$ where $\sqrt{g} \equiv \mathbf{e}_\psi \cdot \mathbf{e}_\theta \times \mathbf{e}_\zeta = (\nabla\psi\cdot\nabla\theta\times\nabla\zeta)^{-1}$.

4. Definition of fieldline: $d\mathbf{l} \propto \mathbf{B}$.

   - Cartesian (x,y,z) coordinate basis: $dx\,\mathbf{i} + dy\,\mathbf{j} + dz\,\mathbf{k} = B^x\,\mathbf{i} + B^y\,\mathbf{j} + B^z\,\mathbf{k}$.
   - Arbitrary (ψ,θ,ζ) coordinate basis: $d\psi\,\mathbf{e}_\psi + d\theta\,\mathbf{e}_\theta + d\zeta\,\mathbf{e}_\zeta = B^\psi\mathbf{e}_\psi + B^\theta\mathbf{e}_\theta + B^\zeta\mathbf{e}_\zeta$, where $B^\psi \equiv \mathbf{B}\cdot\nabla\psi$, $B^\theta \equiv \mathbf{B}\cdot\nabla\theta$, $B^\zeta \equiv \mathbf{B}\cdot\nabla\zeta$.

5. $\dot{\psi} \equiv \dfrac{d\psi}{d\zeta} = \dfrac{B^\psi}{B^\zeta} = -\dfrac{\partial\chi}{\partial\theta}, \quad \dot{\theta} \equiv \dfrac{d\theta}{d\zeta} = \dfrac{B^\theta}{B^\zeta} = \dfrac{\partial\chi}{\partial\psi}$;
   $\chi \equiv$ poloidal flux$\equiv$fieldline Hamiltonian.

6. If $\chi = \chi(\psi)$, $\dot{\psi} = 0$ and $\dot{\theta} = \iota(\psi)$: magnetic field is "integrable", and fieldlines lie on nested flux surfaces.

7. Generally, $\chi = \chi(\psi,\theta,\zeta) = \sum_{m,n} \chi_{m,n}(\psi)\cos(m\theta - n\zeta)$, and "islands" open where $m\dot{\theta} - n = 0$.

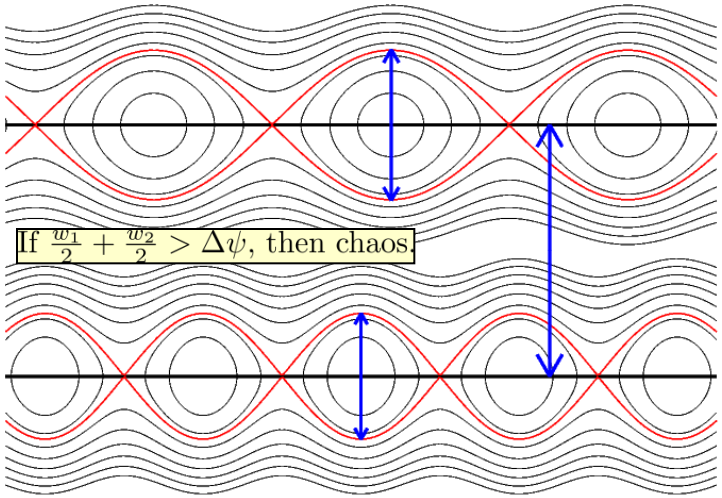

In the beginning, there was Hamiltonian mechanics

Hamilton, Lagrange, et *al*. identified integrals of motion,
Boltzmann's postulated the ergodic hypothesis,
Poincaré described the "chaotic tangle".

Quotations from ["Regular and Chaotic Dynamics", by Lichtenberg & Lieberman]

1) "These deep contradictions between the existence of integrability and the existence of ergodicity were symptomatic of a fundamental unsolved problem of classical mechanics."

2) "Poincaré contributed to the understanding of these dilemmas by demonstrating the extremely intricate nature of the motion in the vicinity of the unstable fixed points, a first hint that regular applied forces may generate stochastic motion in nonlinear oscillator systems."

3) "Birkhoff showed that both stable and unstable fixed points must exist whenever there is a rational frequency ratio (resonance) between two degrees of freedom."

4) "..the question of the ergodic hypothesis, whether a trajectory explores the entire region of the phase space that is energetically available to it, or whether it is constrained by the existence of constants of the motion, was not definitively answered until quite recently. The KAM theorem, originally postulated by Kolomogorov (1954), and proved under different restrictions by Arnold (1963) and Moser (1962) . .